PB81-122368

REPORT NO.
UCB/EERC-80/05
SEPTEMBER 1980

EARTHQUAKE ENGINEERING RESEARCH CENTER

SHAKING TABLE RESEARCH ON CONCRETE DAM MODELS

by
AKIRA NIWA
RAY W. CLOUGH

Report to the National Science Foundation

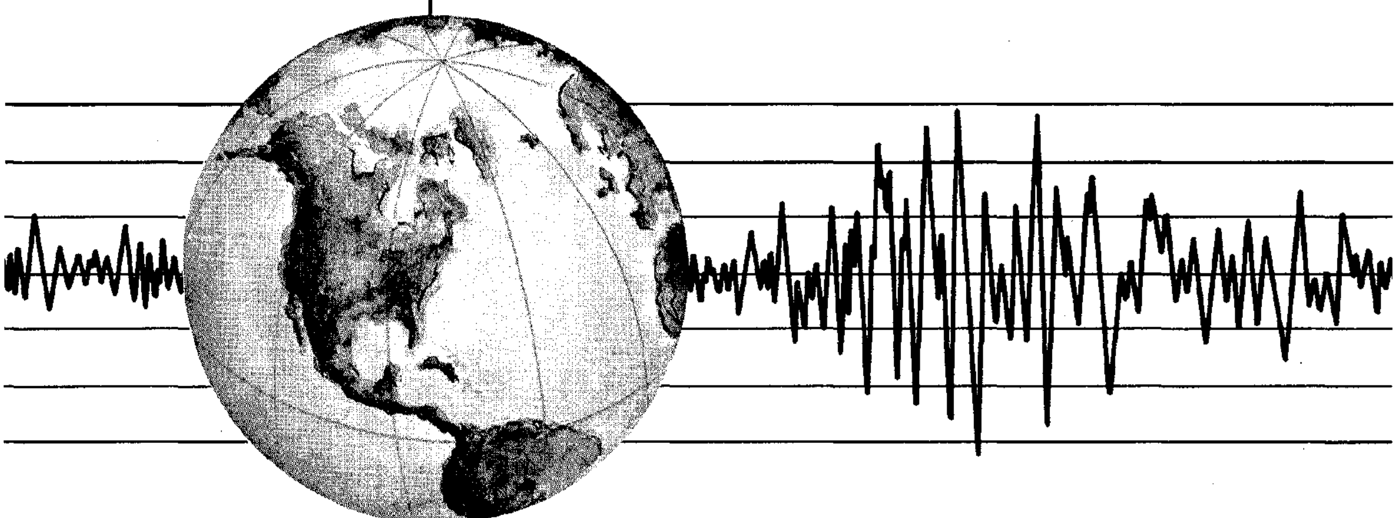

COLLEGE OF ENGINEERING

UNIVERSITY OF CALIFORNIA · Berkeley, California

For sale by the National Technical Information Service, U.S. Department of Commerce, Springfield, Virginia 22161.

See back of report for up to date listing of EERC reports.

50272-101

REPORT DOCUMENTATION PAGE	1. REPORT NO. NSF/RA-800192	2.	3. Recipient's Accession No. PB81 122368

4. Title and Subtitle
Shaking Table Research on Concrete Dam Models

5. Report Date
September 1980

6.

7. Author(s)
Akira Niwa and Ray W. Clough

8. Performing Organization Rept. No.
UCB/EERC-80/05

9. Performing Organization Name and Address
Earthquake Engineering Research Center
University of California, Richmond Field Station
47th and Hoffman Blvd.
Richmond, California 94804

10. Project/Task/Work Unit No.

11. Contract(C) or Grant(G) No.
(C)
(G) PFR78-19333

12. Sponsoring Organization Name and Address
National Science Foundation
1800 G Street, N.W.
Washington, D. C. 20550

13. Type of Report & Period Covered

14.

15. Supplementary Notes

16. Abstract (Limit: 200 words)
The basic purpose of this research was to investigate the feasibility of studying the nonlinear response behavior of concrete arch dams on a 20 ft square shaking table. Assuming a length scale of 1/150, suitable model material of plaster, celite, sand and lead powder was developed. The proportions and properties of adopted materials are listed.

Shaking table tests are described of a segmented arch rib model designed of this material to simulate the monolith joint opening behavior of an arch dam. Also, the test of a model of Koyna Dam is mentioned, where the model behavior simulated reservoir cavitation mechanism and the observed cracking of the prototype. The principal conclusion of the investigation is that shaking table research is a practical means of studying the nonlinear earthquake response of concrete arch dams, including their actual failure mechanisms.

17. Document Analysis a. Descriptors

b. Identifiers/Open-Ended Terms

c. COSATI Field/Group

18. Availability Statement: Release Unlimited	19. Security Class (This Report)	21. No. of Pages
	20. Security Class (This Page)	22. Price

(See ANSI-Z39.18) See Instructions on Reverse OPTIONAL FORM 272 (4-77)
(Formerly NTIS-35)
Department of Commerce

SHAKING TABLE RESEARCH ON CONCRETE DAM MODELS

by

Akira Niwa

Ray W. Clough

Prepared with support from the
National Science Foundation

Report No. UCB/EERC-80/05
Earthquake Engineering Research Center
College of Engineering
University of California
Berkeley, California

September 1980

ABSTRACT

The basic purpose of this research was to investigate the feasibility of studying the nonlinear response behavior of concrete arch dams on a 20 ft square shaking table. Assuming a length scale of 1/150, suitable model material of plaster, celite, sand and lead powder was developed. The proportions and properties of adopted materials are listed.

Shaking table tests are described of a segmented arch rib model designed of this material to simulate the monolith joint opening behavior of an arch dam. Also, the test of a model of Koyna Dam is mentioned, where the model behavior simulated reservoir cavitation mechanism and the observed cracking of the prototype. The principal conclusion of the investigation is that shaking table research is a practical means of studying the nonlinear earthquake response of concrete arch dams, including their actual failure mechanisms.

ACKNOWLEDGEMENTS

This research was carried out with financial support of the National Science Foundation as part of a U.S.-Taiwan Cooperative Research program on the earthquake behavior of Techi Dam. This support is gratefully acknowledged. The authors wish to express their appreciation for technical advice and encouragement received from Professor Jerome Raphael, Mr. Lou J. Trescony and Mr. George Hayler, during the construction of model material. Many thanks also due to Messrs. David Steere, Ivo Van Asten, John McNab, Steve Miller and Derald Clearwater of the Earthquake Engineering Research Center for their help in the tests. The authors are grateful to students Ming-san Yang and Tsutomu Hirata for their assistance during many tedious hours of specimen preparation and performing the tests.

The typing was done by Ms. Toni Avery and the drafting by Ms. Gail Feazell.

TABLE OF CONTENTS

TABLE OF CONTENTS (Cont'd) Page

LIST OF TABLES

LIST OF FIGURES

LIST OF FIGURES (Cont'd)

LIST OF FIGURES (Cont'd)

1. INTRODUCTION

Earthquake safety of dams is a matter of increasing concern in seismically active regions of the world because the potential hazard presented by a large reservoir is proportional to the increasing population downstream of the dam. Consequently, both existing structures and proposed new designs are being subjected to seismic safety evaluations; these involve estimation of the maximum earthquake motions that may be expected at the site, and evaluation of the dynamic response to these motions. The current practice in the seismic analysis of concrete dams is to assume that the structure as well as its interaction mechanisms with reservoir and foundation are linearly elastic, because of problems involved in the analytical representation of nonlinear behavior. Unfortunately, however, such linear analyses do not adequately represent the true behavior of concrete arch dams, and it is difficult to establish consistent design criteria based on results of linear analyses.

Three major types of structural nonlinearities (see Fig. 1.1) can be expected in the response of concrete arch dams to strong earthquake motions. The mechanism that occurs most commonly results from movement of the vertical joints that are formed between the concrete monoliths during the construction process. Under static condition, these joints are forced closed by the hydrostatic pressure of the reservoir, and the structure resists these loads as a single unit. During the dynamic response to a severe earthquake, however, bending and upstream motion of the arch tend to cause opening of these joints, and it is evident that a linear analysis which neglects the possibility of joint opening may produce misleading results. Specifically, tensile stresses that may be indicated in the arch ring direction cannot be transmitted across the monolith joints.

The second type of nonlinearity that may result from an intense earthquake is horizontal cracking of the vertical monoliths. Such cracking is most likely when the dam is deflecting upstream so that the monolith joints open; at such a time, the arch action is eliminated and the structural resistance is provided only by cantilever bending. The typical dynamic response analysis does not predict the cracking of the concrete, and no estimate is made of the displacements that may occur in the post-cracking condition.

Reservoir cavitation is the third form of nonlinearity that may be associated with earthquake response. This occurs when negative dynamic fluid pressure at dam face offsets the hydrostatic plus atmospheric pressure during a intense earthquake motion. Consequently, recurrent separation and subsequent impact action is generated between the reservoir and dam face. The separation action tends to reduce the dam response because it suppresses the dynamic negative pressure beyond the static level; but the subsequent impact action, which causes instantaneous large positive pressures in the upper parts of the dam, might increase the stress response at these locations. The impact actions in concurrence with the second or higher mode response of dam may enhance the tendency toward tensile cracking in the upper sections of the vertical monoliths. The typical dynamic response analysis in the design does not predict the cavitation impact, and no estimate is made of the extent of stress redistribution due to the cavitational response.

Although nonlinear finite element analysis procedures have been developed that could deal in principle with these nonlinearities, no calculations have yet been made that account for the monolith joint opening in a realistic fashion[1], the analytical prediction of cracking has proven to be very difficult because the results are so sensitive to the failure criteria assumptions[2], and the only studies of the cavitation mechanism to date are grossly over-simplified in that they treat the reservoir effect as "added mass"[3]. For these reasons, it is important to carry out experimental studies of the seismic behavior of concrete arch dams, both to provide quantitative evidence about their actual dynamic response and to serve in verification of non-linear analytical procedures as they are developed.

The purpose of the investigation reported here was to determine the feasibility of carrying out meaningful model studies of concrete arch dam response to earthquakes, using the 20 ft. square earthquake simulator at the University of California Earthquake Engineering Research Center. The research was carried out with financial support of the National Science Foundation as part of a U.S.-Taiwan Cooperative Research program on the earthquake behavior of Techi Dam; this support is gratefully acknowledged. Funds provided in this grant were not sufficient to test a complete model of the Techi Dam; moreover, preliminary studies were needed to determine whether a complete model test was feasible. Therefore, this investigation was limited to three objectives: (1) development of a model material that would adquately maintain similitude with the prototype at a length scale of about 1/150, (2) shaking table tests of a segmented arch rib constructed from this model material, to demonstrate the effect of joint opening on the dynamic response, and (3) shaking table testing of a cantilever monolith made from the model material and retaining a reservoir, to determine cracking mechanisms and post-cracking behavior of the system.

Results of the work done on these three topics are presented in the following chapters of this report.

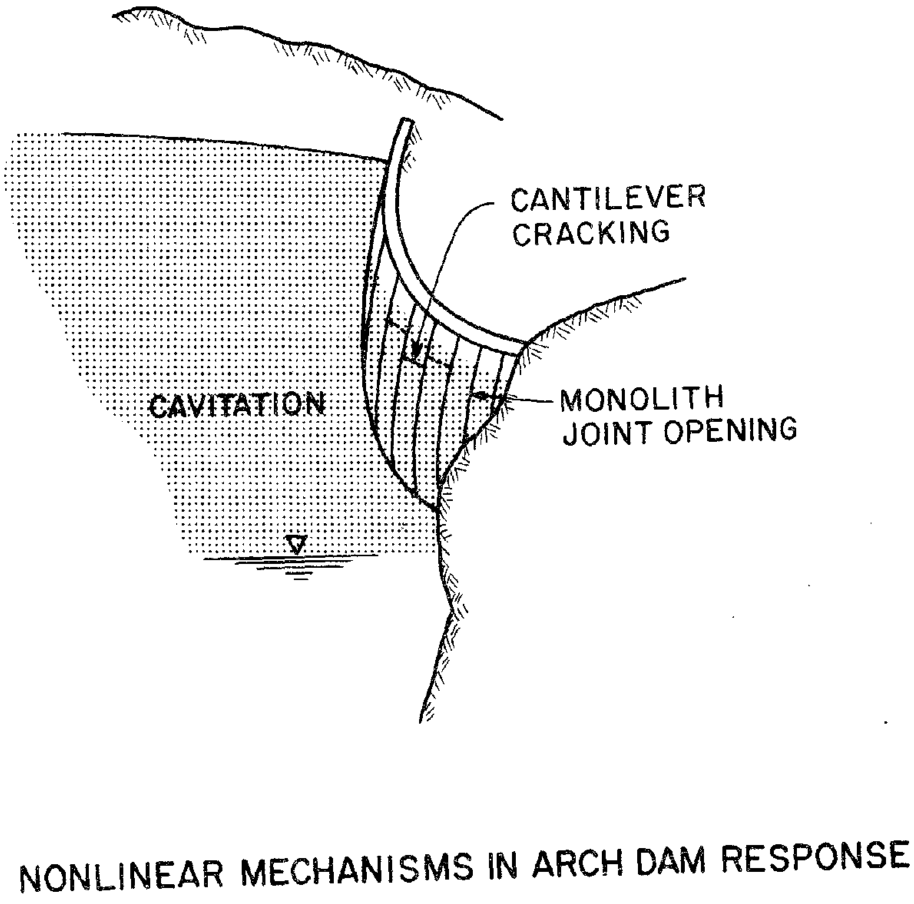

Fig. 1.1 Nonlinear Mechanisms in Arch Dam Response

2. MATERIAL DEVELOPMENT

2.1 Similitude Requirements

In earthquake response of an arch dam, the significant forces controlling the behavior up to the point of failure are those due to gravity (including hydrostatic pressure), to the earthquake acceleration, and to elastic as well as inelastic deformation. In order for the prototype response behavior to be truly reproduced in a model test on the shaking table, the following relationship is imposed by similitude laws:

$$S_E = S_W \cdot S_L$$

where

S_E = Modulus and strength ratio

S_W = Unit weight ratio

S_L = Length scale

It is also required in any nonlinear test that strains in the model should equal those of the prototype - as is necessary to maintain true geometric similitude.

In this study, the length scale was set at 1/150 because this provided a model size that could be constructed and tested conveniently on the shaking table. The unit weight ratio was fixed to unity by the condition that the liquid in the model reservoir would be water, the same as in the prototype. Thus, the scales for strength and modulus of the model material must be equal to the length scale. In addition, the time scale was controlled by the fact that the gravitional accelerations in the model would be the same as in the prototype, thus, requiring that the dynamic acceleration scale also be unity. With both acceleration ratio and length scale fixed, the time scale is found to be the square root of the length scale. In previous dynamic model tests of arch dams, these material requirements have not been satisfied[4].

A summary of the similitude requirements established for this investigation is presented in Table 2.1. It will be noted that two of the requirements expressed for the model liquid are not satisfied if water is used in the model test, i.e., effects due to viscosity and compressibility will be distorted. The authors do not consider these to be critical factors in typical arch dam response, although some researchers would differ with regard to the importance of compressibility [5].

2.2 Development of Test Materials

The foregoing discussion of model similitude has led to the following requirements to be met by the model material: the unit weight must be the same as the prototype material, and both strength and modulus must be 1/150 of those properties in the prototype. Table 2.2 lists the material properties that have been assumed for the prototype, and the resulting target values that are imposed on the model material. Clearly, the development of a material which weighs the same as concrete, with a modulus of 27,000 psi, and 27 psi compressive and 2.7 psi tensile strength is a major challenge. A value of 70,000 psi is the smallest modulus developed in past tests dealing with such plaster materials. The effort to produce a plaster material having such a small tensile strength also is new; the tensile cracking mechanism in arch dam response had been ignored in these previous tests [4,6].

To begin the development it was decided to ignore the unit weight requirement at first; thus, the objective during this phase was to develop a material having appropriate strength and modulus values. The materials used in this initial development were casting plaster, celite and water. The study was based on work done previously at Berkeley by Professor J. M. Raphael [7]. Subsequently, sand was added to the mixture to help control bleeding of the mixing water and also to improve the ratio between the strength and the modulus. In the final stage of development, lead powder was added to the mixture to provide the desired unit weight. In general, the addition of each constituent caused changes in all the material properties; thus, a very extensive test program was required involving casting and testing of nearly 300 3 x 6 in. cylinder specimens. Table 2.4 lists data from all the mixing tests performed in this study.

Mixing and casting procedures varied with the type of material and also with ratio of water to plaster in the mix. In order to minimize bleeding and/or segregation, the cylinders were cast only after the consistency had stiffened to a specified value as indicated by tests with a brass cone consistometer; this requirement led to longer mixing times for higher water/plaster ratios. Control of segregation became difficult when lead powder was included in the mix, and a greater degree of stiffening was required before the heavy plaster mixes were cast. Thus, the addition of lead increased the mixing time before casting, and prolonged mixing caused some variation in the material properties. Test cylinders usually were cast in a set of six from a single batch of material; generally they were removed from the molds about half hour after casting to avoid development of shrinkage cracks along the mold wall. Drying was done at 95°F in a circulating air oven and was continued until the weight of the specimens became constant.

The modulus of elasticity and compressive strength of the materials were determined by standard compression test procedures. Typically the cylinder was preloaded to take up slack in the compressometer; load was then applied at a rate of 200 lbs/minute until a strain of 0.000333 was reached. The process was repeated three times with each cylinder, and the "secant" modulus was determined from the load increment required to produce the strain level of 0.000333. The ultimate compressive strength was determined by loading the cylinders to failure, and the corresponding failure strain was measured in some cylinders with strain gages. The ultimate tensile strength was measured by a lateral splitting test. A special splitting-tension fixture was used for this test, and the tensile strength was calculated from the formula:

$$\sigma_t = \frac{2\,P_{max}}{\pi hd}$$

where hd is the area of the longitudinal section on which splitting occurred. Flexural tests of some 4 x 4 x 26 in. beam specimens also were performed to evaluate the ultimate strain for tension failure.

2.3 Mechanical Properties of the Materials

The significant properties of the four types of material developed in this study are summarized in Figs. 2.1 to 2.5. Properties measured for the light weight mixes are denoted in these figures by circles while the heavy weight mixtures made by the addition of lead powder are indicated by triangles. "Open" symbols are used to identify mixes without sand, and the addition of sand is denoted by "solid" (filled in) symbols.

The ratio of water to plaster was found to be the most important parameter in controlling the mechanical properties of the materials, and Fig. 2.1 shows the variation of Young's modulus (E) with the water/plaster ratio (by weight) for the four types of material. To minimize the experimental effort, a wide range of water/plaster ratios was studied only for the mixture without sand; the mixtures with sand were investigated only in the range of water/plaster ratios expected to provide acceptable results. In general, the amount of celite used in the mixes was adjusted to provide good workability and consistency -- it varied with the water/plaster ratio. Also, the sand/plaster ratio was adjusted to give a suitable relationship between modulus and strength in the range of the desired properties; a ratio of 12 was found to be effective.

As is evident in Fig. 2.1, a wide range of E values was obtained for both light and heavy mixtures by varying the water/plaster ratio; however, addition of the lead powder caused a definite increase of modulus, especially with regard to the minimum achievable value. Also, addition of sand increased the modulus of both light and heavy mixtures; as would be expected.

The influence of the water/plaster ratio on the ultimate compressive strength ($\sigma_{u,c}$) of the test cylinders is depicted similarly in Fig. 2.2, and it is evident by comparison with Fig. 2.1 that the compressive strength is closely related to the modulus of elasticity. However, it is interesting to note that the addition of sand did not increase the strength as it did the modulus. Similar conclusions may be drawn with regard to the ultimate tensile strength ($\sigma_{u,t}$) indicated by the splitting test, which is plotted against the water/plaster ratio in Fig. 2.3.

Of particular importance with regard to similitude requirements are the ratios of modulus to compressive strength ($E/\sigma_{u,c}$) and of compressive to tensile strength ($\sigma_{u,c}/\sigma_{u,t}$), because these ratios should be the same for the model material and the prototype concrete. The variation of modulus with compressive strength is shown for the four types of material in Fig. 2.4, and it is clear that this ratio is essentially constant for each material over a wide range of strengths. On the other hand, the ratio varies widely among the four materials. The light plaster with sand has the desired ratio ($E/\sigma_{u,c} = 1000$); each of the other materials would introduce some distortion of model results in this regard.

The variation of compressive strength with tensile strength is presented similarly in Fig. 2.5. Although some scatter is evident in these results, a reasonable straight line approximation can be made for each material. The variation of this $\sigma_{u,c}/\sigma_{u,t}$ ratio among the materials is less than for the $E/\sigma_{u,c}$ ratios. Again the light plaster with sand is seen to best approximate the target ratio for prototype concrete, which is 10.

Based on these results, a light plaster with sand mixtures was adopted for construction of the segmented arch rib model; constituents and properties of the selected mix are listed in Table 2.3. Comparison with the target values in Table 2.2 shows that this material should provide good similitude with the prototype deformations and failure mechanisms. Of course, the unit weight requirement is not satisfied, but for this model lead weights were attached to approximate the static load effects. The compressive stress-strain curve for this material, shown in Fig. 2.6, is similar in shape to that of typical mass-concrete; therefore, it may be assumed that nonlinear deformations will be simulated adequately as well.

To simulate the dynamic cracking behavior of a cantilever section model, it was necessary for the model material to duplicate the unit weight of the prototype concrete because the addition of external weights would lead to distortions. The constituents and mechanical properties of the heavy plaster with sand material that was selected to construct this model also are summarized in Table 2.3; its compressive stress-strain curve also is plotted in Fig. 2.6. The tabulated data and curve for this material demonstrate that it does not satisfy the similitude requirements as well as does the light weight mixture. In particular, it will be noted that the ultimate strain is only 0.8 mils per inch; thus, deformations at compressive failure would be smaller in the model than in the prototype. However, this type of distortion was not introduced in this cantilever section test, because the failure mechanism in that test was associated with tensile cracking.

TABLE 2.1

SIMILITUDE REQUIREMENTS FOR DAM MODEL

Component	Variable	Required Scale Ratio $\frac{\text{model}}{\text{prototype}}$
Dam	Unit Weight	$\rho = 1$
	Length	$L = 1/150$
	Elastic Modulus	$E = 1/150$
	Ultimate Strength	$\sigma = 1/150$
	Poisson's Ratio	$\nu = 1$
	Strain	$\varepsilon = 1$
	Force	$F = (1/150)^3$
Reservoir Liquid	Unit Weight	$\rho = 1$
	Speed of Sound	$c = (1/150)^{1/2}$
	Viscosity	$\mu = (1/150)^{3/2}$
Earthquake Motion	Displacement	$L = 1/150$
	Acceleration	$a = 1$
	Duration and Period	$T = (1/150)^{1/2}$

TABLE 2.2

DAM MATERIAL PROPERTIES

Property	Assumed Prototype Concrete	Modal Material Targets
Unit Weight (pcf)	150	150
Young's Modulus E (psi)	4×16^6	26.7×10^3
Ultimate Strength (psi)		
Compression ($\sigma_{u,c}$)	4000	26.7
Tension ($\sigma_{u,t}$)	400	2.67
Poisson's Ratio	0.20	0.20
$E/\sigma_{u,c}$	1000	1000
$\sigma_{u,c}/\sigma_{u,t}$	10	10

TABLE 2.3

ADOPTED MODEL MATERIALS - CONSTITUENTS AND PROPERTIES

Mix Proportions (by weight)				Mechanical Properties						
Water / Plaster	Celite / Plaster	Sand / Plaster	Lead / Plaster	E (psi)	$\sigma_{u,c}$ (psi)	$\sigma_{u,t}$ (psi)	unit wt. (pcf)	$^{*}\nu$	$E/\sigma_{u,c}$	$\sigma_{u,c}/\sigma_{u,t}$
Light Plaster With Sand										
7.0	1.8	12.0	--	27.7×10^3	26.5	2.81	74.9	0.17	1045	9.43
Heavy Plaster With Sand										
10.0	2.2	12.0	24.12	44.1×10^3	26.7	2.99	146	0.16	1650	8.93

$^{*}\nu$ = Poisson's Ratio

TABLE 2.4

CYLINDER MIXING AND LOADING TEST

(a) LIGHT PLASTER MIXTURES

Mixing Test Ident.	Mix Proportions (by Weight)				Consistency (in.)		Time (min.)		Settle (in.)	Mechanical Properties				Remarks
	W/P	C/P	L/P	S/P	Initial	Cast	Cast	Set		E (10^3 psi)	$\sigma_{u,c}$ (psi)	$\sigma_{u,t}$ (psi)	Specific Density	
121278.1	3.5	1.0			3.7	1.4	21			51.9	122.	11.4	0.51	Mixture considerably hardened just before cast.
121278.2	3.8	1.0			4.6	3.6	24			59.9	100.	18.9	0.48	
121378.1	4.2	1.1			4.5	3.5	31		.01	45.5	77.2	15.7	0.46	
121478.1	3.4	0.9			4.3	3.3	32			55.7	110.	23.4	0.50	Mixture hardened during cast.
121978.1	4.6	1.2			4.8	3.5	23	24½	.03	38.7	84.3	14.3	0.44	
121978.2	5.0	1.35			4.6	3.8	20	26½	.02	33.9	74.2	10.9	0.43	Spiral cracks developed in one cylinder.
121978.3	5.4	1.5			4.5	3.8	20	28	.05	29.1	62.8	9.67	0.42	
122078.1	3.4	0.9			4.3	3.6	15	21		85.1	173.	27.3	0.51	
122078.2	5.8	1.65			4.4	3.6	23	31		24.2	47.1	7.58	0.42	
122078.3	3.0	0.77			4.8	3.3	20	24		112.	224.	31.9	0.53	
011729.1	6.2	1.8			4.3	3.2	34	42		17.8	40.8	6.20	0.41	
012479.1	6.6	1.9			4.4	3.3	29			18.7	42.9	6.47	0.40	
012579.1	6.6	1.9			4.2	2.9	39			17.6	42.3	6.32	0.40	Casting plaster from barrel "Ross High Dam No. 12".
020179.1	7.0	2.0			4.5	3.6	68		Excessive	9.96	19.0	2.60	0.40	In trial cast of arch block, bleeding water leaked through mold joints. Shrinkage was 2.7%.

TABLE 2.4b

LIGHT PLASTER MIXTURE WITH SAND

Mixing Test	Mix Proportions (by Weight)				Consistency (in.)		Time (min.)		Settle (in.)	Mechanical Properties				Remarks
	W/P	C/P	L/P	S/P	Initial	Cast	Cast	Set		E (10^3 psi)	$\sigma_{u,c}$ (psi)	$\sigma_{u,t}$ (psi)	Specific Density	
011779.2	6.2	1.8		2.0	4.4	3.1	41	48½	0.00	19.5	39.2	5.93		
011879.1	6.2	1.8		3.0	4.4	3.4	33	40		21.2	39.3	4.49		
011879.2	6.2	1.8		1.0	4.4	3.5	32	38½		19.9	42.2	5.73		
011879.3	6.2	1.8		1.0	3.7	2.7	29			23.4	51.9	8.01		Sand of No. 20 mesh.
011879.4	6.2	1.8		2.0	4.2	3.0	38	44		19.6	38.2	5.85		Sand of No. 20 mesh.
020879.1	6.5	1.5		13.4	4.8	3.4	25			--	--	--		Cast cylinders were very weak, and damaged in mold release.
020979.1	6.5	1.5		13.4	5.1	3.7	23	28		48.2	42.0	5.80	1.30	
021479.1	6.5	1.5		13.4	4.8	3.8	31	37		40.8	34.5	--	1.29	Shrinkage 1.5%. Trial cast of arch block.
021579.1	6.5	1.5		13.4	4.8	3.8	32	38		--	--	--	1.29	Shrinkage 2.3%. Trial cast of arch block.
021679.1	7.0	1.8		12.0	4.6	3.5	26	32½		26.2	28.1	3.78	1.19	
022279.1	7.5	2.0		12.0	4.6	3.5	24	30	0.03	33.6	30.4	4.44	1.16	
022379.1	7.0	1.8		8.0	5.2	3.5	33	39		27.6	32.1	4.06	1.00	
022379.2	7.5	2.0		8.0	4.8	3.6	26	32½		24.9	33.2	4.48	0.97	
030879.1	7.0	1.8		12.0	4.7	3.7	37	45		29.8	27.1	3.24	1.21	

TABLE 2.4b(CONT'D) - LIGHT PLASTER MIXTURE WITH SAND

Mixing Test	Mix Proportions (by Weight)				Consistency (in.)		Time (min.)		Settle (in.)	Mechanical Properties				Remarks
	W/P	C/P	L/P	S/P	Initial	Cast	Cast	Set		E (10^3 psi)	$\sigma_{u,c}$ (psi)	$\sigma_{u,t}$ (psi)	Specific Density	
031479.1	7.0	1.8		12.0	4.8	4.1	38			27.4	25.1	3.16	1.21	Trial cast of arch block.
032979.1	7.0	1.8		10.0	5.0	3.6	27	34		29.5	28.0	3.38	1.12	
032979.2	7.0	2.0		12.0	3.9	2.7	25	31		31.8	32.5	4.03	1.21	Tiny air bubbles scattered over surface of cylinder just after mold release.
033079.1	7.0	1.6		12.0	5.2	3.9	25	31		32.9	30.2	3.78	1.20	
040279.1	7.0	1.8		11.0	4.9	3.8	41	49		30.1	24.2	2.95	1.16	Shrinkage 2.5%.
040679.1	7.0	1.8		13.0	4.5	3.4	32	38		--	--	--	--	Cast cylinders were weak like jello and badly distorted during mold release.
041379.1	7.0	1.8		12.0	4.7	3.6	42			--	--	--	--	Cast ten arch blocks.
041879.1	7.0	1.8		12.0	4.8	3.9	45	51		27.7	26.5	2.81	1.20	Cast ten arch blocks.
042579.1	7.0	1.8		12.0	4.8	3.8	38	47½		26.5	26.0	3.02	1.20	Cast ten arch blocks.
050479.1	7.0	1.8		12.0	4.6	3.6	44	53		--	--	--	--	Cast three arch blocks.
060679.1	7.0	1.8		12.0	4.9	3.9	45	54		--	--	--	1.21	Cast five 4x4x27 in. beams. Shrinkage 3.0%.
062979.1	7.0	1.8		12.0	5.0	3.9	49			27.2	28.6	--	1.21	Trial cast of Koyna Dam section.
070579.1	7.0	1.8		12.0	4.9	3.8	38							Trial cast of Koyna Dam section.
070779.1	7.0	1.8		12.0	4.7	3.6	36							Trial cast of Koyna Dam section.

TABLE 2.4c - HEAVY PLASTER MIXTURE

Mixing Test	Mix Proportions (by Weight)				Consistency (in.)		Time (min.)		Settle (in.)	Mechanical Properties				Remarks
	W/P	C/P	L/P	S/P	Initial	Cast	Cast	Set		E (10^3 psi)	$\sigma_{u,c}$ (psi)	$\sigma_{u,t}$ (psi)	Specific Density	
121378.2	4.2	1.1	12.92		4.1	1.1	14		0.00	--	--	--	--	All cylinders were cracked inside mold due to delayed release.
121378.3	4.2	0.769	10.35		0.	0.	5		0.22	--	--	--	2.05	Dry litharge substituted. Cylinder stayed soft for many days.
121478.2	4.2	1.0	12.88		4.6	3.0	48			52.0	77.5	--	2.57	
121578.1	4.2	1.1	12.92		4.5	1.7	22			73.0	123.	21.2	2.67	
121578.2	3.8	1.0	11.66		4.6	3.3	18	21½		109.	170.	27.1	2.63	
122178.1	4.2	1.1	12.92		3.7	3.5	37	76½	Excessive	64.0	83.2	14.4	2.62	Cylinder cracks near top due to excessive bleeding.
122178.2	4.2	1.1	12.92		4.0	3.0	52	64		74.0	104.	17.9	2.71	Spiral cracks near top due to delayed mold release.
122778.1	4.6	1.1	14.14		4.3	3.2	94	114		42.8	53.4	10.0	2.72	Egg beater was used first time to help thorough mixing of ingredients
122778.2	5.0	1.2	13.23		4.5	3.1	90	102		35.9	48.7	7.48	2.41	
122878.1	5.4	1.3	14.32		4.5	3.2	90	107½		33.5	41.7	7.24	2.41	
122878.2	3.4	0.9	8.88		3.7	1.5	51	64½		98.8	156.	28.5	2.38	
011079.1	6.2	2.0	16.60		2.8	1.8	70	99	0.10	31.3	48.2	7.35	2.37	Cylinder stayed soft and wet with heavy bleeding.
011679.1	6.2	1.5	16.50		4.5	1.7	95	127	0.08	--	--	--	--	
011679.2	6.2	1.5	16.50		4.5	1.2	77	92	0.04	--	--	--	--	
011679.3	6.2	1.5	16.50		3.0	3.0	168		0.25	--	--	--	--	Powdered lead of Standard Grade (FS-S). Mixture was like a thick paint paste, and never stiffened.
012979.2	7.0	1.8	18.71		4.3	1.7	100		0.30	--	--	--	--	Excessive cracks inside mold before developing enough strength to be released.

TABLE 2.4d - HEAVY PLASTER MIXTURE WITH SAND

Mixing Test	Mix Properties (by Weight)				Consistency (in.)		Time (min.)		Settle (in.)	Mechanical Properties				Remarks
	W/P	C/P	L/P	S/P	Initial	Cast	Cast	Set		E 10^3 psi)	$\sigma_{u,c}$ (psi)	$\sigma_{u,t}$ (psi)	Specific Density	
012679.1	6.2	1.5	16.50	6.0	4.3	1.4	54½	62		--	--	--	2.46	Cracked severely inside mold during oven dry.
012979.1	6.2	1.5	14.24	10.0	3.7	1.1	33	38½	None	42.3	34.1	4.53	2.29	
060779.1	7.0	1.8	15.99	12.0	3.5	0.	28		None	62.8	48.0	6.99	2.28	
061979.1	8.0	1.8	18.68	12.0	4.7	2.0	24	29		49.3	32.0	4.37	2.33	During the first twenty min. of mixing, lead particles deposited at mix bottom.
062079.1	9.0	2.0	21.40	12.0	4.7	1.9	30	41		61.1	35.0	3.88	2.39	
062079.2	10.0	2.2	24.12	12.0	4.6	3.0	63½		0.88	--	--	--	--	Cylinders just after cast was soft like jello.
062179.1	8.0	1.9	19.15	10.0	3.9	1.5	48	58		55.9	30.6	3.81	2.38	
062279.1	8.0	1.9	19.60	8.0	4.3	2.3	60	74		--	--	--	--	Cylinders were soft like paste inside mold even three days after cast.
071079.1	8.0	1.9	19.60	8.0	4.5	1.9	23	26½	None	30.6	29.0	4.49	2.29	
071079.2	9.5	2.1	22.76	12.0	4.5	4.0	30	45½	0.09	35.0	22.6	3.26	2.25	Cylinder cast was made at two different times of mixing.
						3.4	36		0.06	47.7	28.9	--	2.35	
071279.1	10.0	2.2	24.12	12.0	4.5	4.5	40		0.31	31.8	17.8	--	2.07	Cast made at four different times of mixing. Successful mold release at 1-½ hour after cast.
						4.3	50		0.25	42.3	22.6	--	2.34	
						4.0	55		0.13	55.9	26.8	--	2.39	
						4.0	59		0.06	61.2	27.9	2.95	2.35	
071379.1	9.0	2.0	22.30	8.0	4.6	4.5	42		0.16	40.6	27.1	4.08	2.35	
						4.2	48		0.13	41.6	27.1	4.07	2.38	
072479.1	10.0	2.2	24.12	12.0	4.8	4.0	38			47.9	27.9	3.61	2.34	Cast Koyna Dam section.
072779.1	10.0	2.2	24.12	12.0	4.4	4.2	46	62	0.17	--	--	--	--	Cast Koyna Dam section.
073179.1	10.0	2.2	24.12	12.0	4.4	4.0	44	54	0.06	--	--	--	--	Cast Koyna Dam section.
080379.1	10.0	2.2	24.12	12.0	4.7	3.9	25	31½	0.06	44.1	26.7	2.99	2.34	Cast Koyna Dam section

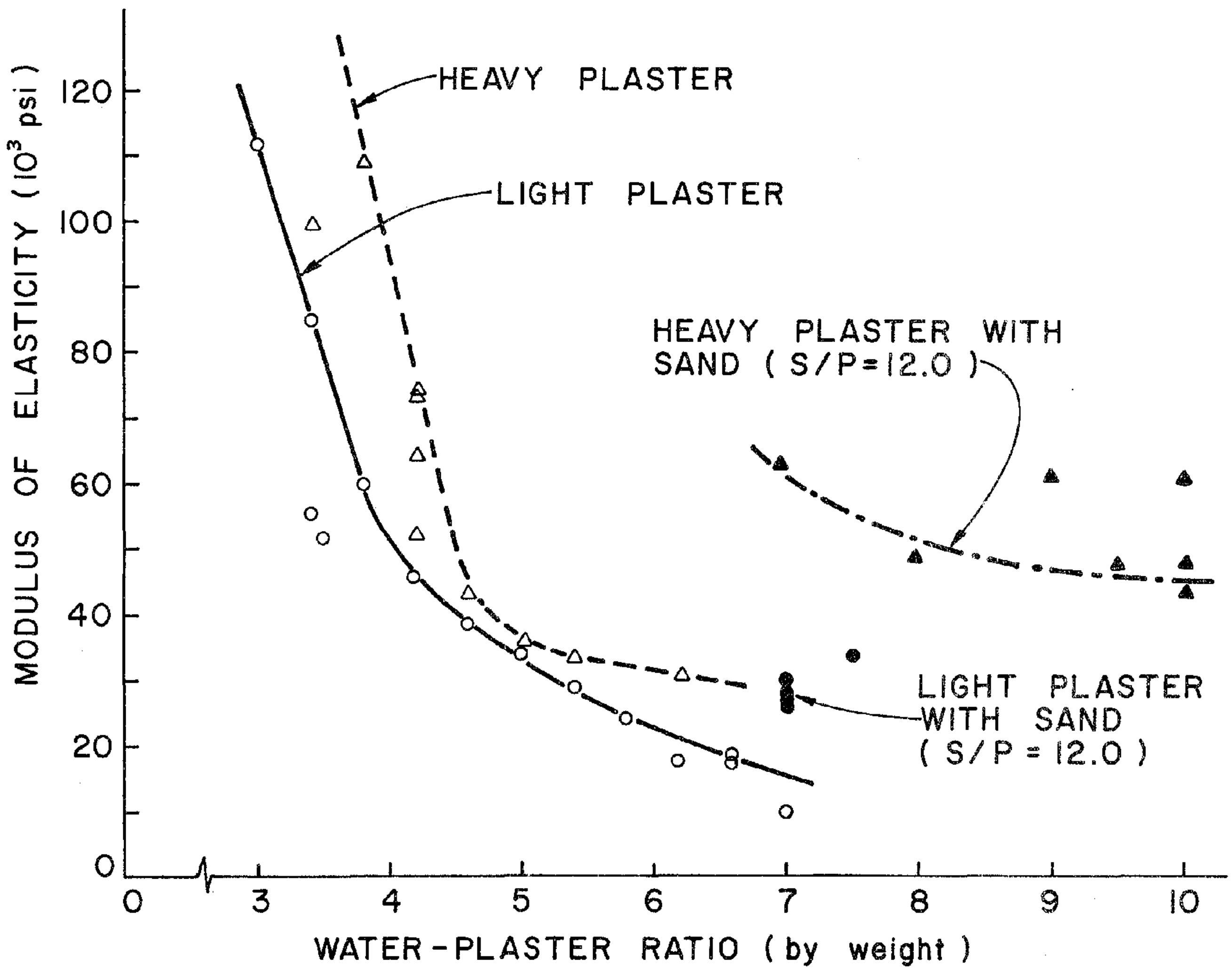

Fig. 2.1 Influence of Water/Plaster Ratio on Young's Modulus

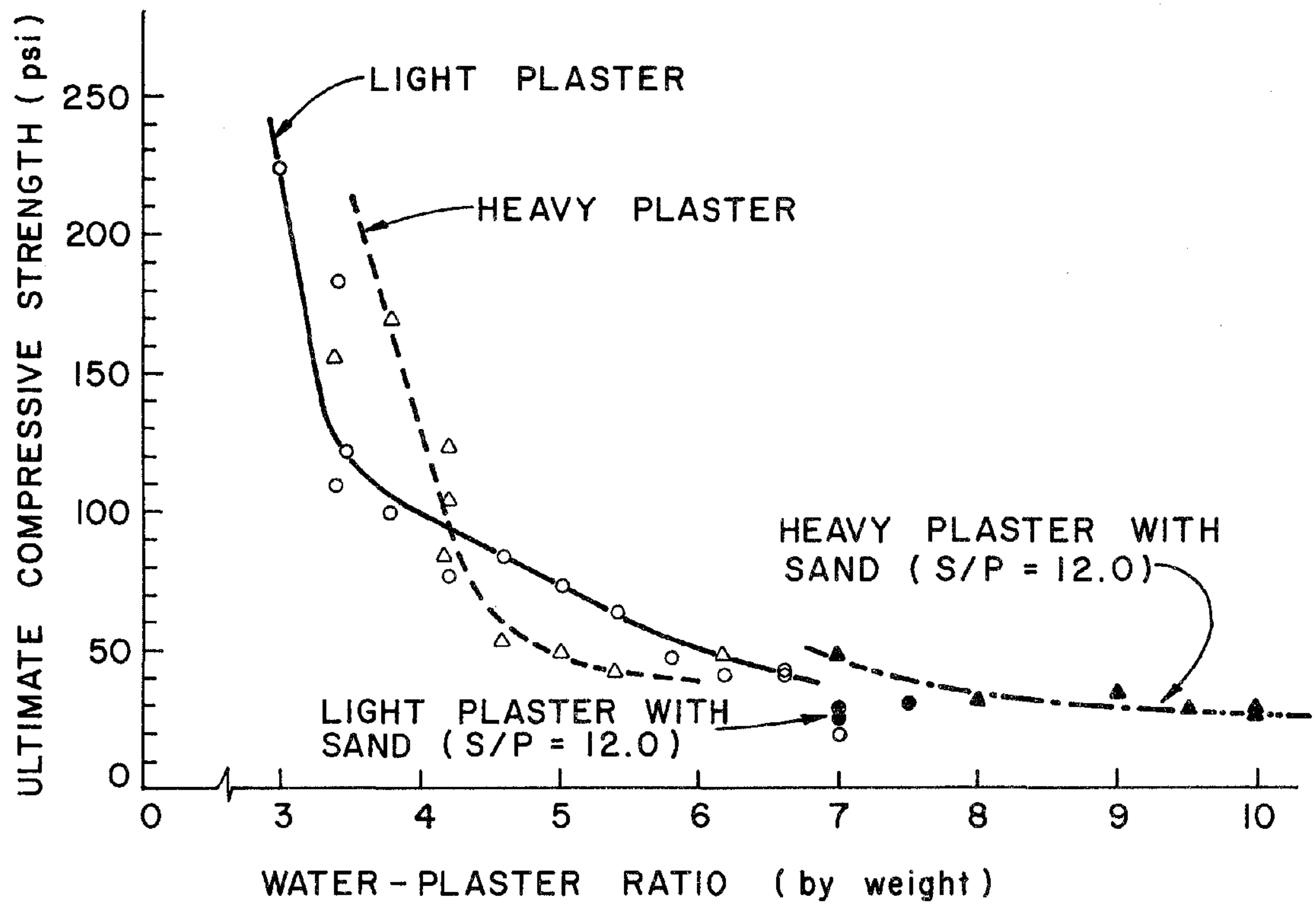

Fig. 2.2 Influence of Water/Plaster Ratio on Compressive Strength

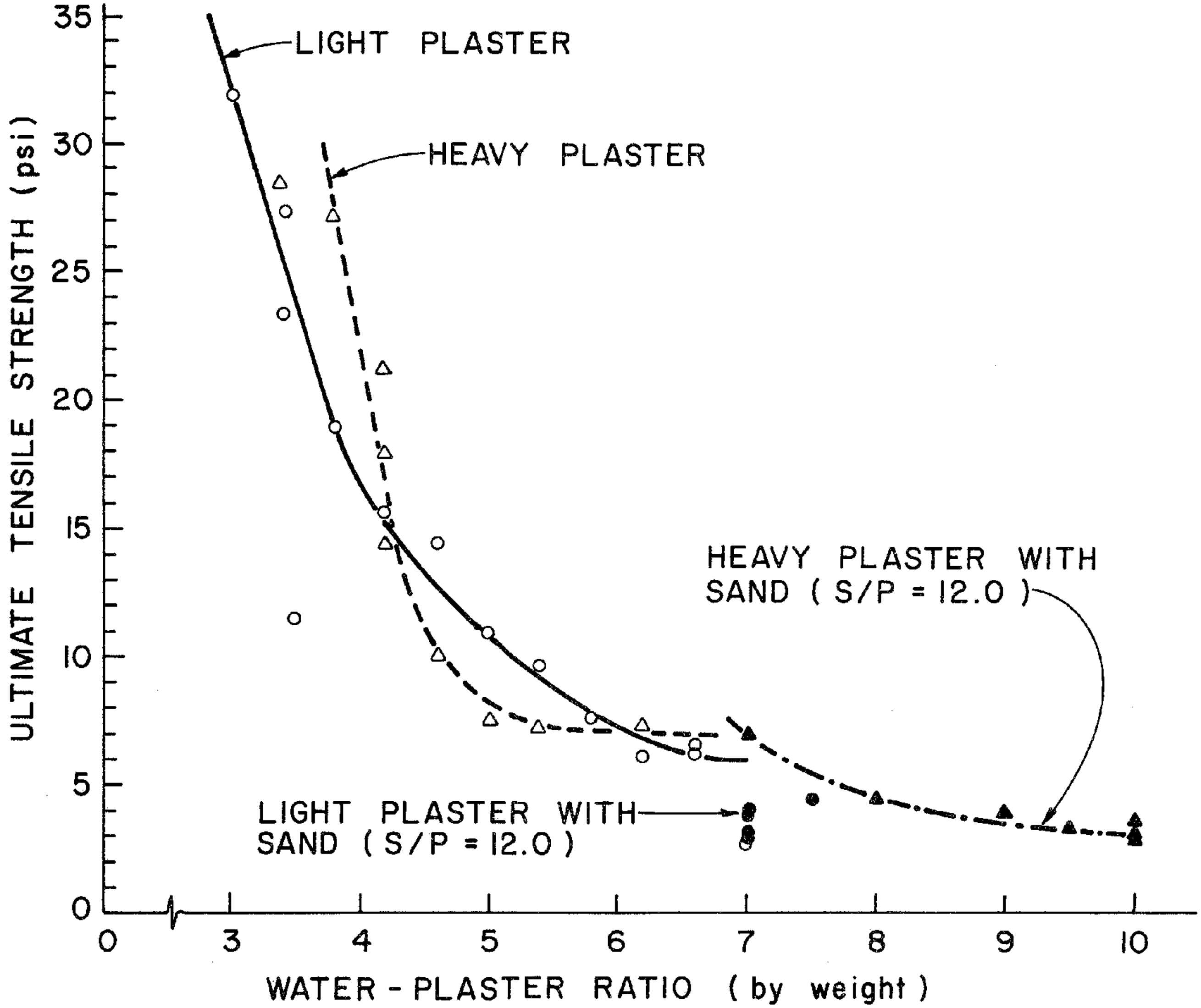

Fig. 2.3 Influence of Water/Plaster Ratio on Tensile Strength

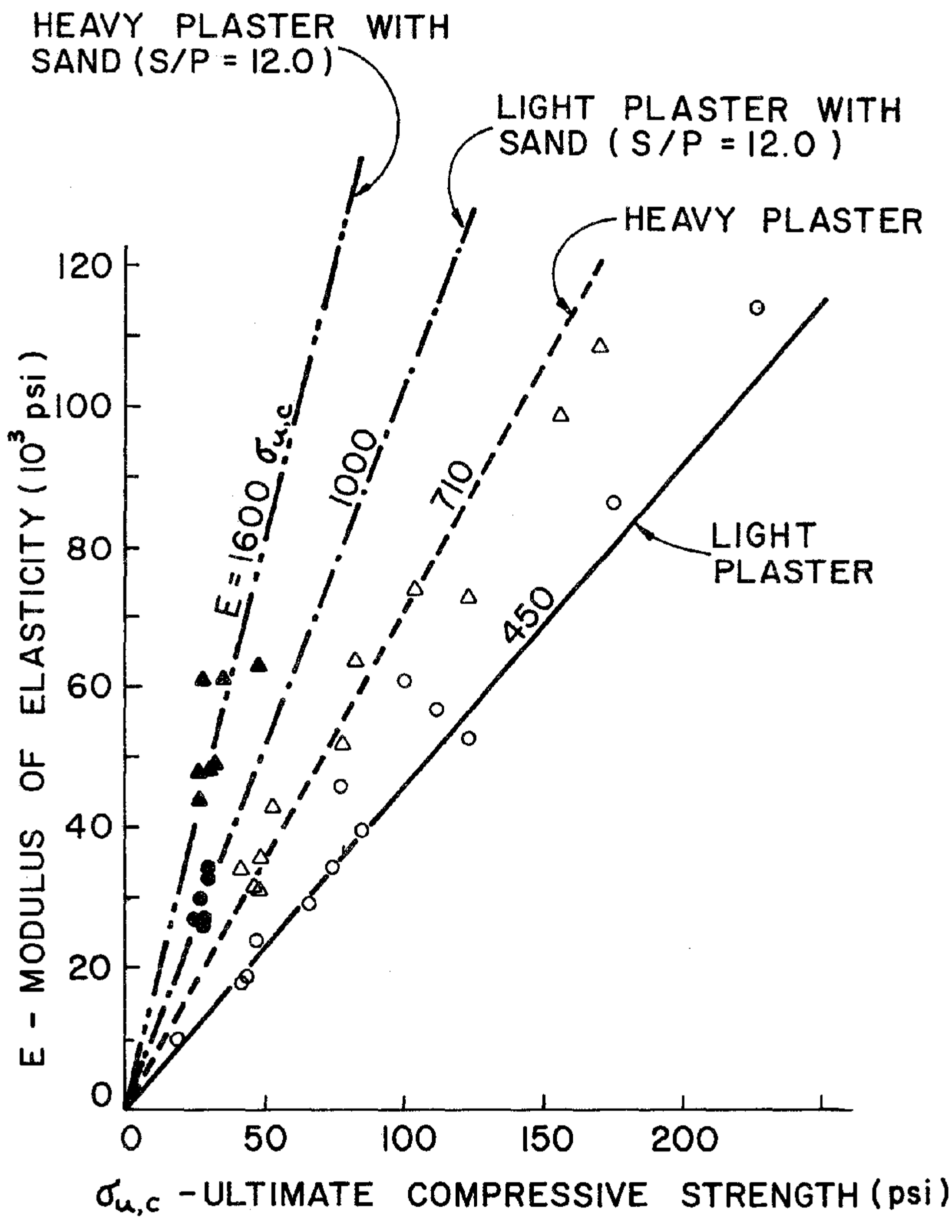

Fig. 2.4 Relation between Young's Modulus and Compressive Strength

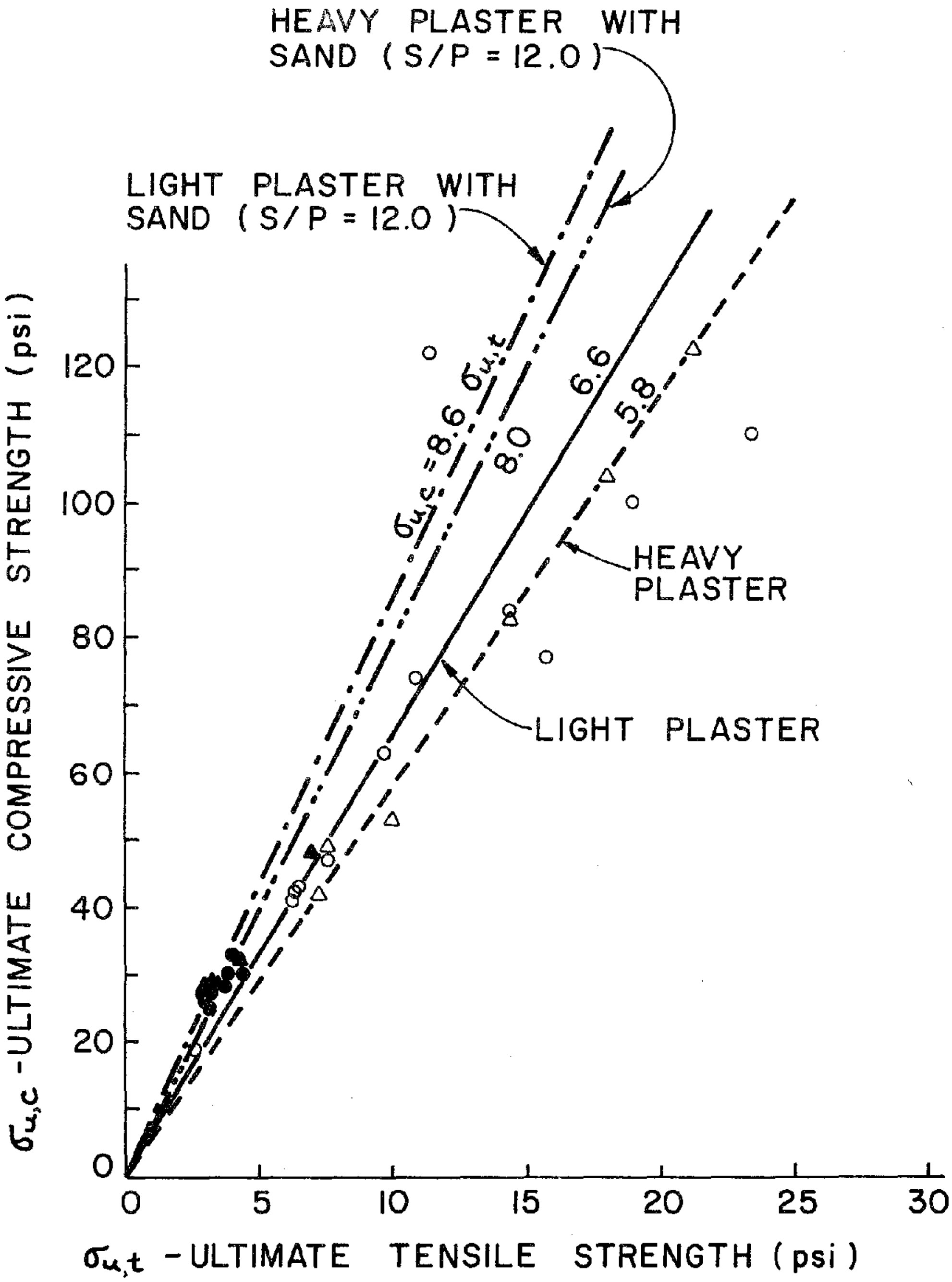

Fig. 2.5 Relation between Compressive and Tensile Strength

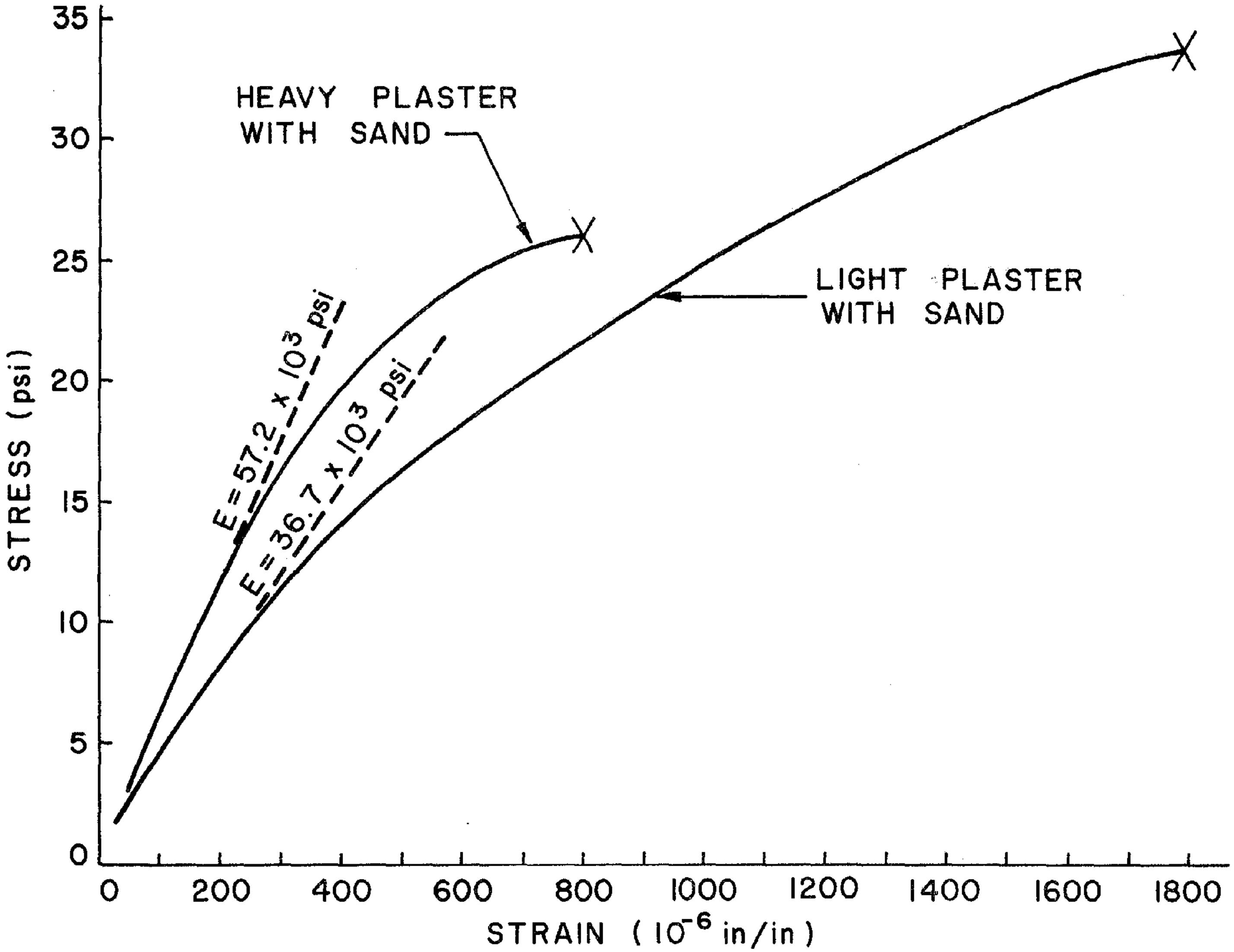

Fig. 2.6 Compressive Stress-Strain Curves for Adopted Materials

3. ARCH RIB TEST

3.1 Model Configuration

The arch rib model was designed to approximate the geometry (span, thickness, and curvature) of the Techi arch dam, Taiwan, at about the mid-height section, using a length scale of 1/150. It was constructed of a rectangular blocks cast of the light plaster with sand mixture, with edges beveled to form the arch shape. Only seven blocks were used for experimental simplicity; it is believed that this is enough to qualitatively characterize the joint opening mechanism. The dimensions of the blocks were 9 in. wide by 3-3/16 in. thick, by 13-5/16 in. long.

To conduct the tests the arch rib was assembled on the shaking table in the vertical plane, as shown in Figs. 3.1 and 3.2. In this arrangement, the dead weight of the blocks simulated the hydrostatic pressure that acts horizontally on the prototype arch rings, so lead weights were attached to the blocks to develop the desired static arch thrust. Two different amounts of weight were added in different tests, giving equivalent unit weights of the material of 151 and 227 pcf; the incremental weight was intended to approximate the dynamic "added mass" effect of the reservoir. With the model constructed in the vertical plane, vertical motions of the shaking table simulated the effect of an upstream-downstream earthquake while horizontal table motions simulated a cross-canyon earthquake.

3.2 Instrumentation

Instrumentation provided to measure the dynamic response of the model included accelerometers, oriented radially at the center of blocks

2, 4 and 6 (see Fig. 3.1), and Direct Current Differential Trans-Formers (DCDT's) measuring radial and tangential displacements at the center of each block, as well as relative "joint opening" displacements at the upper edge of each joint. In addition, strain gages were installed at three points in each block along the extrados center line: at mid-length and one inch from each end. To indicate opening of the joints, contact sensors were installed near the upper and lower edges of the blocks on adjacent faces. The photographs presented in Figure 3.3 show the DCDT's, contact sensors, and the arch rib end support.

To define the response during each test, output from sixty-nine data channels was recorded in digital form at a rate of about 100 samples per second per channel.

3.3 Test Procedure

Free vibration tests of the arch rib models were made during the first stage of testing. To excite the motion, a weight was suspended by a wire from an appropriate point on the model and was released suddenly by cutting the wire (see Fig. 3.4). Either symmetric or anti-symmetric vibration modes were induced by attaching the suspended weight at suitable locations; the first three mode shapes are plotted in Fig. 3.5. Vibration frequencies of the first three modes were 12, 24 and 38 Hz, respectively.

Earthquake excitations of the model were applied first in the vertical component alone, then in the horizontal component alone, and finally with both vertical and horizontal motions applied simultaneously. The motion used in this study was derived from the El Centro 1940 accelerogram, but was speeded up by a factor of $\sqrt{150}$ as required for model similitude. The testing in each series was started at a low intensity, and subsequent tests were made with sequentially increased accelerations. During the final biaxial input tests, the intensity of the combined motions was increased gradually until collapse occurred. The entire sequence of test cases is listed in Table 3.1.

3.4 Test Results

3.4.1 Vertical excitations

The vertical table acceleration history applied to the model in a typical test is shown in Fig. 3.6a. This vertical input excited primary the two lowest symmetric vibration modes (Fig. 3.5); the time histories of the response in these modes is shown in Fig. 3.6b and 3.6c. These modal amplitudes were derived from the radial displacements recorded at seven points on the arch, making use of the orthogonality properties of the mode shapes. Strains recorded near one end of the arch rib, shown in Fig. 3.6d, demonstrate reasonable correlation with these modal amplitudes and suggest that the response during this test (which had a peak table acceleration of 0.226 g) was essentially linear.

3.4.2 Linear response to horizontal excitation

The antisymmetrical modes of vibration excited by horizontal table motions are associated with large flexural deformations, and thus tend to induce joint openings between the arch segments. Therefore, the first horizontal input was applied at low intensity (0.039 g peak acceleration) to minimize joint opening and provide essentiallly linear response for correlation with analytical results. The time variation of the first antisymmetric mode amplitude induced by this test is shown in Fig. 3.7a; the corresponding strain history recorded near one end support of the arch is plotted in Fig. 3.7b. Again the fact that the local strain correlates well with the modal amplitude suggests that little joint opening is occurring near the end of the model.

3.4.3 Nonlinear response to horizontal excitation

The first mode response to a more intense horizontal excitation (0.152 g peak), about four times greater than that discussed above, is shown in Fig. 3.8a. Both the reduced frequency of vibration (from 12 to 8 Hz.) and the increased response relative to the input (response amplitude increased about 8 times) demonstrate that this behavior is significantly nonlinear. The occurrence of joint opening is evident in Fig. 3.8b which depicts the top surface strain of the arch adjacent to an end support; clearly the dynamic "tensile" strain in this test is limited to the amount of preexisting compressive strain induced by the dead load. Joint opening prevents the development of actual (total) tensile strains, but no such limitation is operative in the compressive direction. Motions indicated by the DCDT and the contact sensor at the same joint (Figs. 3.8c and 3.8d) provide corroboration of the joint opening response mechanism. The fact that the strain history shown in Fig. 3.8b continued after the termination of the joint opening suggests that the final stage of the response is linearly elastic.

3.4.4 Configuration of opened joint

The exact configuration of the block faces of an opened joint can not be identified directly from joint displacement or contact sensor data. A much more meaningful quantity, the "joint opening ratio", was evaluated by means of a simple data transformation. The radial, tangential and joint displacement measured at each block were transformed into the relative block rotation angle (θ) and the localized compressive deformation (C), according to the mechanism presented in Fig. 3.9.

The joint opening ratios for joints 1 and 3 during the "Moderate Intensity Horizontal Test" are shown in Fig. 3.10; joint 2 never opened in this test. It is interesting to note that at joint 1, at one end of the arch model, nearly 90 percent of the original contact area opened; thus, only ten percent of the area of the joint face carries the compressive load at this time. Thus, it is evident that intense joint opening causes greatly amplified compressive stresses in return for suppressing development of tensile stresses in an arch ring.

3.4.5 Nonlinear response to intense biaxial excitation

The first mode response to a severe biaxial excitation (0.739 g peak in horizontal direction and 0.788 g peak vertical), is shown in Fig. 3.11a. In the horizontal component alone, this is about five times greater than the input discussed above. Greatly enhanced nonlinear behavior is evident in the result. The frequency of vibration is further reduced (from 8 to 4 Hz) and the response relative to the input increased again about 1.5 times. Moreover, the shift of the modal response towards the negative direction indicates that the arch rib vibrates with a shape substantially distorted toward the up-south direction (Fig. 3.2). Strain recorded near one end support of the arch model, shown in Fig. 3.11b, indicates no significant response corresponding to intense joint opening except for the first compressive cycle. From these results it is concluded that significant joint degradation occurred at the arch end, probably due to local crushing at one edge. Subsequently, the shape of the arch became distorted, and the stress was redistributed at the support.

3.4.6 Compressive failure in arch rib

During a biaxial excitation test with peak accelerations of 1.34 g in the horizontal and 0.91 g in the vertical direction, the arch rib model collapsed as shown in Fig. 3.13. Time history responses of the strain and contact sensors at the end support of the model are shown in Figs. 3.12a and 3.12b; no displacement response was measured in this test because these instruments had been removed to protect them from damage. It is evident in these results that the model remained in place during the first two seconds of earthquake shaking (Fig. 3.6a); in spite of undergoing intense joint opening response, the collapse occurred surprisingly close to the end of excitation. This failure pattern reinforces the conclusion that significant joint degradation at one end of the arch rib model caused major distortion of shape in the up-south direction; the model stability was finally lost by a compressive failure at the end support. The photograph of Fig. 3.13 showing the debris of plaster material at the arch end support corroborates this conclusion. It should be noted that there was no indication of slip in adjacent joint faces or tensile cracking within the model prior to the collapse in compression.

3.5 Correlation With Elastic Analysis

Nonlinearities in the segmented arch rib response to severe earthquake excitation are related to recurrent opening and closing of the joints. During severe opening action, the arch rib also demonstrates substantial nonlinear degradation of the joints, leading eventually to compressive failure in the joint faces. The nonlinear computer programs at Berkeley have not yet been adapted to account for the joint opening mechanism of an arch rib, so analytical correlation cannot be made at this time with the intensely nonlinear response. However, a linearly elastic finite element model of the arch rib was subjected to the measured low and moderate intensity table accelerations to examine the analytical correlation with these responses. To match the observed vibration frequency, the elastic modulus of the mathematical model was set to 42,900 psi, about 17 percent greater than the measured tangent modulus shown on Fig. 2.6. The analytical damping ratio was set to 3 percent, as measured in free vibration tests of the model.

The analytically determined time histories of the first and second symmetric mode amplitude, and also of the strain near the end support are compared with the corresponding experimental results from the vertical acceleration test in Fig. 3.14. The correlations are good enough to verify that the behavior is essentially linear, as assumed. Correlation between analysis and experiment for the low intensity horizontal test is shown in Fig. 3.15. These results suggest that even in this minor motion the response is slightly nonlinear; both the observed displacement response amplitude and its period of vibration are somewhat greater than the analytical values. The displacement correlation for the moderate intensity test, shown in Fig. 3.16a, demonstrates much greater discrepancies in both period and amplitude. The observed strain in Fig. 3.16b, shows its significant nonlinearity by the limited tensile strain as well as intensified compressive strain. Of course, no such phenomena are demonstrated in the analytical response, because the linear mathematical model cannot duplicate the behavior of the physical model undergoing significant joint opening.

TABLE 3.1

TEST CASES OF ARCH RIB MODEL NO. 3
(Equivalent Unit Weight of 151 pcf)

Test Run	Peak Table Acceleration (g)		Remarks
	Horizontal	Vertical	
110579.01		0.060	
110579.02		0.095	
110579.03		0.226	
110579.04	0.039		
110579.05	0.068		
110579.06	0.152		
110579.07	0.157	0.238	
110579.08	0.274	0.340	
110579.09	0.561	0.517	Minor compressive damages at upper edges of joint - 1 and 3.
110579.10	0.739	0.788	Several blocks of localized damage at lower edges of joint face.
110579.11	0.983	0.944	DCDT's (for radial, tangential and joint displacement) were dismantled.
110579.12	1.344	0.908	Arch collapsed. Block 7 completely were crashed near end support of arch.

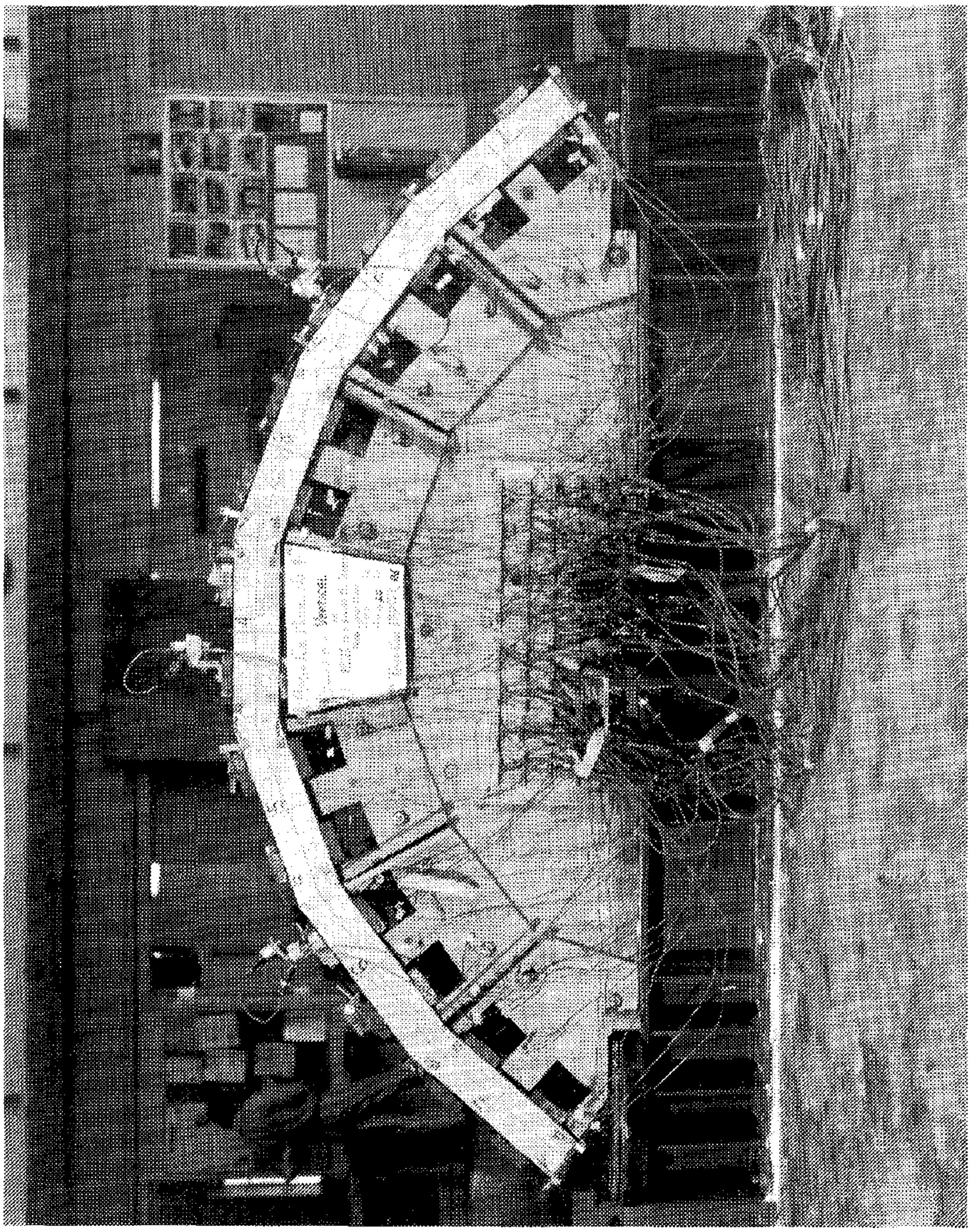

Fig. 3.1 Segmented Arch Model on Shaking Table

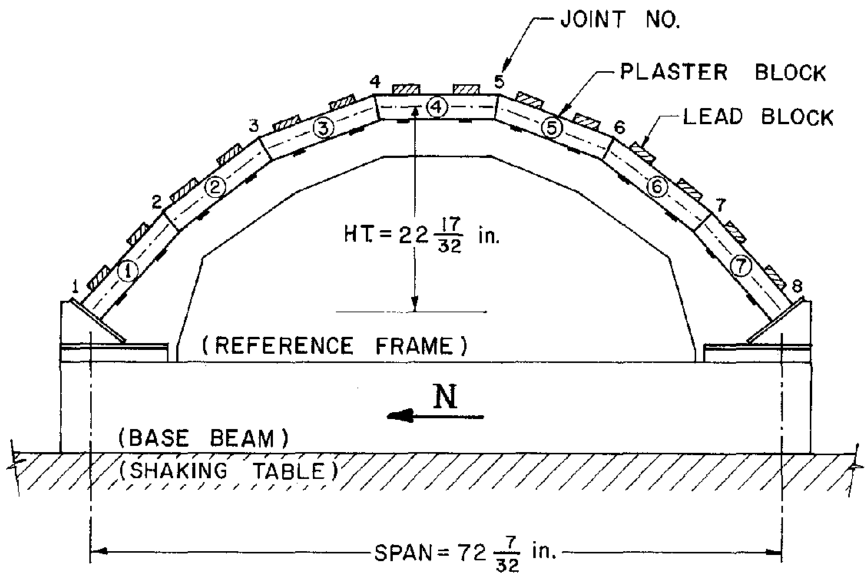

Fig. 3.2 Arrangement of Segmented Arch Model

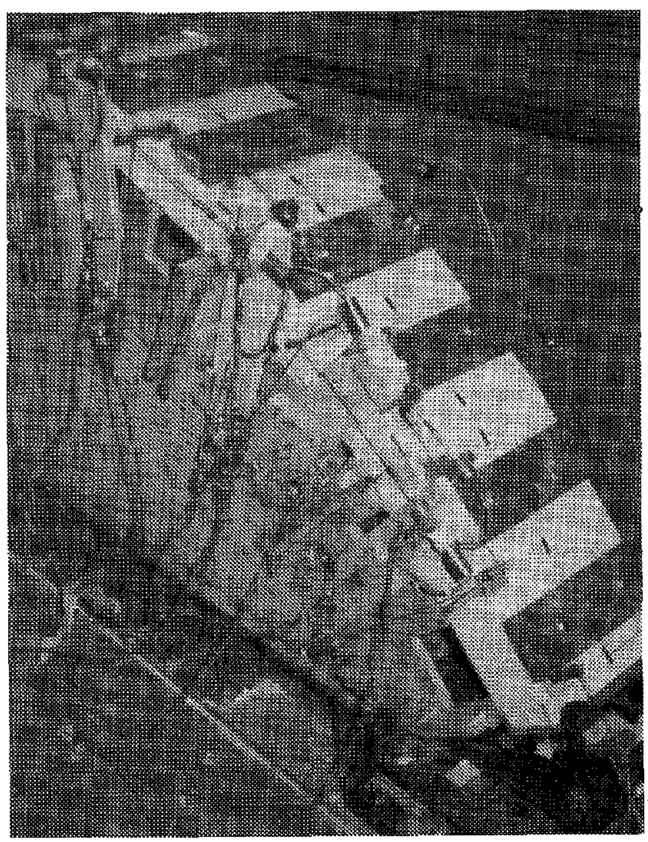

(a) View of DCDT's

Fig. 3.3 Instrumentation of Arch Model

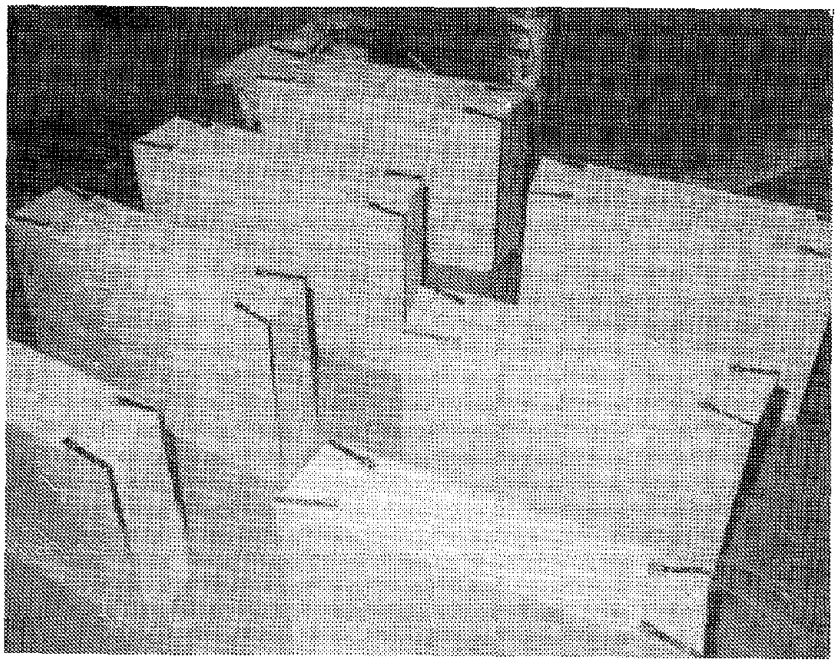

(b) Contact Sensors on Arch Rib

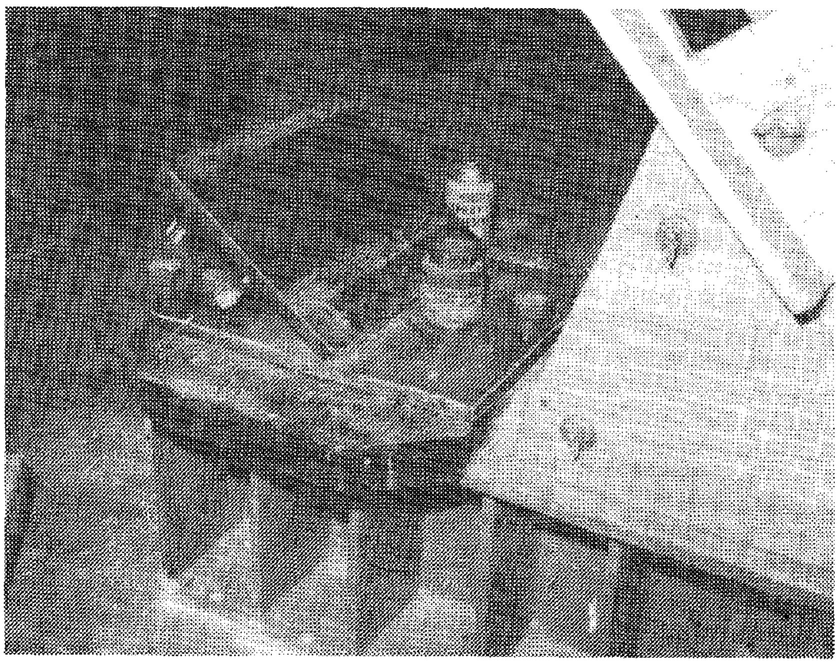

(c) End Support of Arch Model

Fig. 3.3 (Cont.) Instrumentation of Arch Model

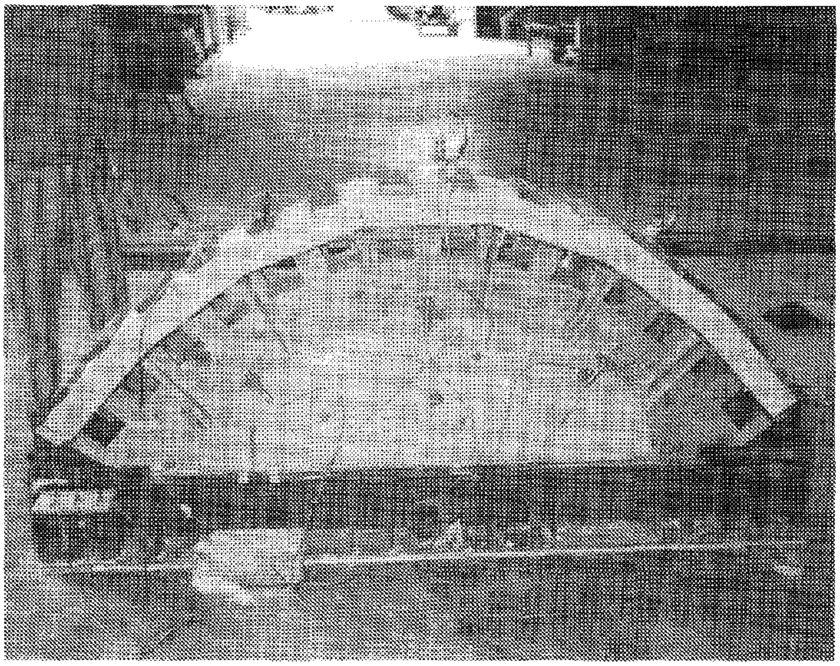

Fig. 3.4 Free Vibration Test of Arch Model

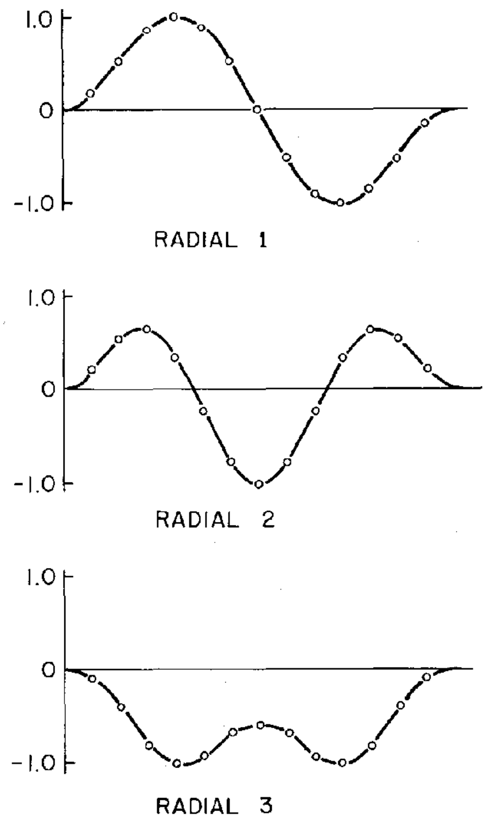

Fig. 3.5 Elastic Vibration Mode Shape of Arch Model

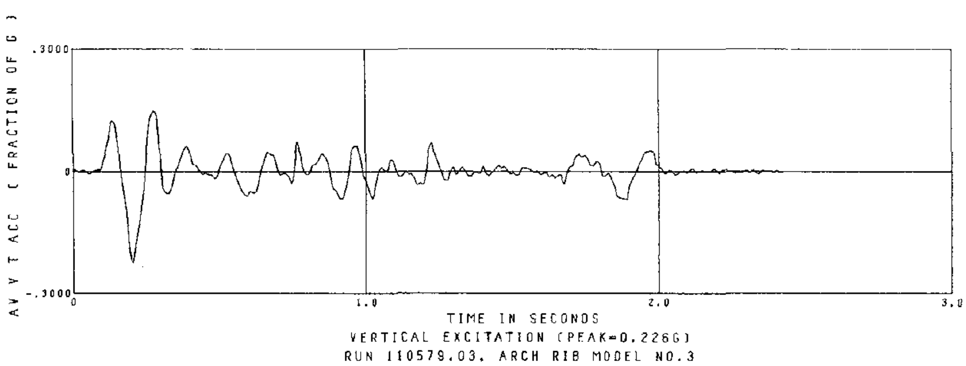

(a) Vertical Table Accelerations

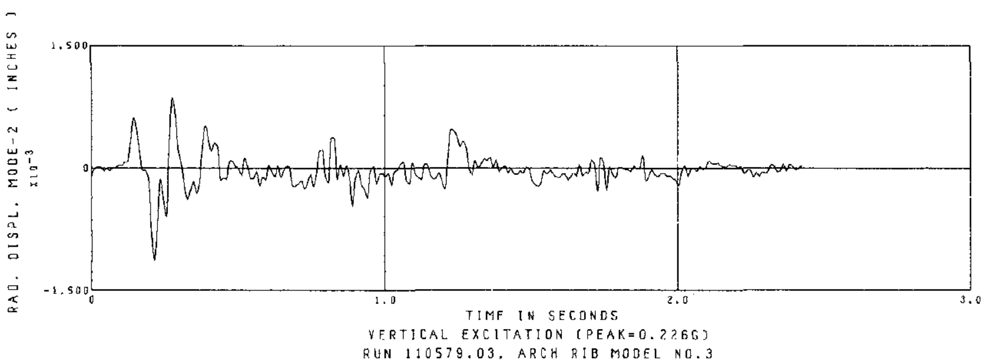

(b) First Symmetric Mode Response

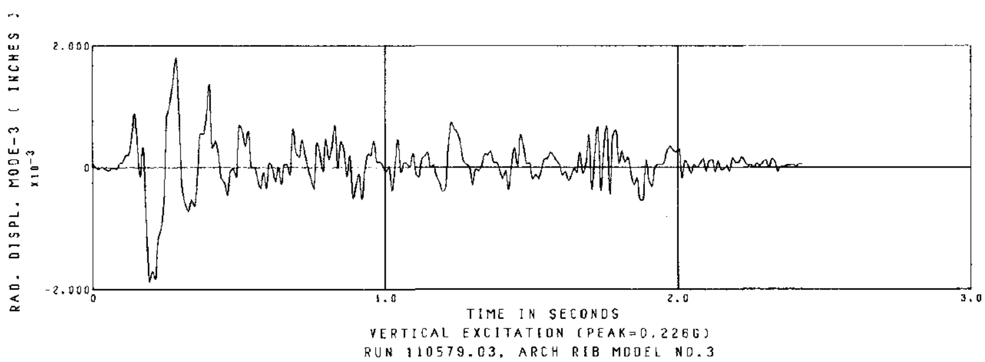

(c) Second Symmetric Mode Response

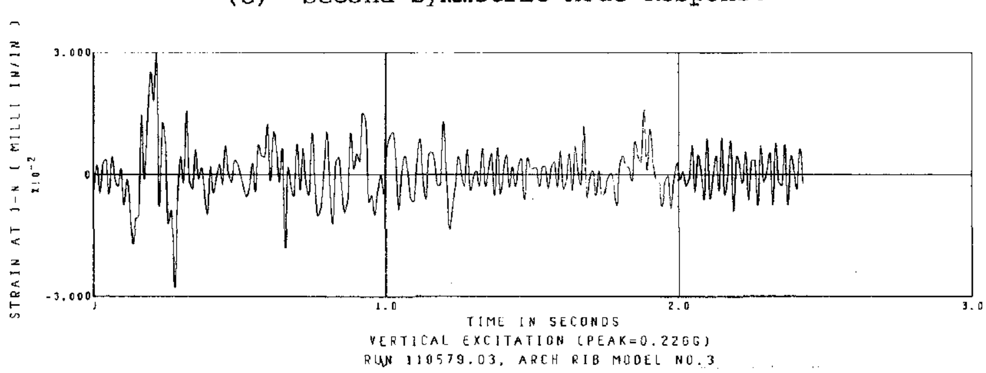

(d) Measured Strain near Support

Fig. 3.6 Vertical Excitation Test of Arch Model

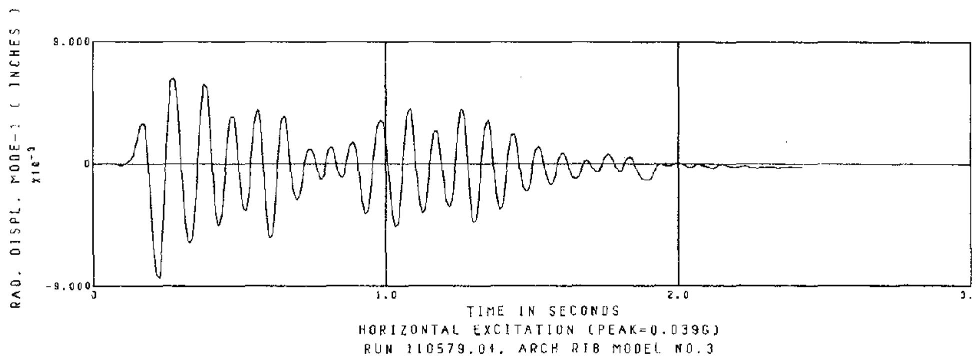

(a) First Antisymmetric Mode Response

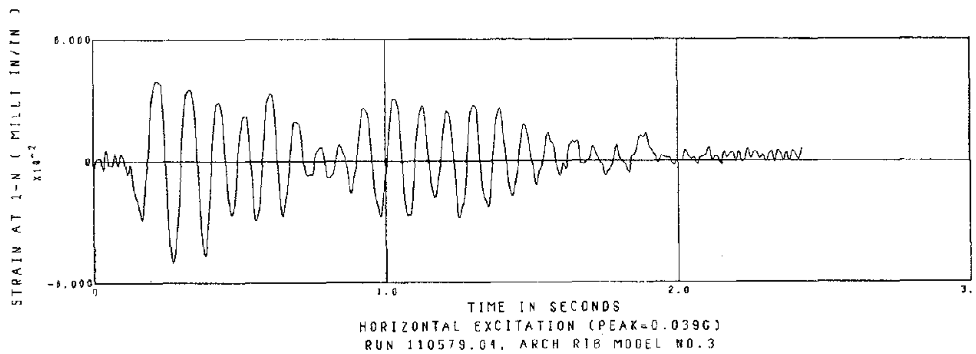

(b) Measured Strain near Support

Fig. 3.7 Low Intensity Horizontal Test of Arch Model

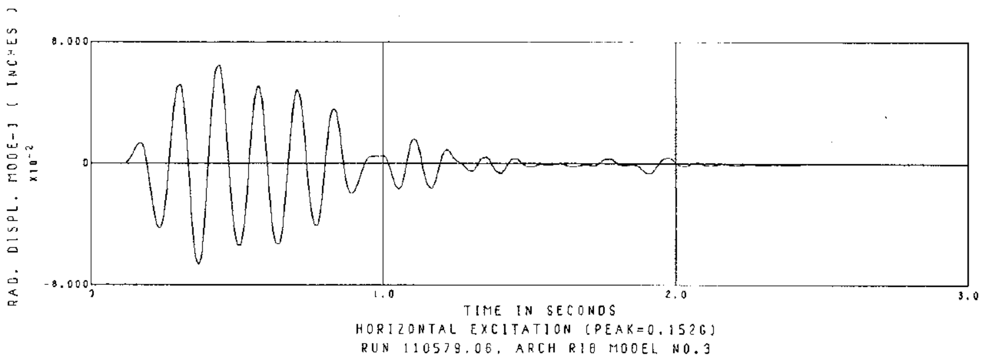

(a) First Antisymmetric Mode Response

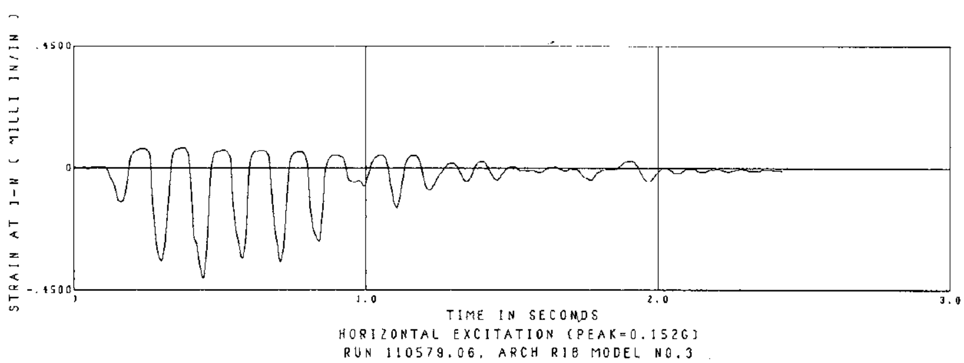

(b) Measured Strain near Support

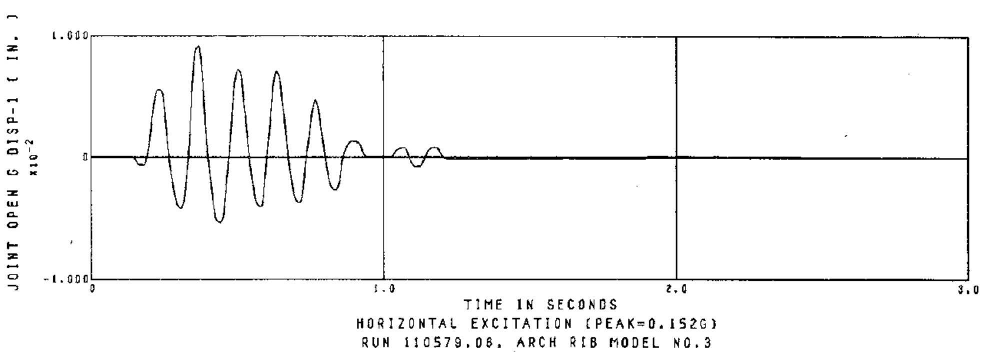

(c) Joint Motion at Support

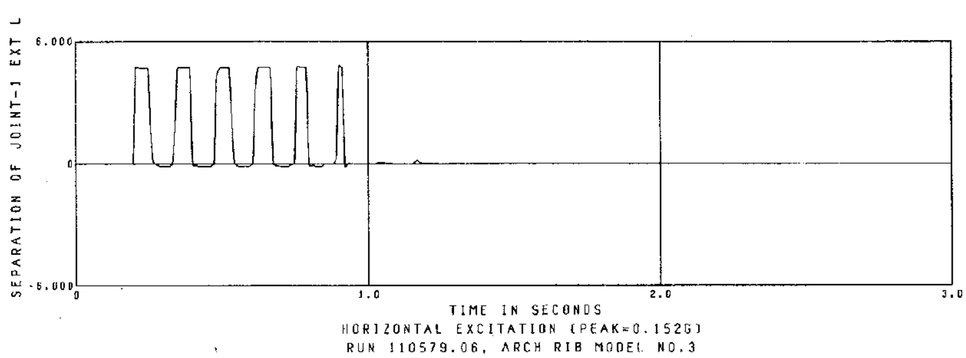

(d) Joint Opening at Support

Fig. 3.8 Moderate Intensity Horizontal Test of Arch Model

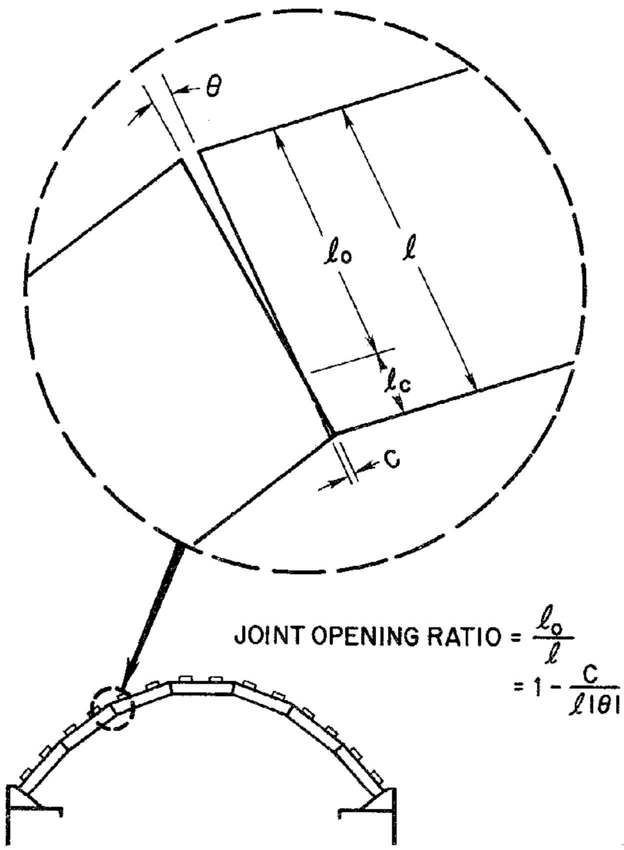

Fig. 3.9 Definition of Joint Opening in Arch Model

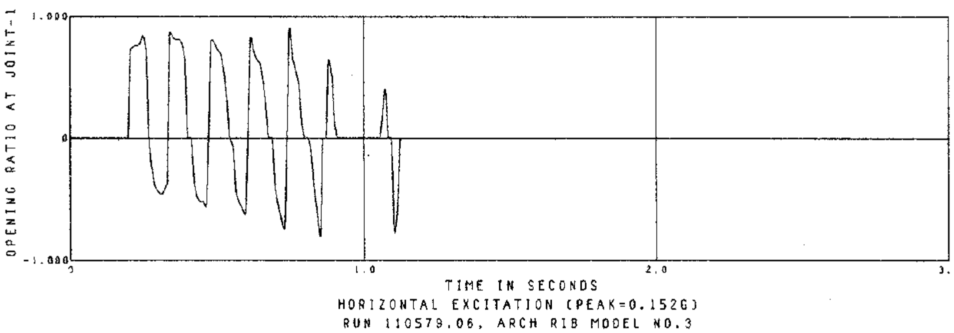

(a) Joint Opening Ratio at Support

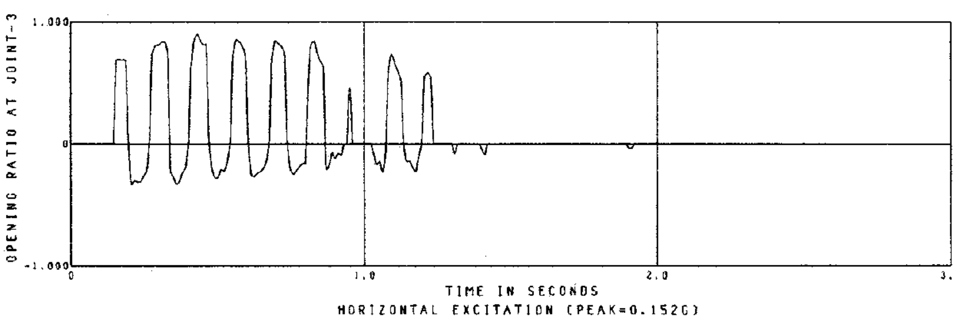

(b) Joint Opening Ratio at Joint-3

Fig. 3.10 Joint Opening Ratio of Arch Model

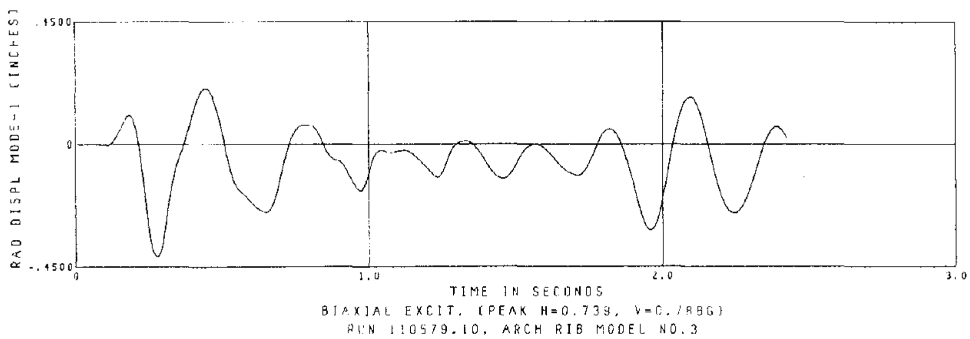

(a) First Antisymmetric Mode Response

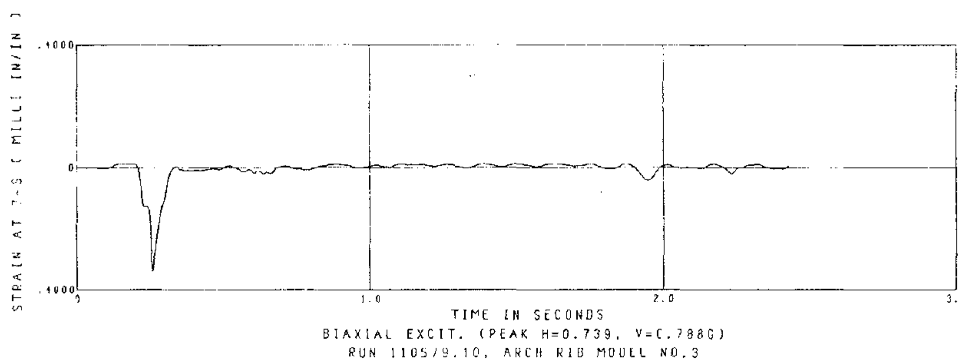

(b) Measured Strain near Support

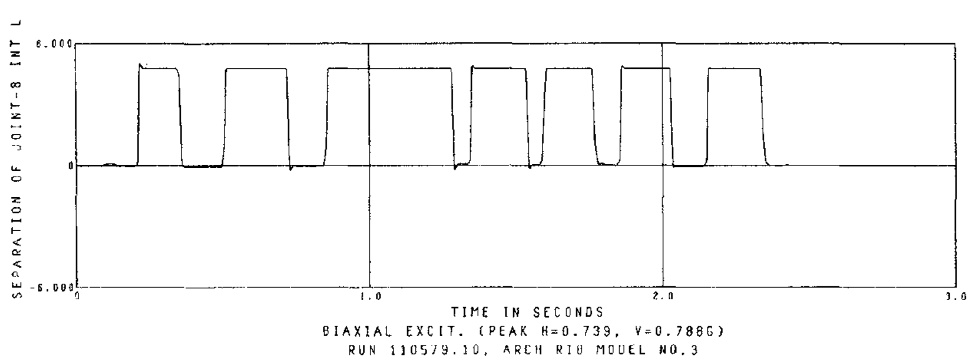

(c) Joint Opening at Support

Fig. 3.11 High Intensity Biaxial Test of Arch Model

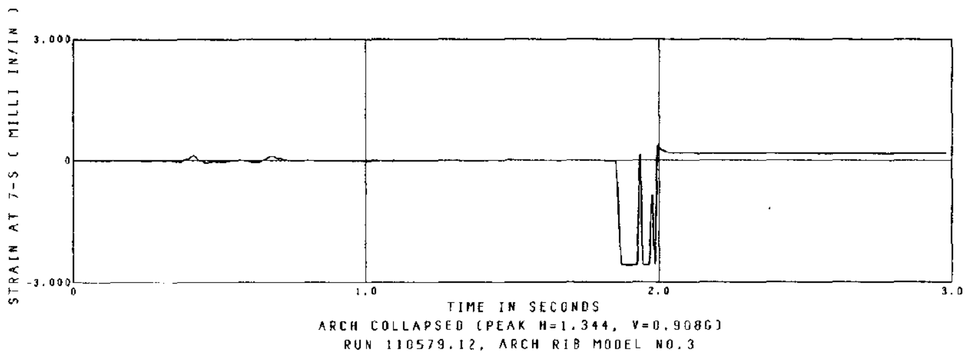

(a) Measured Strain near Support

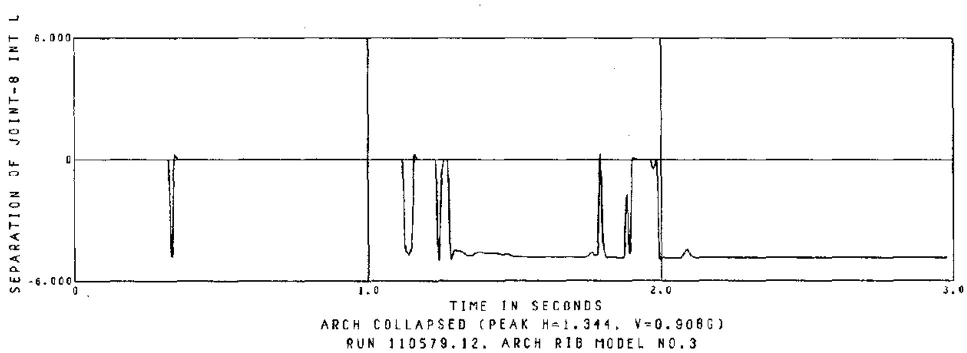

(b) Joint Opening at Support

Fig. 3.12 Collapse Test of Arch Model

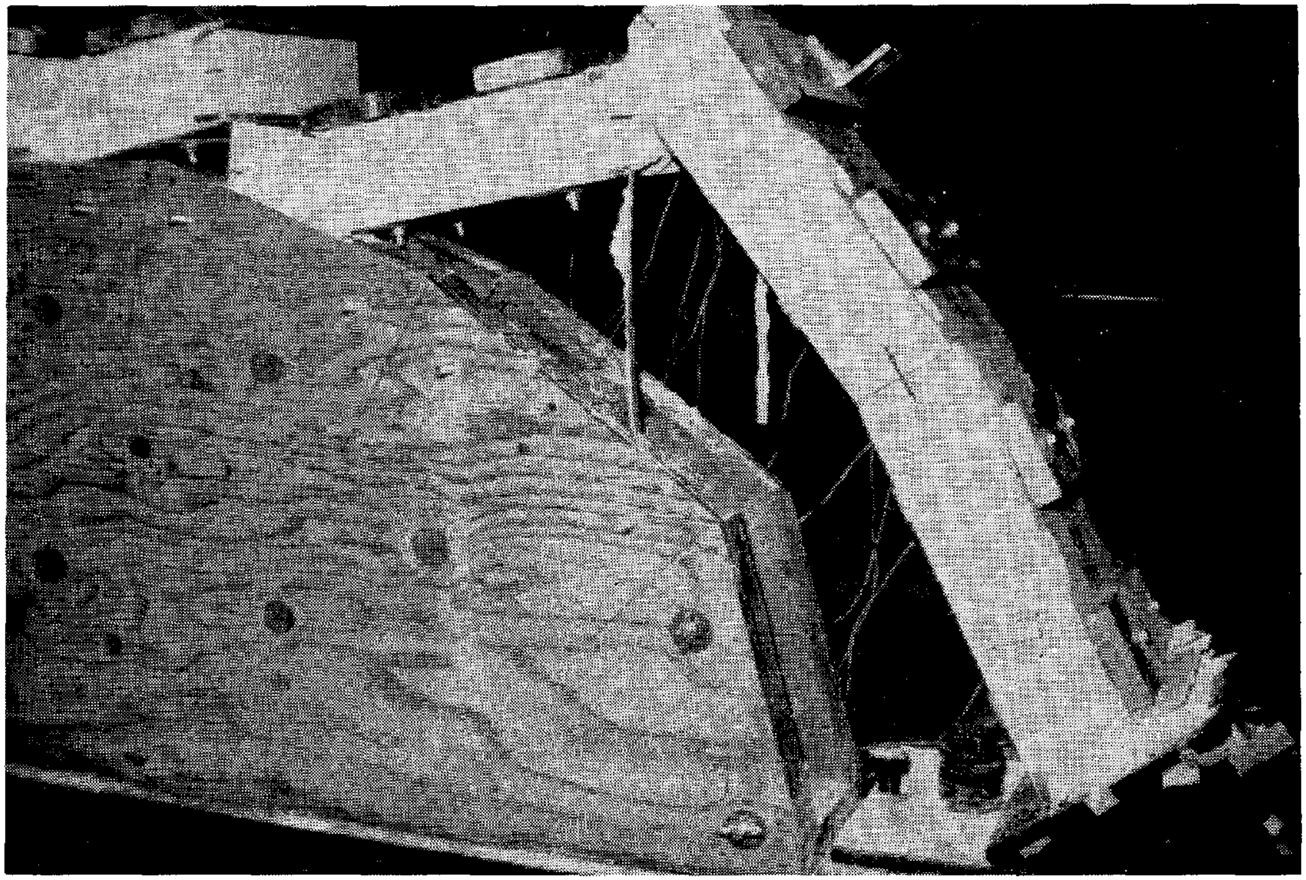

Fig. 3.13 Collapsed Arch Model - Note for débris at the right end support of arch

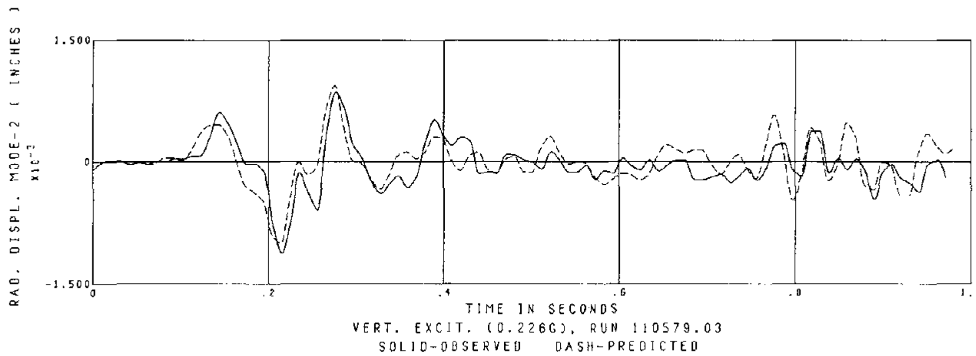

(a) First Symmetric Mode

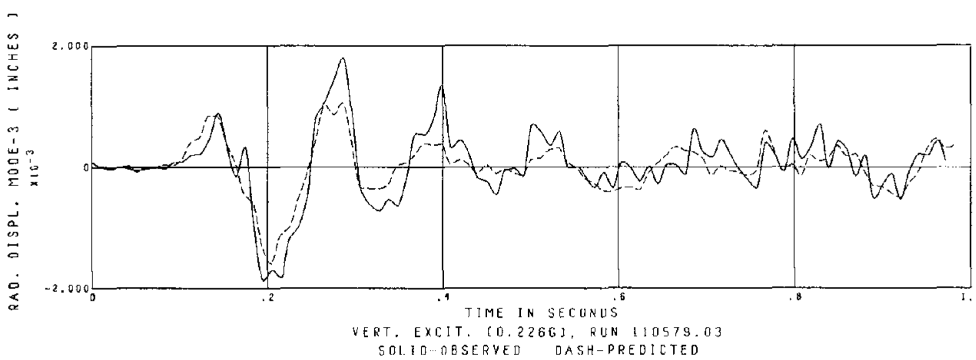

(b) Second Symmetric Mode

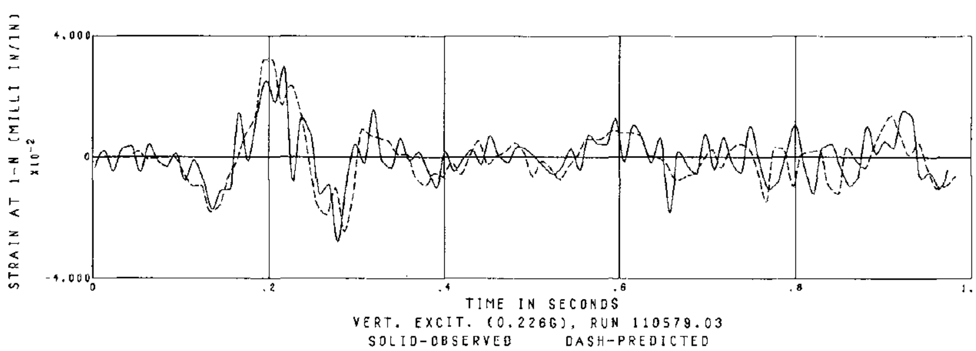

(c) Strain near Support

Fig. 3.14 Correlation in Vertical Test

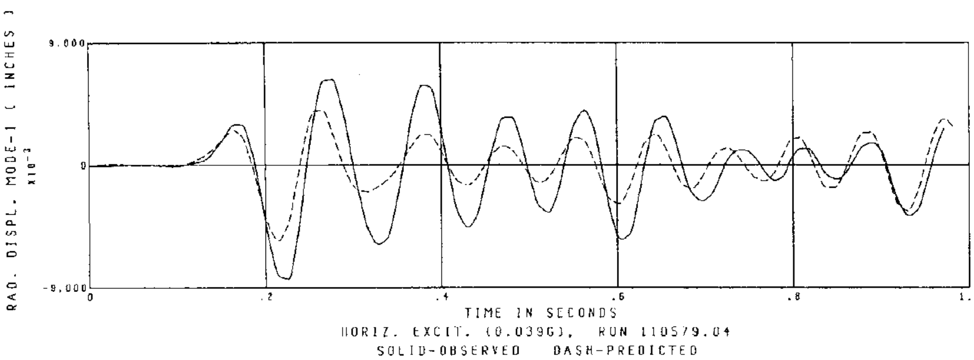

(a) First Antisymmetric Mode

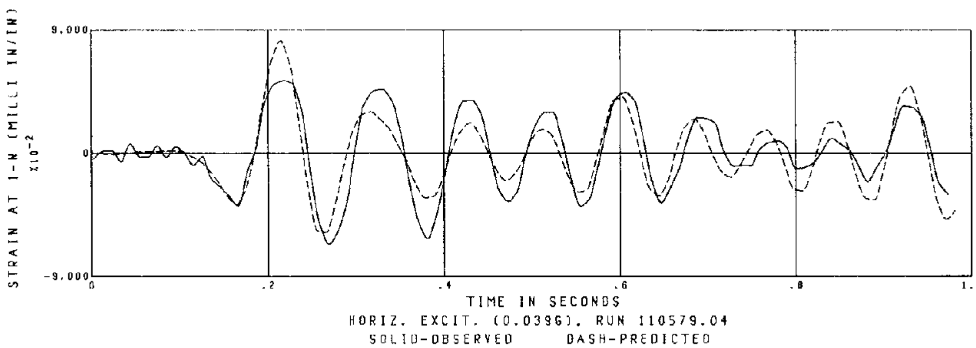

(b) Strain near Support

Fig. 3.15 Correlation in Low Intensity Horizontal Test

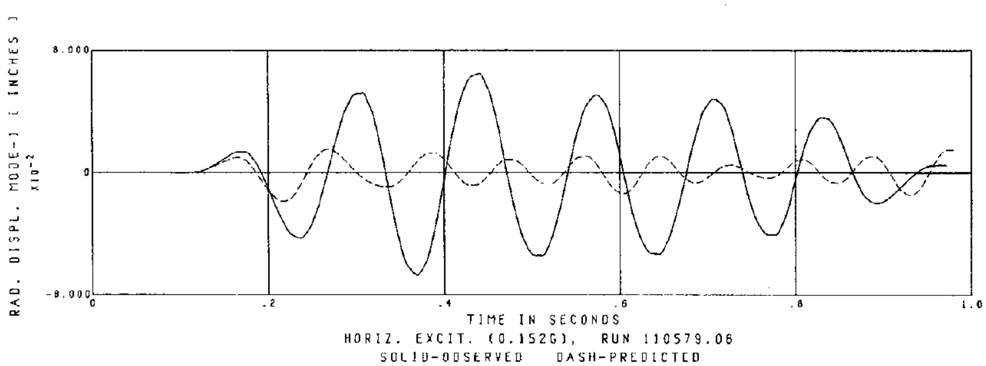

(a) First Antisymmetric Mode

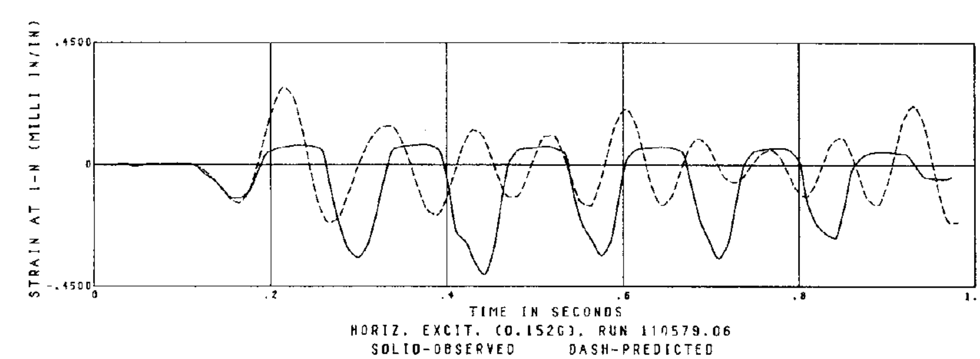

(b) Strain near Support

Fig. 3.16 Correlation in Moderate Intensity Horizontal Test

4. GRAVITY DAM SECTION TEST

4.1 Model Configuration

Although the basic purpose of this general research effort was to evaluate the seismic behavior of a concrete arch dam, a gravity dam section was selected for studying the dynamic cracking and cavitation mechanisms because an individual thin shell arch dam monolith is not suitable for resisting horizontal loads. Construction and testing of a single monolith model was considered to be essential as a preliminary step to testing of a complete arch dam model. A non-overflow section of the Koyna Dam in India was chosen because that dam suffered earthquake damage in 1966 and a seismograph record was obtained of the damaging ground motions[8]. Thus, the objective of this study was to subject a 1/150 scale section model of the Koyna Dam to the scaled base motions, and to observe its cracking and post-cracking behavior. At the same time, an investigation was made of the reservoir cavitation mechanism observed during this model test.

The model was made of the heavy plaster with sand mixture by casting at 4-inch thick section in a horizontal form in a single pour. After drying, the model was rigidly attached to the shaking table at the end of a rectangular water tank, 10 ft. long by 4-1/2 inches wide and 30 inches high. The end of the tank was sealed by a thin, plastic sheet that was supported by the face of the dam section; the plastic had negligible strength and stiffness, but protected the plaster from water. Figures 4.1 and 4.2 show the dimensions of the model, and a photograph of the model dam at the end of the plywood reservoir tank. Because of the plastic sheet at the end of reservoir, this model setup is, in fact, capable of simulating one aspect of the cavitation mechanism in a prototype reservoir. Specifically, this model exhibits response related to the recurrent separation and subsequent impact between reservoir and dam face whenever the negative dynamic pressure offsets the initial hydrostatic pressure. Figure 4.3 illustrates the concept of the cavitation mechanism in a prototype and model reservoir. It should be noted that the atmospheric pressure effect is not introduced in this model because the plastic film prevents wetting of the plaster and thus allows access of the air pressure to the upstream face. If the atmospheric pressure were permitted to act in this model response mechanism, its effect would be greatly exaggerated because the pressure would not be suitably scaled. To take proper account of the atmospheric pressure at model scale would require use of a reduced pressure chamber around the model. Lacking this capability, a lesser distortion is achieved by using the plastic film to avoid atmospheric pressure effects completely.

4.2 Instrumentation

Instrumentation provided to measure the model response included dynamic pressure gages mounted on the plywood tank wall near the face of the dam; gage 1 located at 2 in. depth, gages 2 to 5 at 5 in. depth increments and gage 6 at the bottom of the reservoir. Horizontal crest acceleration of the model was recorded by an accelerometer rigidly attached to the model top. Deflections were monitored at every one-fourth level of the dam by DCDT's mounted on a stiff reference frame at the downstream end of the model. Also, strains were measured at several locations around the level where there is an abrupt change in the downstream slope (the term "critical section" will be used hereafter in this report in reference to this level) and at the dam base.

Two types of wire gage with paper backing were used: single component gages 0.812 in. long and rosettes of 0.750 in. gage length. Strain gages of these sizes were deemed suitable for accurate strain measurement. Figure 4.4 shows the strain gage locations.

Each of these tranducers in addition to the shaking table instrumentation, a total of 46 channels, was sampled at a rate of about 150 samples per second to define the response during each test.

4.3 Test Procedure

Frequency sweep tests of the model dam were made during the first stage of testing. The sinusoidal excitation was gradually varied in frequency in order to identify the model fundamental frequency with and without reservoir water; the frequency response functions showing the ratio of measured top to base acceleration are plotted in Fig. 4.5. The results from these tests were particularly useful for the construction of an artificial excitation signal.

Although the original test plan was to subject the gravity dam model to the scaled Koyna base motions, a simulated earthquake excitation signal was employed in this test. The actual shaking table motion produced by the time scaled Koyna displacement signal (speeded up by a factor of $\sqrt{150}$) did not simulate the true time scaled earthquake because the shaking table excitation system greatly attenuated the amplitude for frequencies higher than 16 Hz. Thus, a simulated earthquake displacement signal containing amplified frequency components close to the model fundamental frequency was applied instead, in order to generate a large amplification response in the model. This artificial earthquake was a combination of harmonic motions, with frequencies of 6, 20 and 33 Hz. These harmonics were applied with intensity increasing linearly for one second, constant for one second and then decreasing linearly for one second. Figure 4.6 shows the table displacements and accelerations produced by this artificial signal. Figure 4.7 is the velocity response spectrum of this motion.

Earthquake tests were started with a very low intensity signal, then the intensity of the signal was increased by increments up to cracking of the model. Simulated earthquake accelerations with a peak value about equal to the acceleration of gravity induced cracking of the model very similar to that observed at Koyna. As a final test, a similar intensity shaking was applied to the cracked dam, simulating an "aftershock" situation to demonstrate the post-cracking stability of the dam.

Table 4.1 lists all the tests of the model, with excitation intensity and some remarks recorded during the tests.

4.4 Test Results

4.4.1 Linear elastic response to low intensity excitation

The time history of crest acceleration and displacement, dynamic pressure at the base, and strain near the critical section, recorded in a test of 0.156 g peak acceleration, are shown in Fig. 4.8. These results, showing nearly perfect correlation with each other, clearly indicate the linear elastic response behavior of the model when subjected to low intensity excitation. It should be noted that the model responds in its first mode of vibration at 33 Hz in strong correlation with the highest frequency component of the excitation signal (Fig. 4.7); there is no indication of second or higher mode response in the response.

4.4.2 Cavitation response

Cavitation occurs in a prototype reservoir when the pressure in the water is reduced to the vapor pressure, 0.363 psi absolute at $70^{\circ}F$. In this model test, however, the plastic film allowed air pressure to act on the dam face; hence, a simulated cavitation mechanism was induced when the negative dynamic pressure equaled the hydrostatic pressure. This phenomonen occurred in these model tests for excitation intensity above moderate level (0.225 g peak acceleration). In fact, during the test of 0.441 g peak acceleration, direct evidence of this impact mechanism first was observed by emission of smoke-like dust from the face of the model. It was evident that the surface of the plaster model was being abraded by the recurrent impact action during the test. Time histories of the dynamic pressures measured in this test are shown in Fig. 4.10. The cavitation response is evidenced in the results by the biased response toward the positive direction; pressure changes in the negative direction were cut-off at the hydrostatic pressure level. It will be noted in Fig. 4.9 that the pressure response to low intensity shaking (0.156 g peak) does not indicate such distortions. The results for the much more intense test (1.210 g peak) in Fig. 4.11 demonstrate the cavitation region extending to below half the reservoir depth.

The influence of the cavitation phenomenon on the dynamic pressure response is much more evident in Fig. 4.12, which shows extreme values of dynamic pressure at several depths below the surface in each test, plotted as a function of peak base acceleration. The negative peak pressure in the results at all location demonstrates a definite tendency to level-off at about the amplitude of hydrostatic pressure for each depth.

A trend curve of dynamic pressure distribution along the dam height was constructed at every time step in each test, using a parabolic fairing technique with the set of pressures measured at several depths below the surface (see Fig. 4.14 for an example of the calculated pressure distribution). Then, the dynamic pressure over the entire area of the dam upstream face was integrated by Simpson's rule to obtain a time history of "resultant pressure force". The extreme value of this force in each test is shown in Fig. 4.13a, plotted as a function of peak base acceleration. The result indicates a significant difference in the positive and negative peaks in each test. Specifically, in the test of 1.08 g peak acceleration, the negative resultant pressure force was close to its maximum limit of 53 lbs, which represents the hydrostatic pressure force.

To evaluate the total shearing force acting over the base section (1-1/4 in. above the base), a data reduction technique similar to that described above was applied for a set of shearing strain measured at this level. Figure 4.13b shows its extreme values in each test plotted as a function of peak base acceleration. A significant difference in the positive and negative response is evident in the results for tests with base acceleration peaks above 0.8 g, showing the influence of the biased dynamic pressure loading on the model.

For a detailed evaluation of the cavitation mechanism, isometric plots of the dynamic pressure together with the corresponding dam deflection response were found to be most suitable. The dynamic pressure distribution along the height of the dam face and its variation with time are shown in the upper part of Fig. 4.14a, for a selected interval during a low intensity test (0.156 g peak acceleration).

The lower part of this figure shows the deflection of the dam section relative to its base. The results of this "non-cavitational" test demonstrate that the dynamic pressure profile is nearly identical in each time increment, and also that the pressure variation is in strong correlation with the dam deflection; the deformation towards upstream direction coincides with negative dynamic pressure, and the downstream displacement is concurrent with positive dynamic pressure.

The corresponding plots for the most intense shaking test (1.21 g peak acceleration) are shown in Fig. 4.14b. At each of the time-slice grids, the hydrostatic pressure level is indicated by a dotted line on the negative side. The dynamic pressure profile and the time variation in this test are quite different from those discussed above for the non-cavitational test. The pressure response at the upper part of reservoir is quite erratic even before the dam cracking at time 1.1693 sec; of course, pressure in this region becomes more correlated with the rocking motion of the top profile of the dam after cracking. Of particular importance in this plot is a definite indication of "impact action" caused by the separated reservoir subsequently coming back in contact with dam face. The sudden appearance of positive pressure above 7 in. depth of reservoir from time 1.0886 sec. to 1.0954 sec. in the excitation history is one such example. It is believed that such "top heavy" pressure response would create a local bending of the upper section of dam, and significantly contribute to the initiation of tensile cracking at these location. Suppression of negative dynamic pressure above the hydrostatic level is also demonstrated in the results for this prominent cavitational test. The negative pressure profile is strictly confined within the dotted line marking the hydrostatic level.

The response tendency of the crest acceleration and displacement shown in Figs. 4.15a and 4.15b reflect the cavitation effect in a "global" sense; a relative reduction is seen in the upstream response due to the limited dynamic negative pressure. A similar cavitation effect is also evident in the vertical strain at the dam base, which is shown in Fig. 4.15d. A relative reduction in the tensile response at the dam base near the downstream face correlates to the dam deflection biased downstream. The vertical strain measured at the downstream side of the critical section, shown in Fig. 4.15c, has quite a different character. The result does not indicate any influence of a relative reduction in the upstream response causing similar reduction in tension at this location; on the contrary, the tensile peaks exceed the compressive peaks at all levels of excitation intensity, except for the non-cavitational test at 0.156 g peak acceleration. It is evident that the second or higher displacement mode response was excited "locally" in the upper part of the dam due to the cavitational impact.

4.4.3 Cracking response

The model cracked in a manner very similar to that observed at Koyna Dam during a simulated earthquake test with a peak value of 1.21 g (see Fig. 4.18). The time history of crest acceleration and displacement, dynamic pressure at the base, and strain near the critical section, recorded in this cracking test are shown in Fig. 4.16. The cracking was initiated by tensile failure at the downstream edge of the critical section at 1.17 sec., and propagated through to the upstream face in one swing of the dam deflection. The comparison of the crest displacement history in this test (Fig. 4.16b) with the corresponding results in the low intensity shaking test (Fig. 4.8b) reveals the marked influence of cracking on the dam response behavior. After cracking, the part of the dam above the cracked section was excited into a prominent rocking motion. The rocking response is strongly correlated with the 6 Hz component of the simulated earthquake motion (Fig. 4.6a), and the response amplitude relative to the input acceleration intensity was increased by a factor of twenty from the "linear elastic" test. The history of pressure at the dam base, which is shown in Fig. 4.16c, also indicates the 6 Hz rocking effect superimposed on the 33 Hz elastic vibration response. It should be noted that a similar 6 Hz response in the result before the cracking at 1.17 sec. is related to the reservoir cavitation effect: the reservoir separation and impact action was greatly influenced by that frequency component of the simulated earthquake signal. The most significant phenomenon demonstrated in this test is that the upper part of the dam section continued to retain the reservoir, even though it was completely severed from the lower part: the stabilizing effect of the gravitational force acting on the upper part of the dam was very important in preventing overturning of the top profile.

4.4.4 Post-cracking response

Subsequent to the cracking test described above, a similar intensity shaking was applied to the cracked dam. The response obtained in this "aftershock" test is shown in Fig. 4.17. The crest acceleration and displacement histories, shown in Fig. 4.17a and 4.17b, indicate that the top profile of the dam above the cracked section was excited into the same type of rocking motions as observed in the "cracking test". A motion picture taken during this test showed that some damages were developed at the downstream edge of the cracked section by impact action due to the rocking motion (see Fig. 4.19). The cracked dam section, however, continued to retain its reservoir during and after the severe aftershock test. It is evident that the cracked dam is a stable structure, as was demonstrated analytically many years ago by Dr. Jai Krishna[8].

4.5 Correlation With Elastic Analysis

At present, no analytical procedure is capable of realistically considering the cracking and cavitation effects observed in the gravity dam response. However, to demonstrate the limitations of a simple elastic analysis, the response observed in two test cases (the low intensity shaking and the cracking tests) have been compared with the predicted response obtained from linear elastic finite element analysis including hydrodynamic interaction[5].

Figures 4.20 and 4.21 present comparisons of the observed and predicted time histories of crest displacement and strain near the critical section, in the low intensity shaking test (0.156 g peak acceleration) and the severe shaking test (1.210 g peak acceleration), respectively. Figure 4.20 demonstrates reasonably close correlation between the observed and predicted responses in the low intensity shaking. Of course, such relatively good agreement between the observed and predicted responses was expected because the model response in this low intensity test was "linearly elastic", as assumed in the analysis.

Referring to Fig. 4.21, it is seen that there is no consistent relationship between the observed and predicted response peaks and frequencies in this intense shaking test. The observed crest displacement (Fig. 4.21a) demonstrates a prominent vibration response with substantially reduced frequency, and the predicted response differs considerably from the observed. These discrepancies are due mainly to the cracking of the dam, which was not considered in the linear elastic analysis.

A similar comparison between the observed and predicted response for a hydrostatic test is shown in Fig. 4.22. The response in this case is due to filling of the reservoir. Close agreement between the observed and predicted crest deflection is seen in Fig. 4.22a. The correlation for the strains observed at two levels is seen in Fig. 4.22b to be not as good as that for the deflection. The difference between the observed and the predicted result is particularly big for strains at the downstream face. Of course, strain gages of nearly one-inch length cannot accurately measure any strain concentration, but also the predicted strain might be exaggerated by numerical inaccuracy at the level where the downstream slope changes abruptly.

TABLE 4.1

TEST CASES OF KOYNA MODEL NO. 3
(27" Water Depth)

Test Run	Peak Base Acceleration (g)	$\frac{\text{Crest Accel.}}{\text{Base Accel.}}$ Amplification	Remarks
280879.04	0.075	3.4	
280879.05	0.156	3.2	
280879.09	0.235	3.5	
280879.10	0.441	3.5	Cavitation Appeared. White smoke emitted from the upstream face.
280879.11	0.610	3.0	
280879.12	0.794	2.8	
280879.13	0.929	2.9	
280879.14	1.082	3.0	
280879.15	1.210	2.8	Crack developed from downstream face.
280879.16	1.218	2.4	"After Shock" test for cracked model.

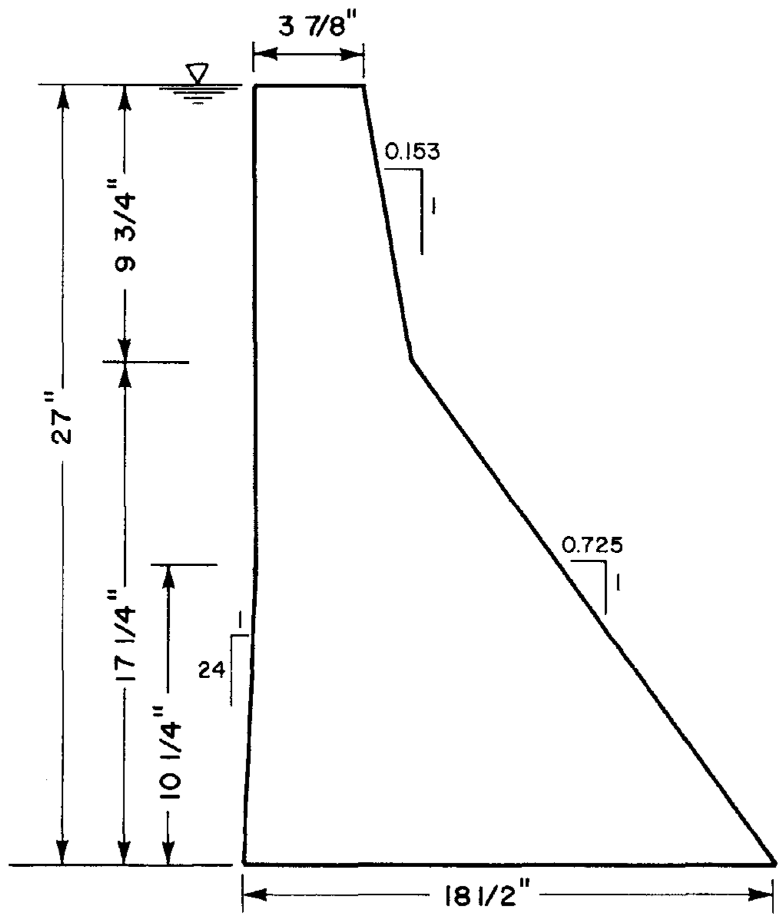

Fig. 4.1 Geometry of Koyna Dam Model

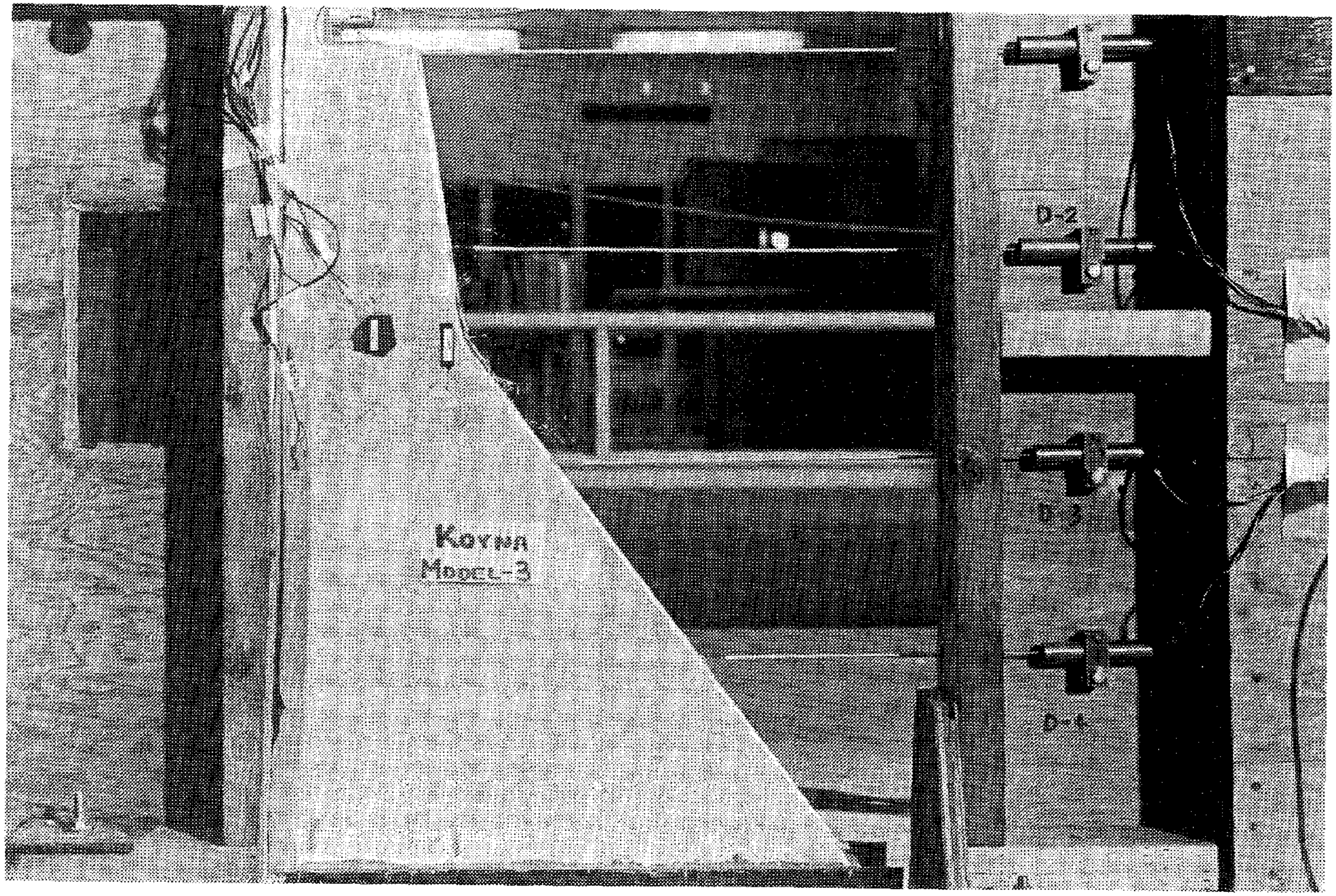

Fig. 4.2 Koyna Dam Model and Reservoir Tank on Shaking Table

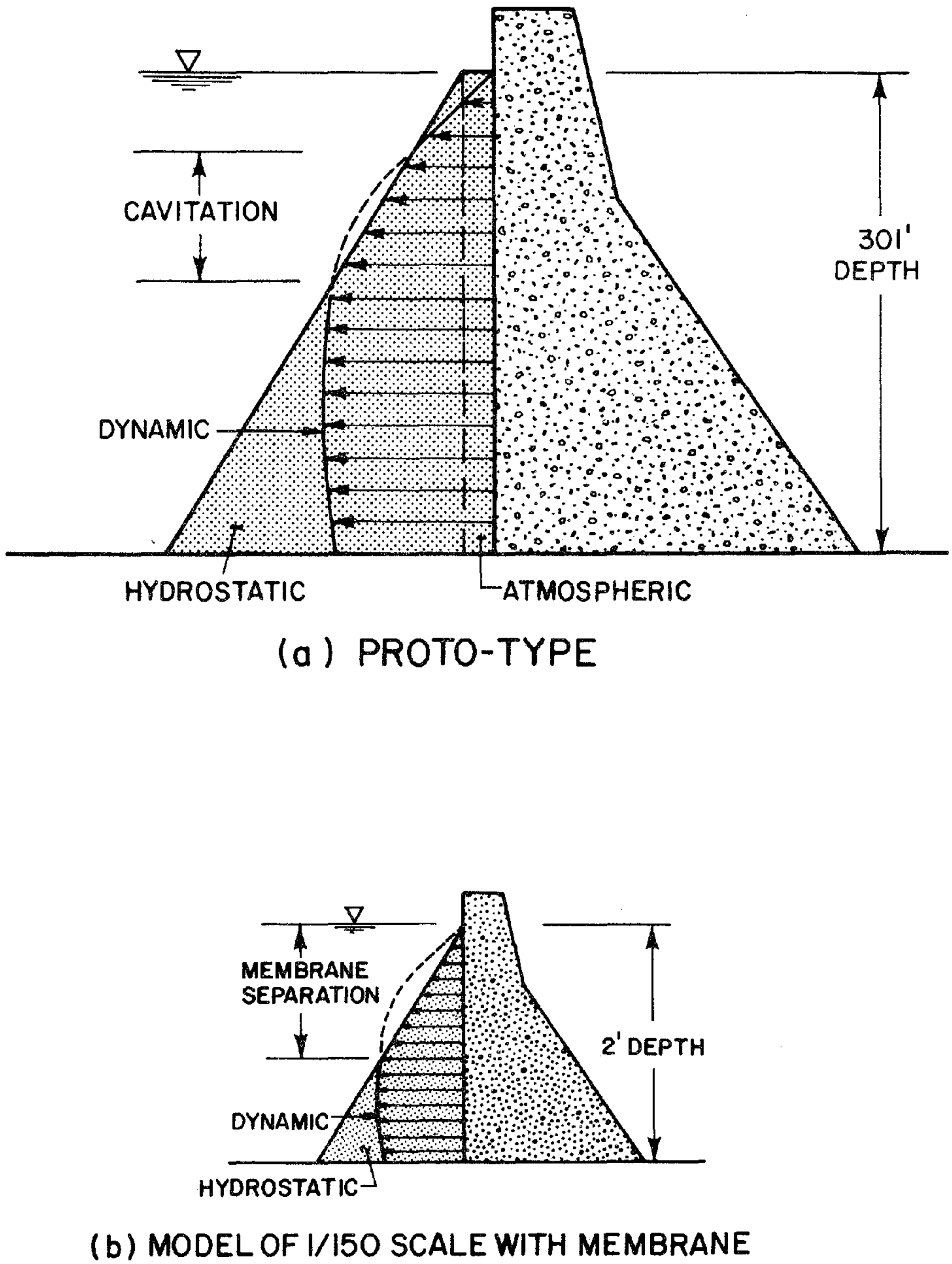

Fig. 4.3 Cavitation Mechanisms in Gravity Dam

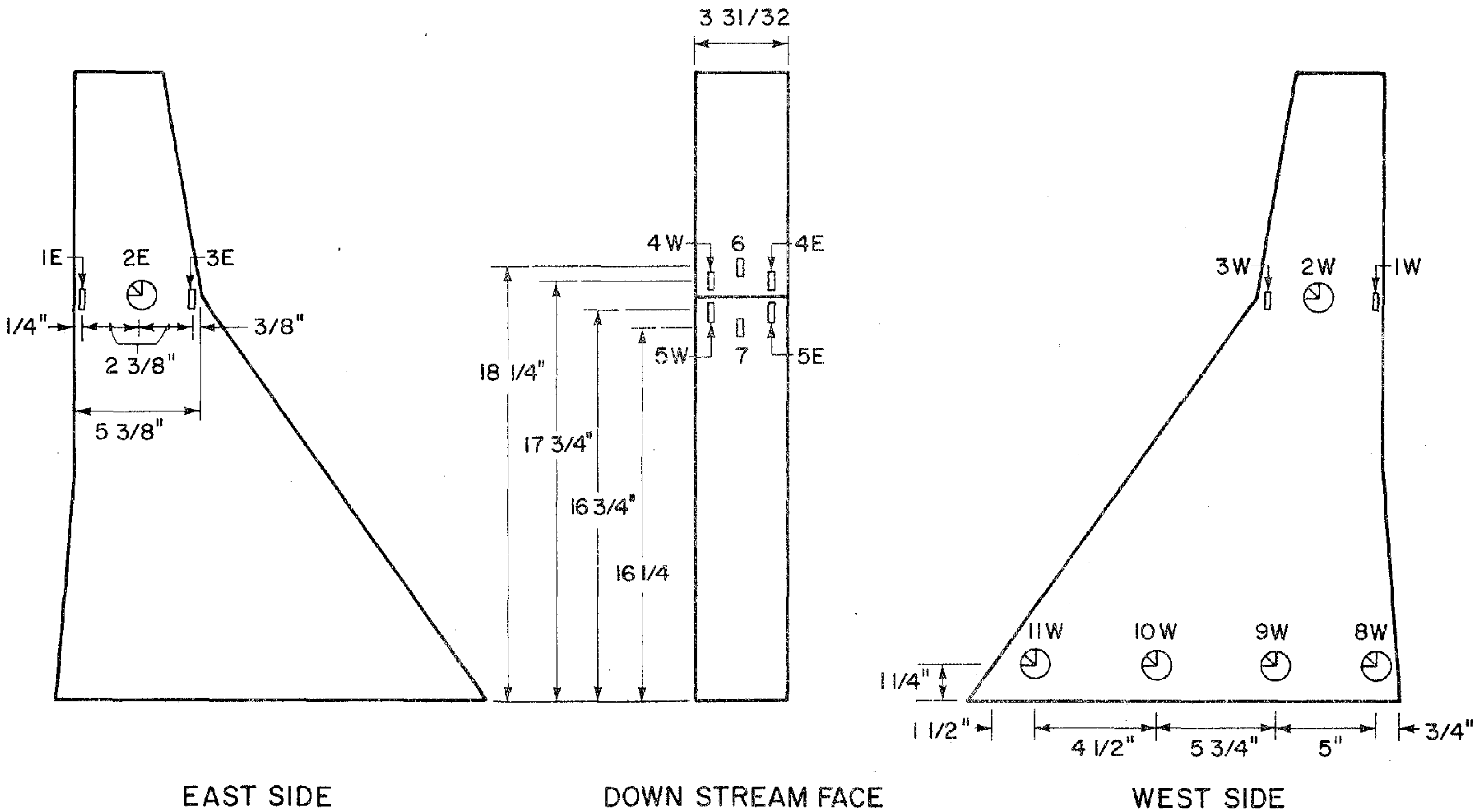

Fig. 4.4 Strain Gage Location of Koyna Model

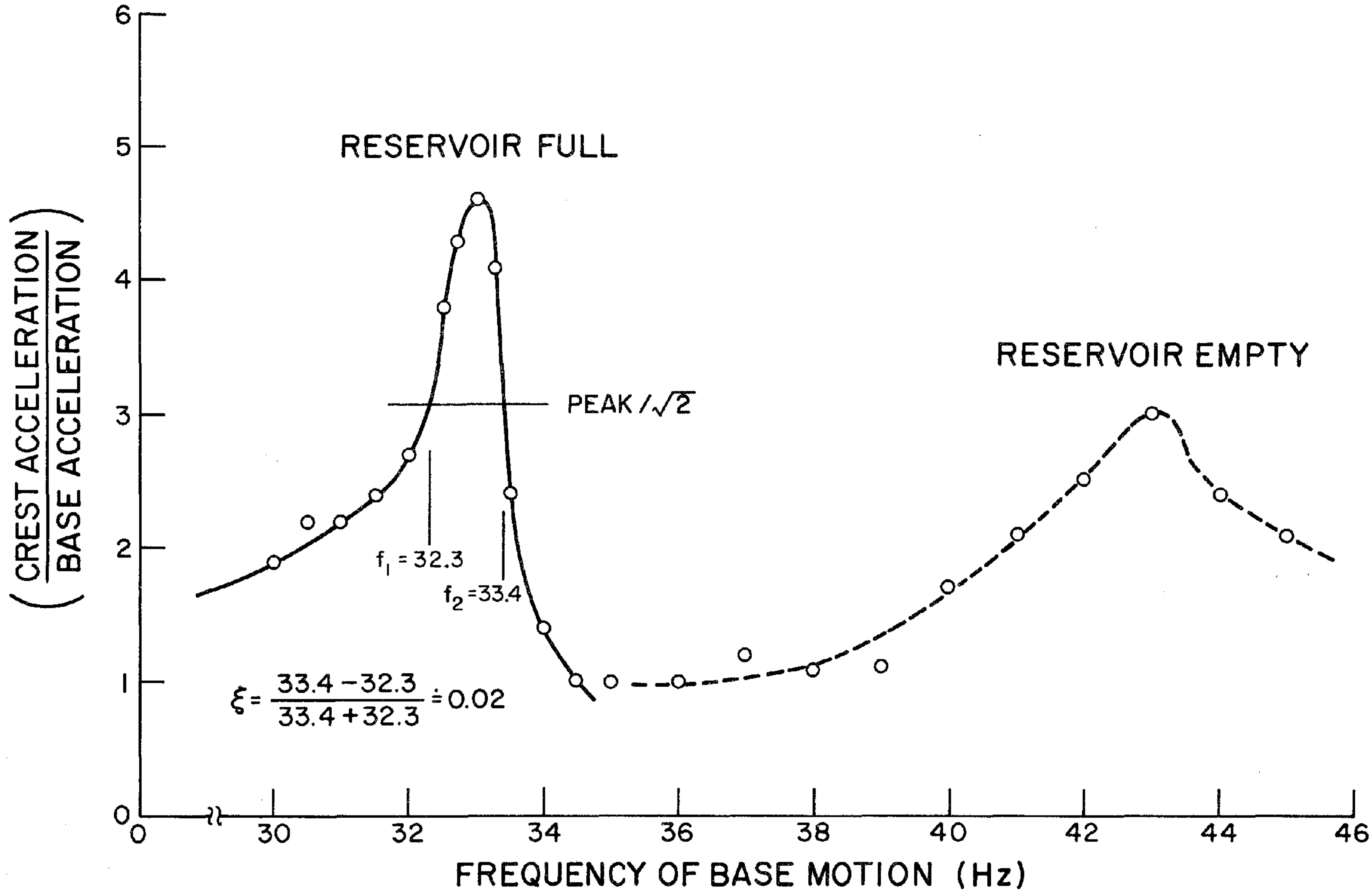

Fig. 4.5 Frequency Response Curves of Koyna Model

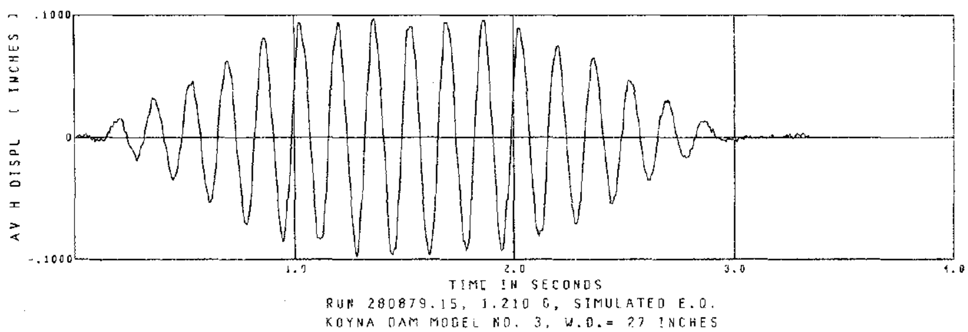

(a) Actual Table Displacements

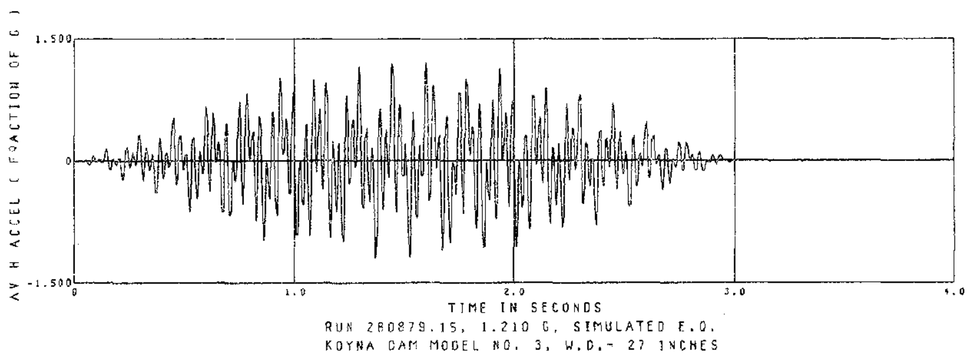

(b) Actual Table Accelerations

Fig. 4.6 Simulated Earthquake of Koyna Model Test

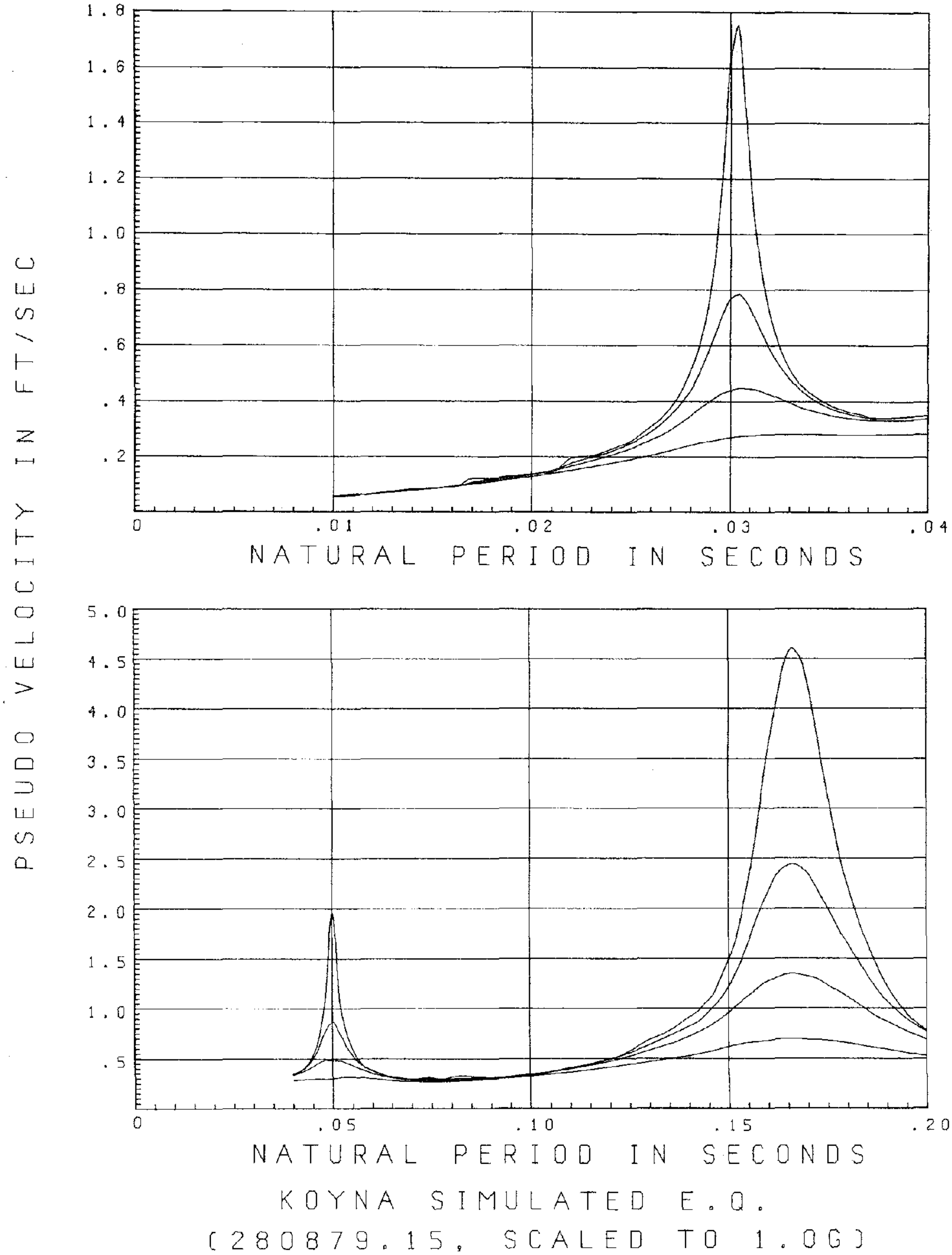

Fig. 4.7 Response Spectra of Koyna Simulated Earthquake

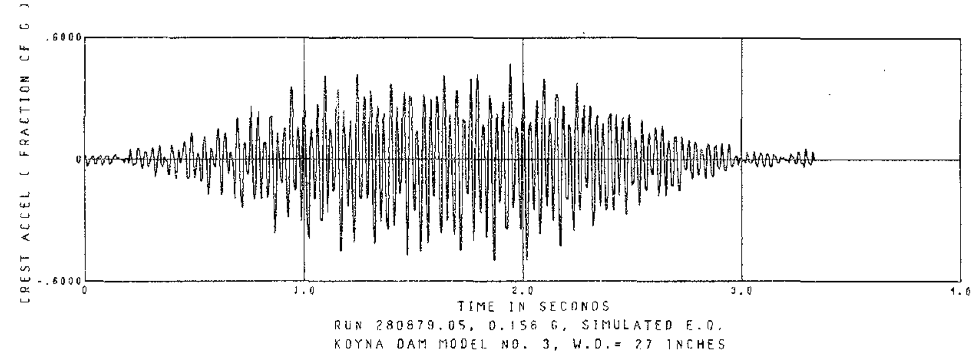

(a) Crest Accelerations

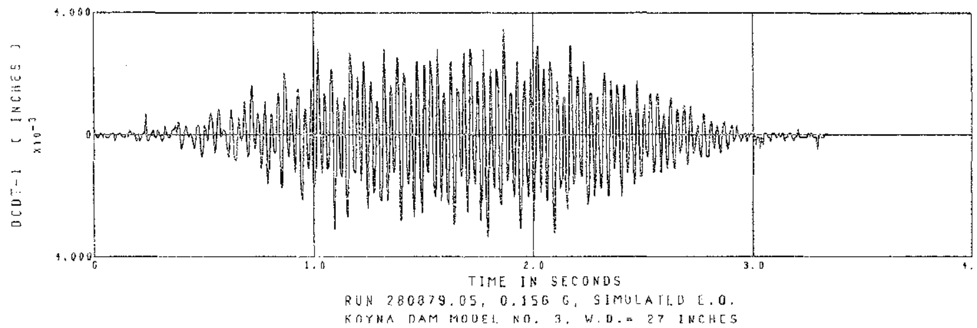

(b) Crest Displacements

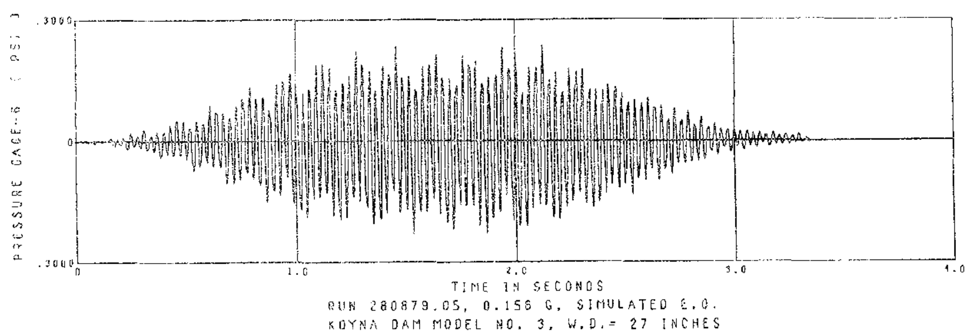

(c) Pressure at Base

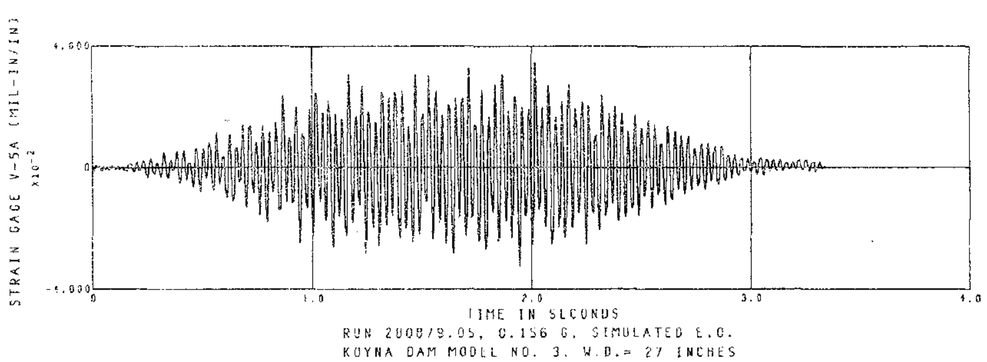

(d) Strain near Critical Section

Fig. 4.8 Low Intensity Excitation Test of Koyna Model

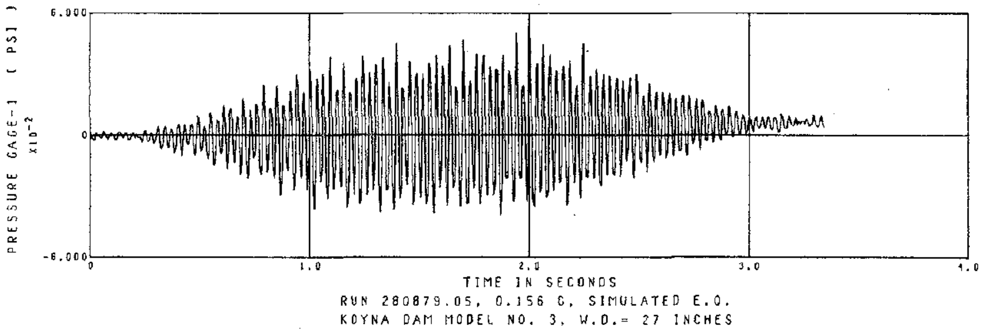

(a) Two in. Depth

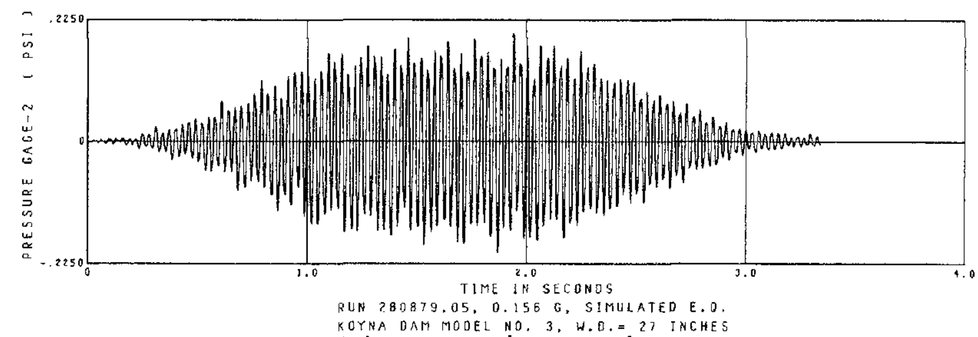

(b) Seven in. Depth

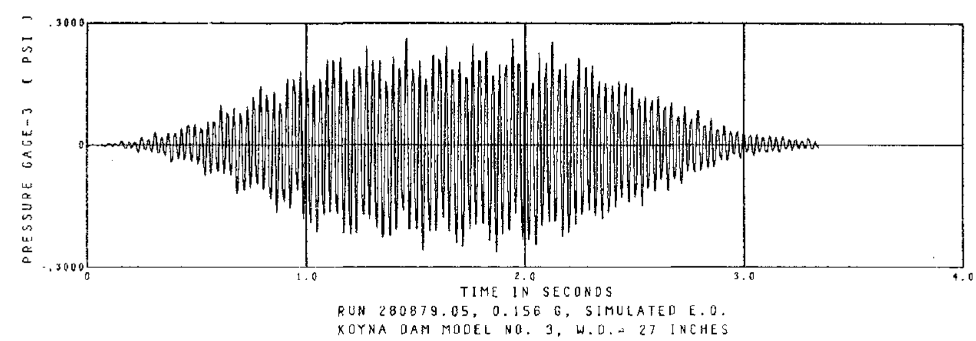

(c) Twelve in. Depth

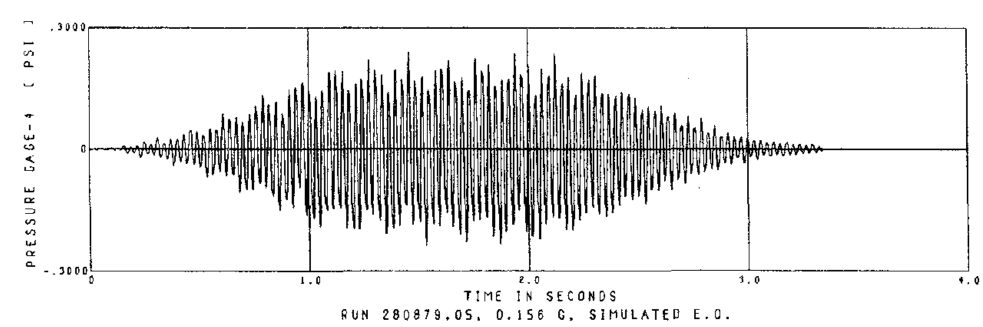

(d) Seventeen in. Depth

Fig. 4.9 Pressure Response in Low Intensity Excitation Test of Koyna Model

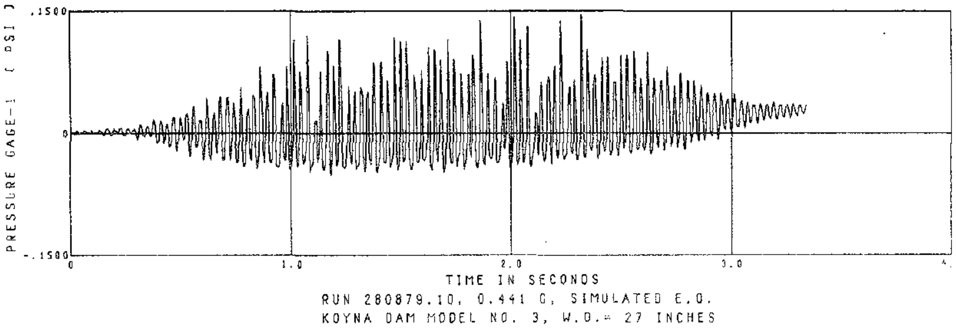

(a) Two in. Depth

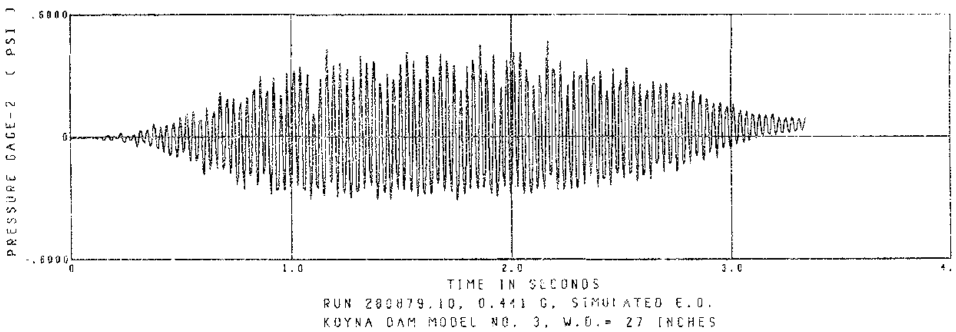

(b) Seven in. Depth

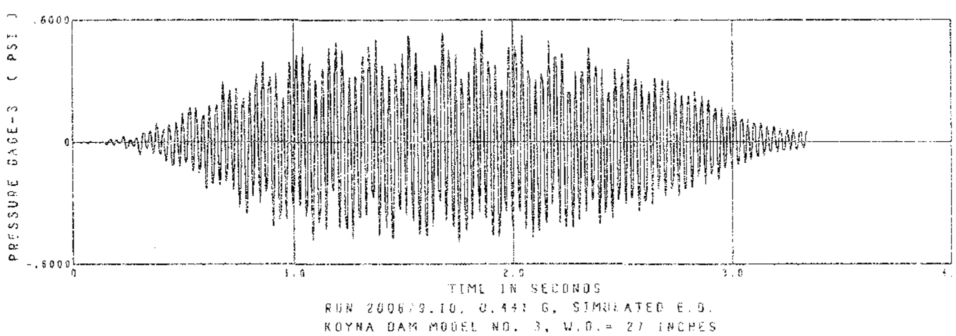

(c) Twelve in. Depth

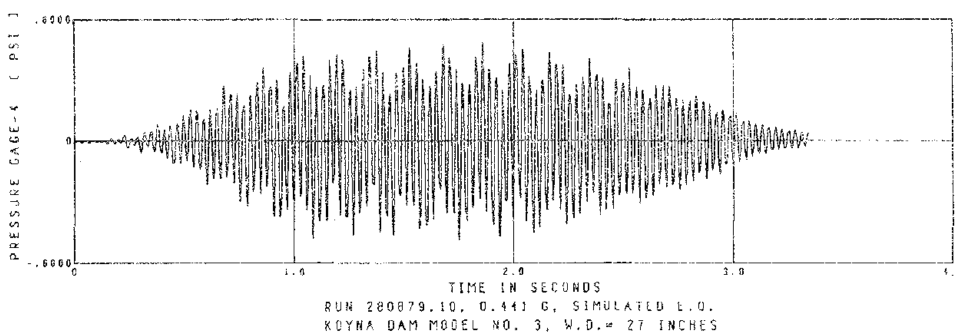

(d) Seventeen in. Depth

Fig. 4.10 Pressure Response in Moderate Intensity Excitation Test of Koyna Model

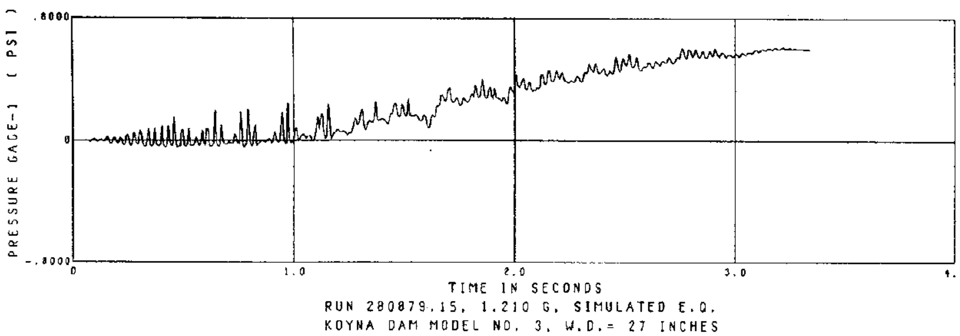

(a) Two in. Depth

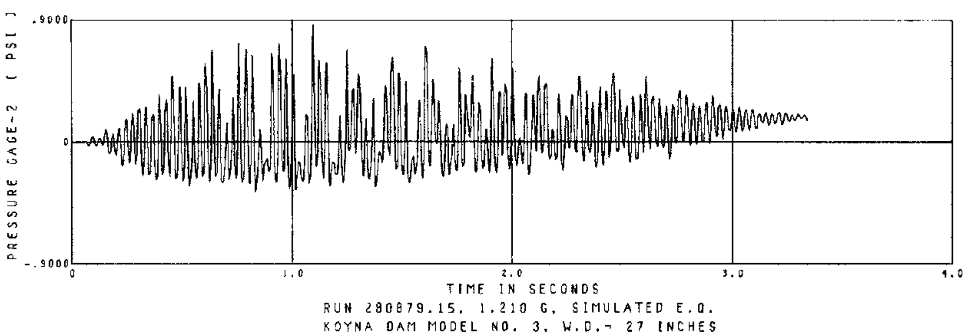

(b) Seven in. Depth

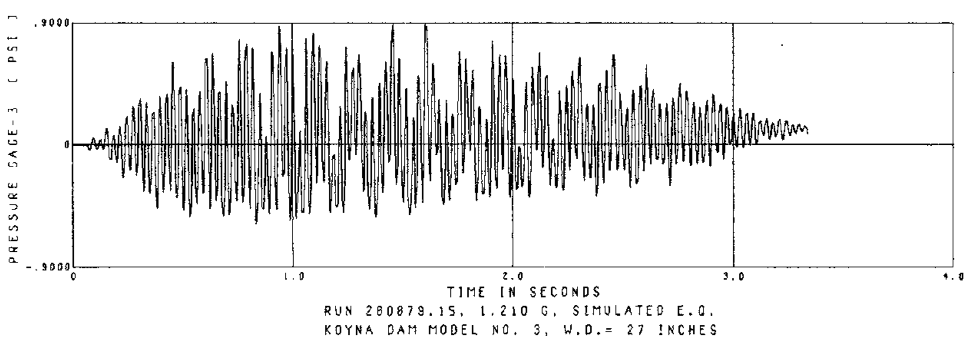

(c) Twelve in. Depth

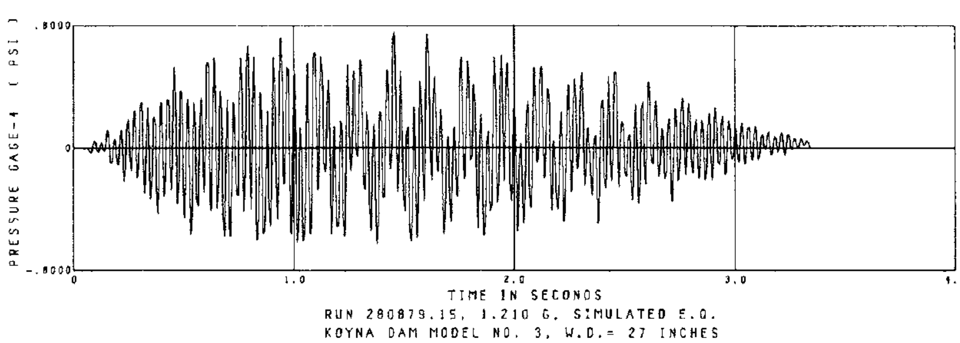

Fig. 4.11 Pressure Response in Severe Intensity Excitation Test of Koyna Model

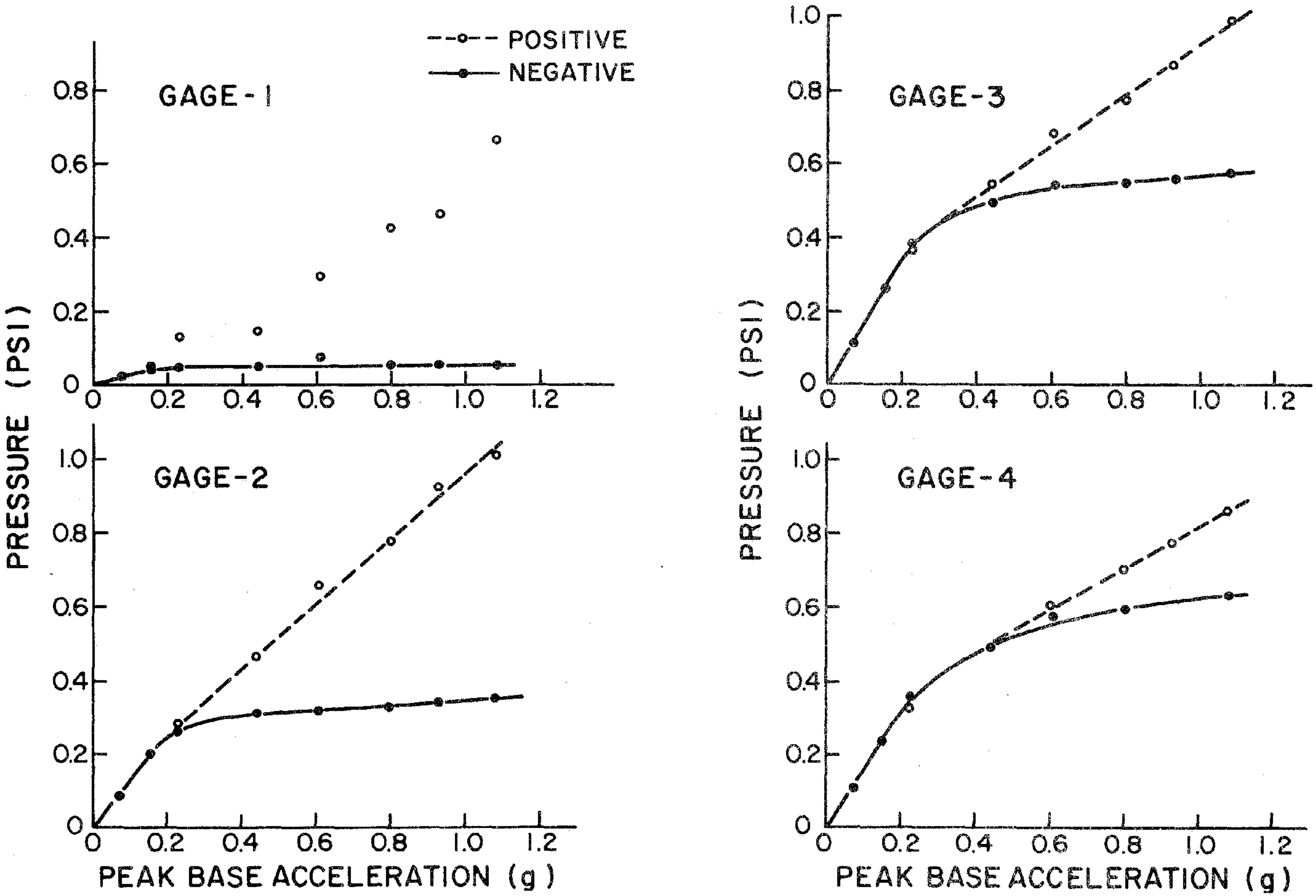

Fig. 4.12 Influence of Excitation Intensity on Pressure Response of Koyna Model

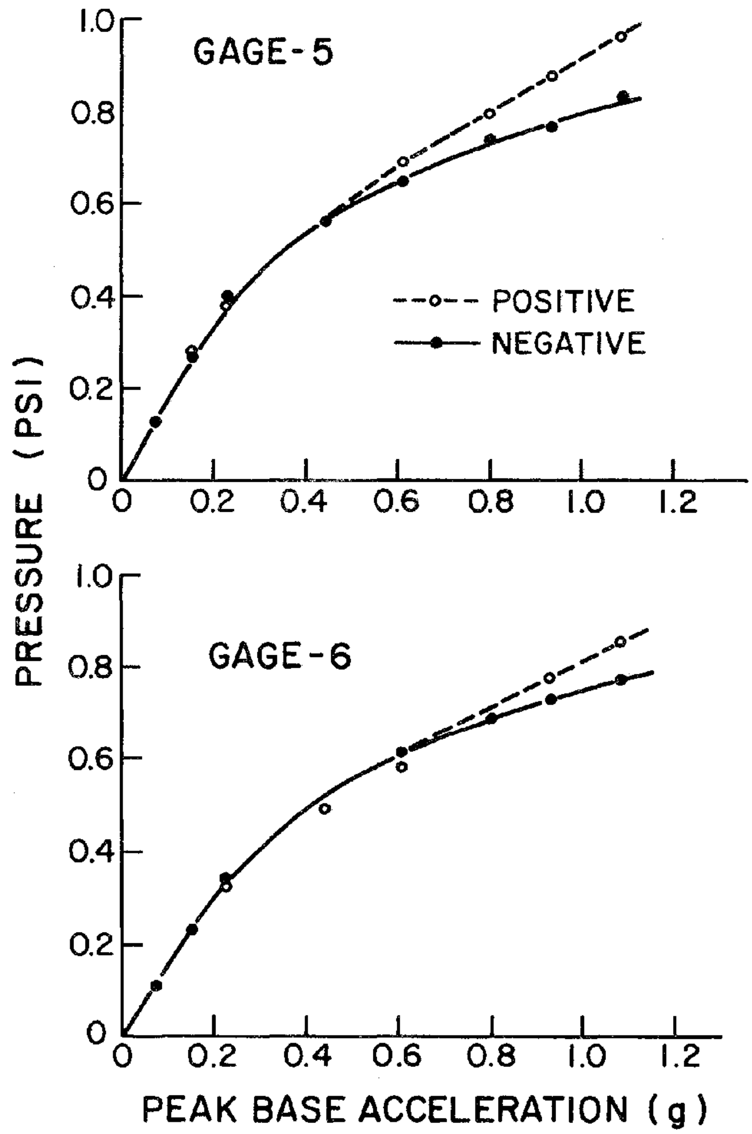

Fig. 4.12 (Cont.) Influence of Excitation Intensity on Pressure Response of Koyna Model

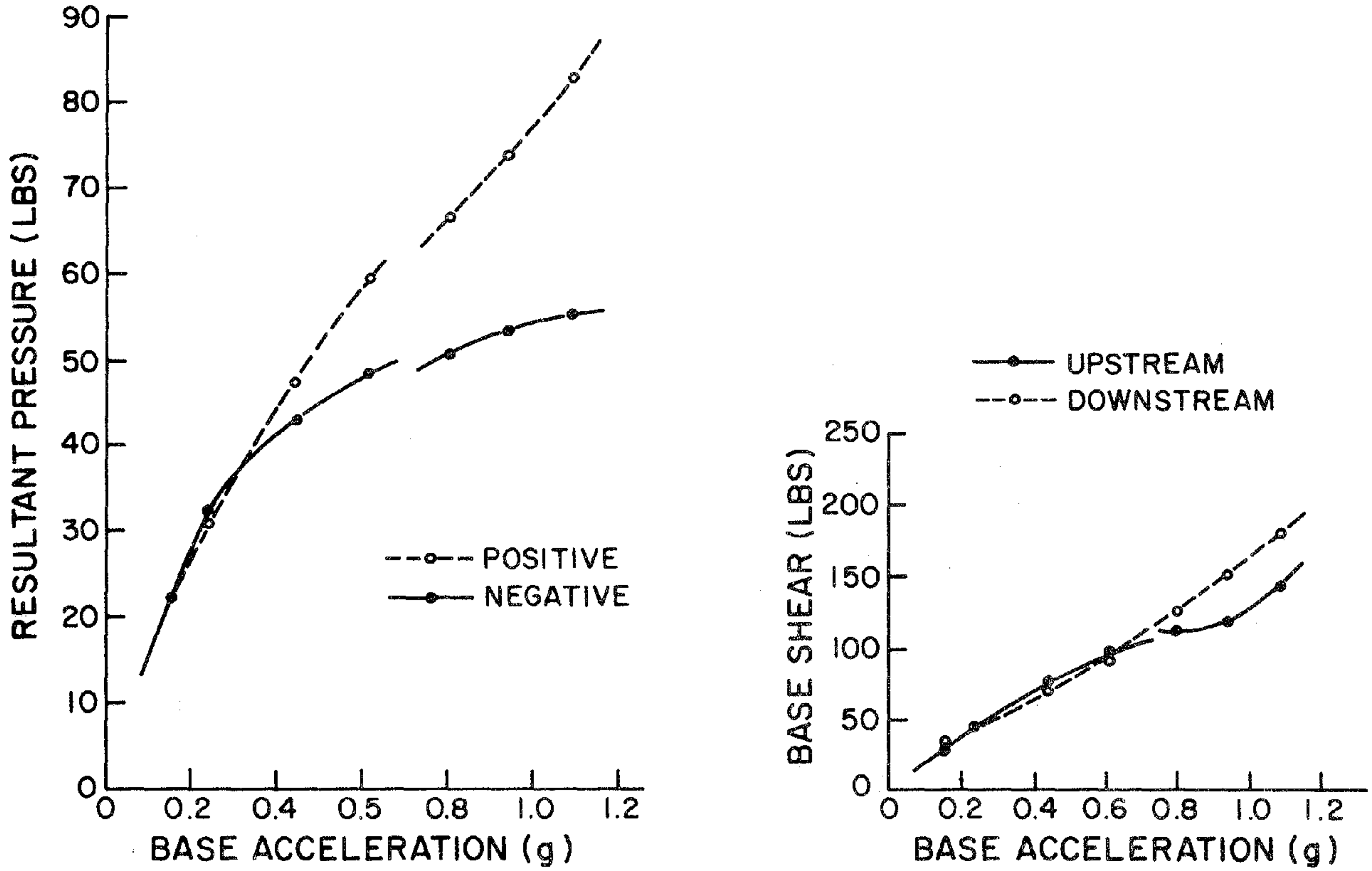

(a) Resultant Pressure

(b) Base Shear

Fig. 4.13 Influence of Cavitation Response on Resultant Pressure and Base Shear Response of Koyna Model

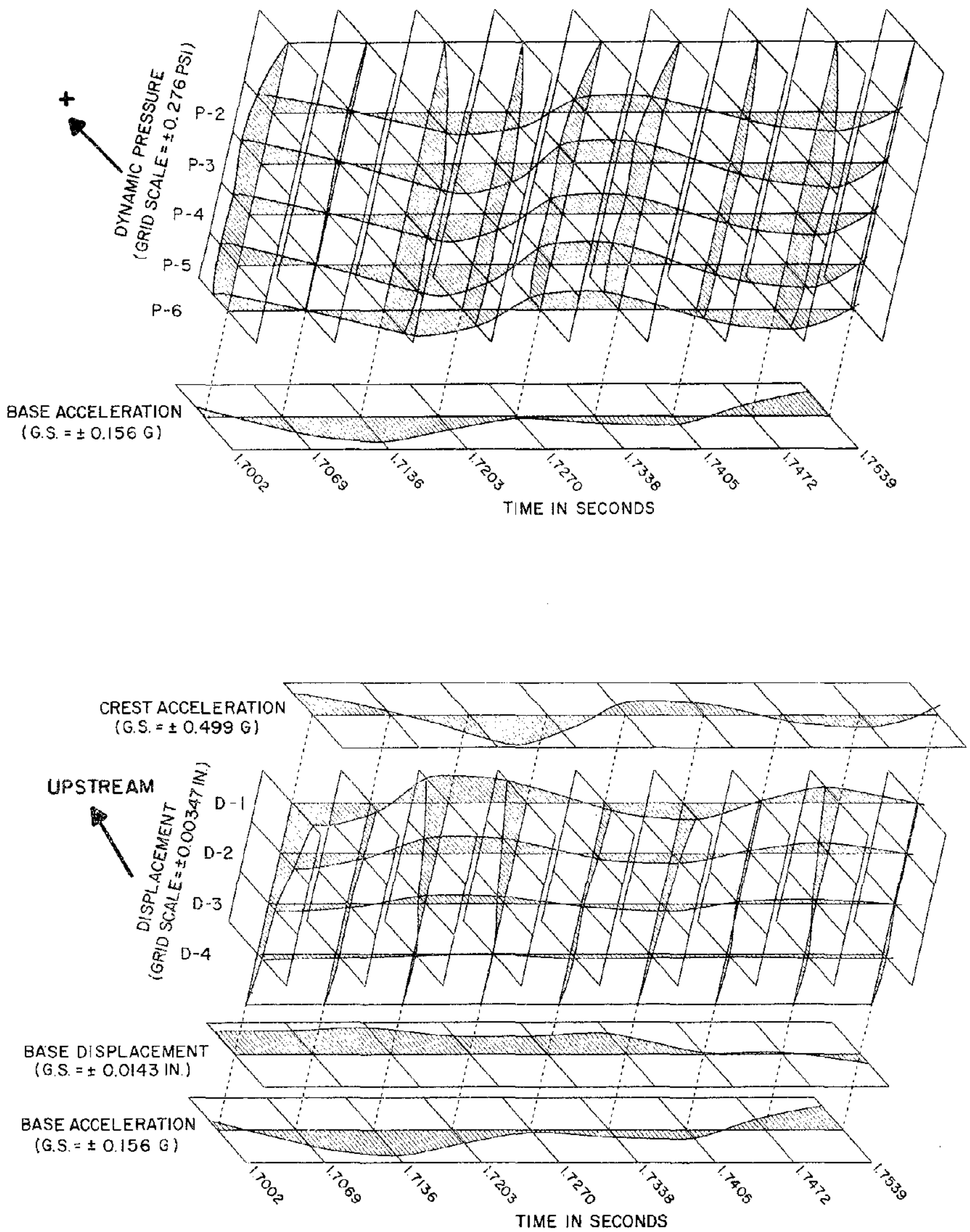

(a) Low Intensity Excitation Test

Fig. 4.14 Isometric Plot of Pressure and Displacement of Koyna Model

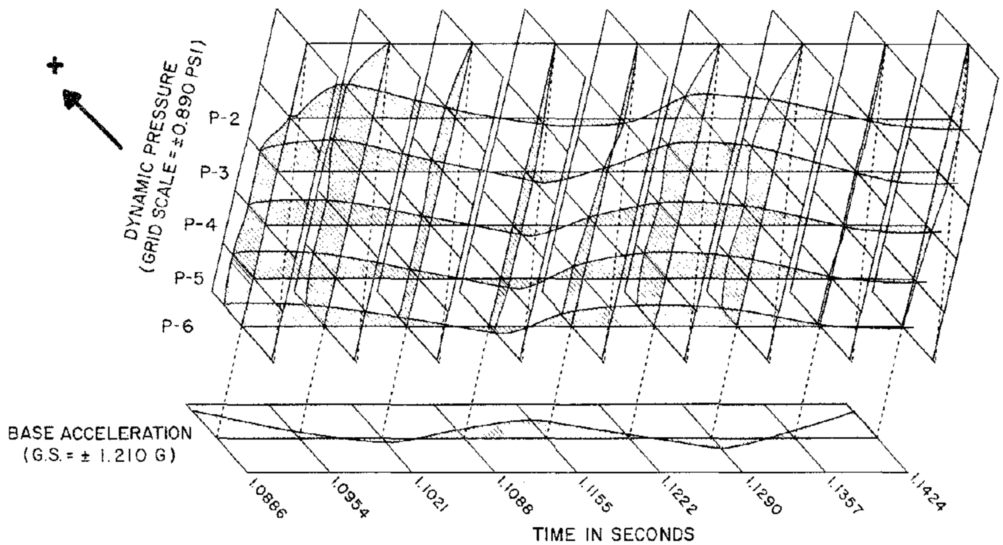

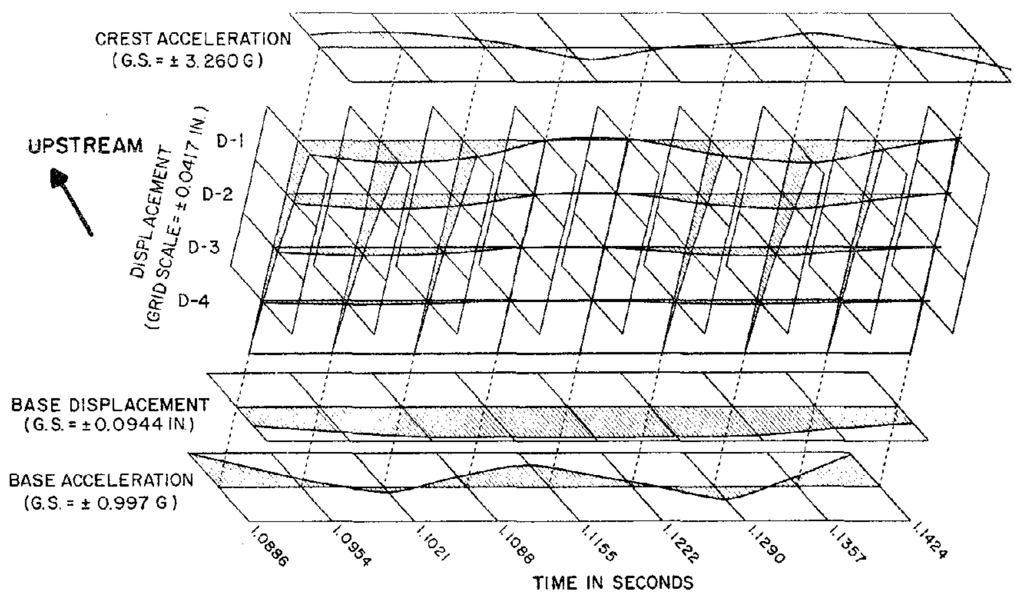

(b) Intense Excitation Test

Fig. 4.14 (Cont.) Isometric Plot of Pressure and Displacement of Koyna Model

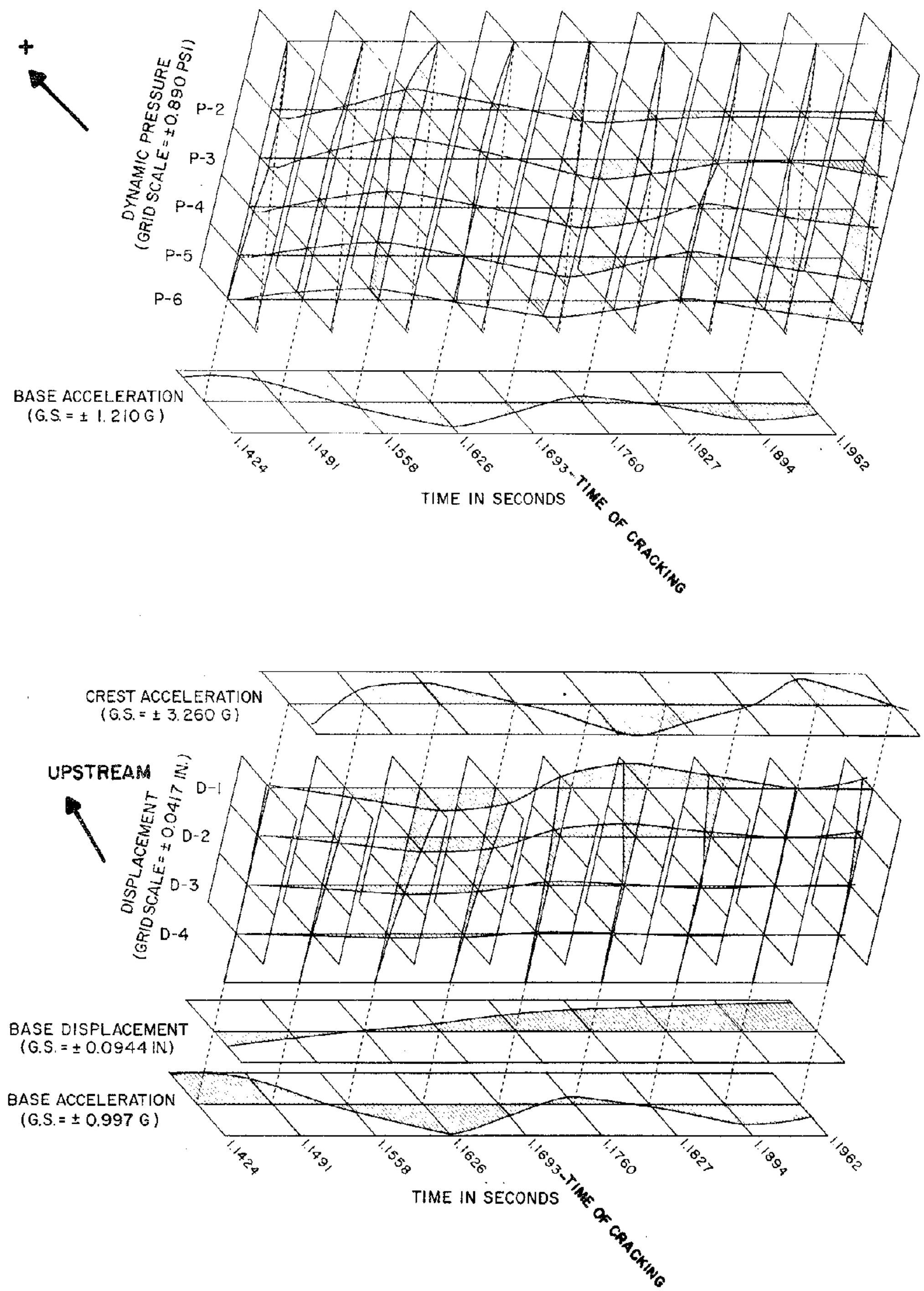

Fig. 4.14b (Cont.) Intense Excitation Test, Isometric Plot of Pressure and Displacement of Koyna Model

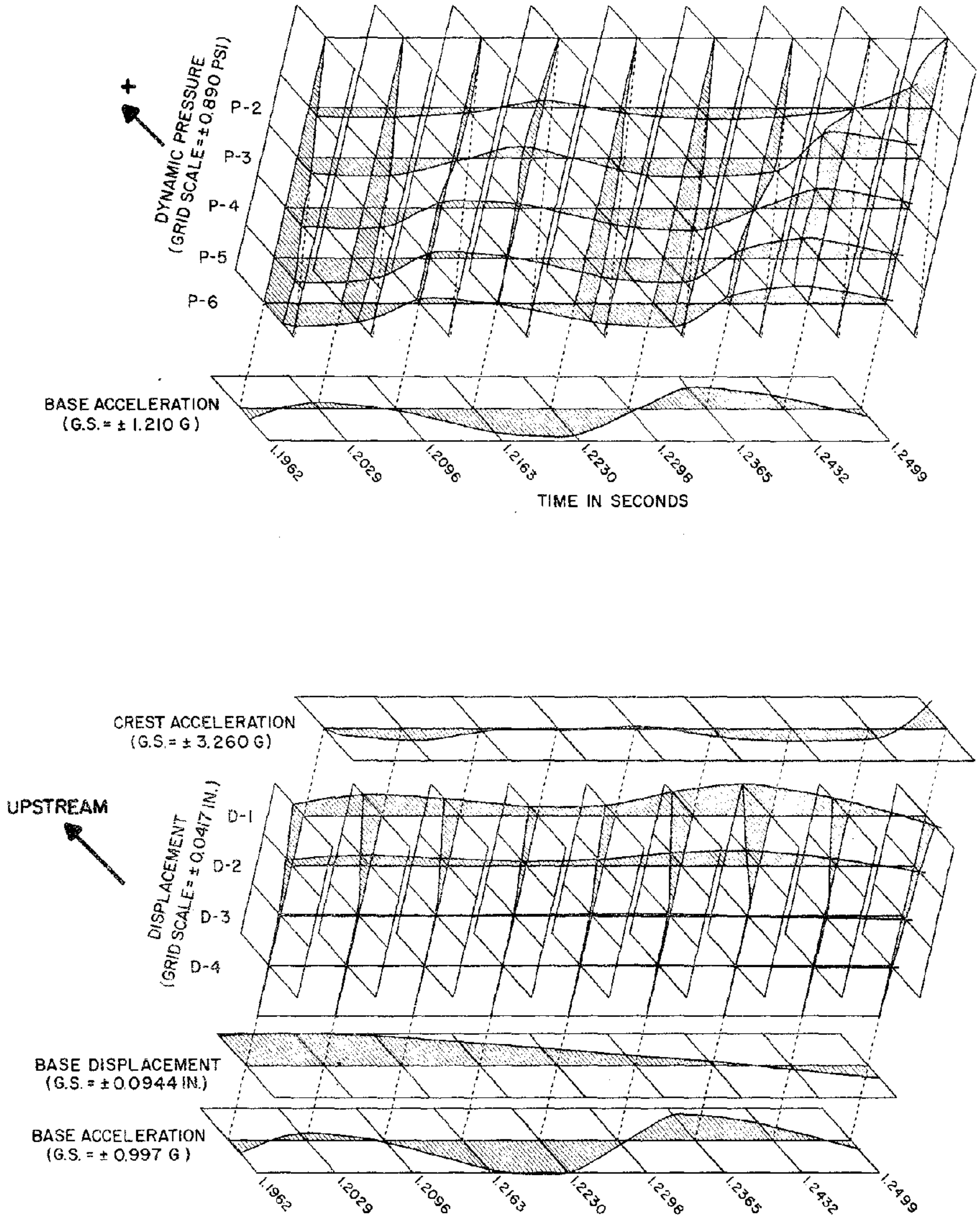

Fig. 4.14b (Cont.) Intense Excitation Test, Isometric Plot of Pressure and Displacement of Koyna Model

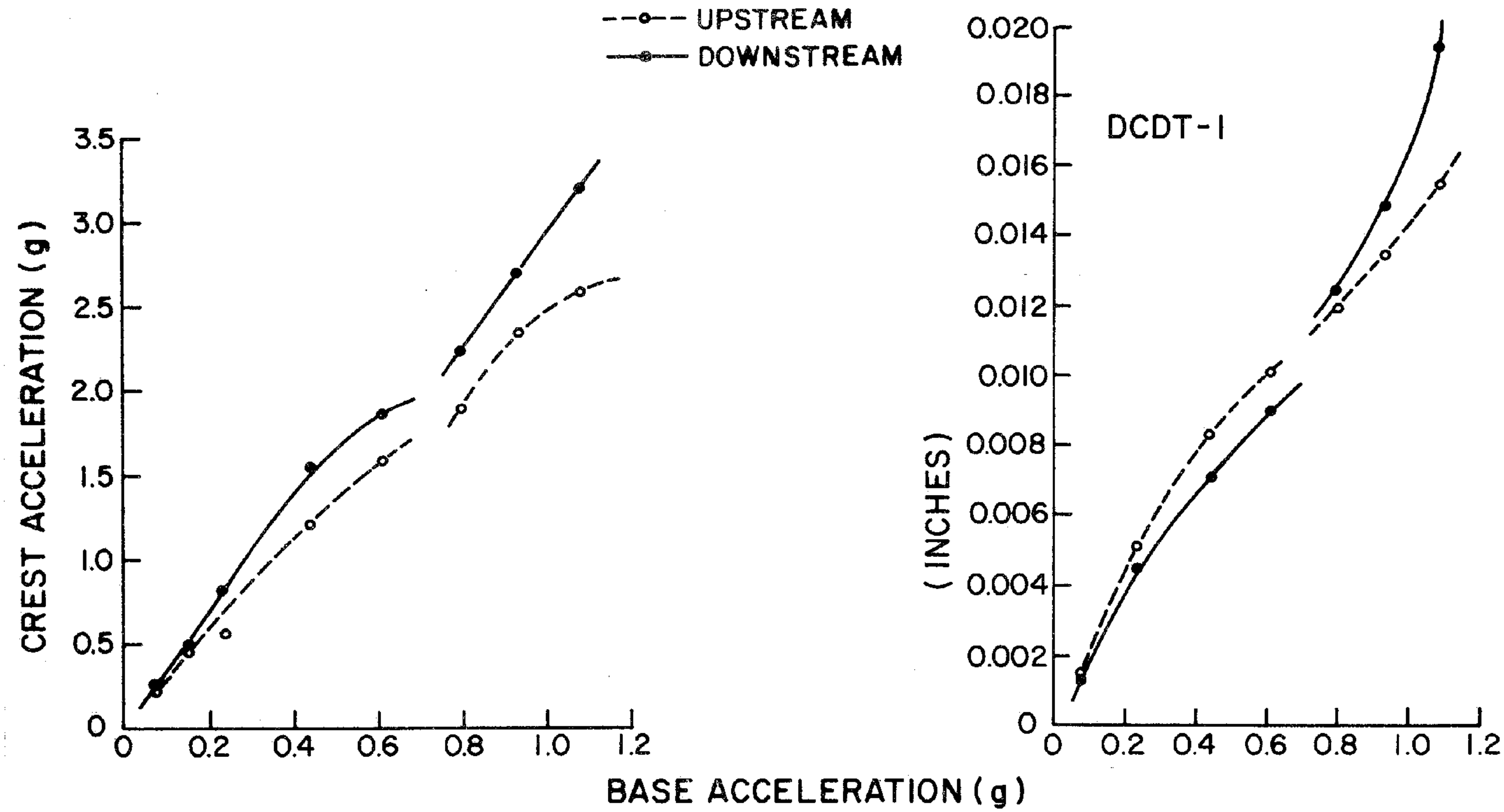

(a) Crest Acceleration

(b) Crest Displacement

Fig. 4.15 Influence of Cavitation on Response of Koyna Model

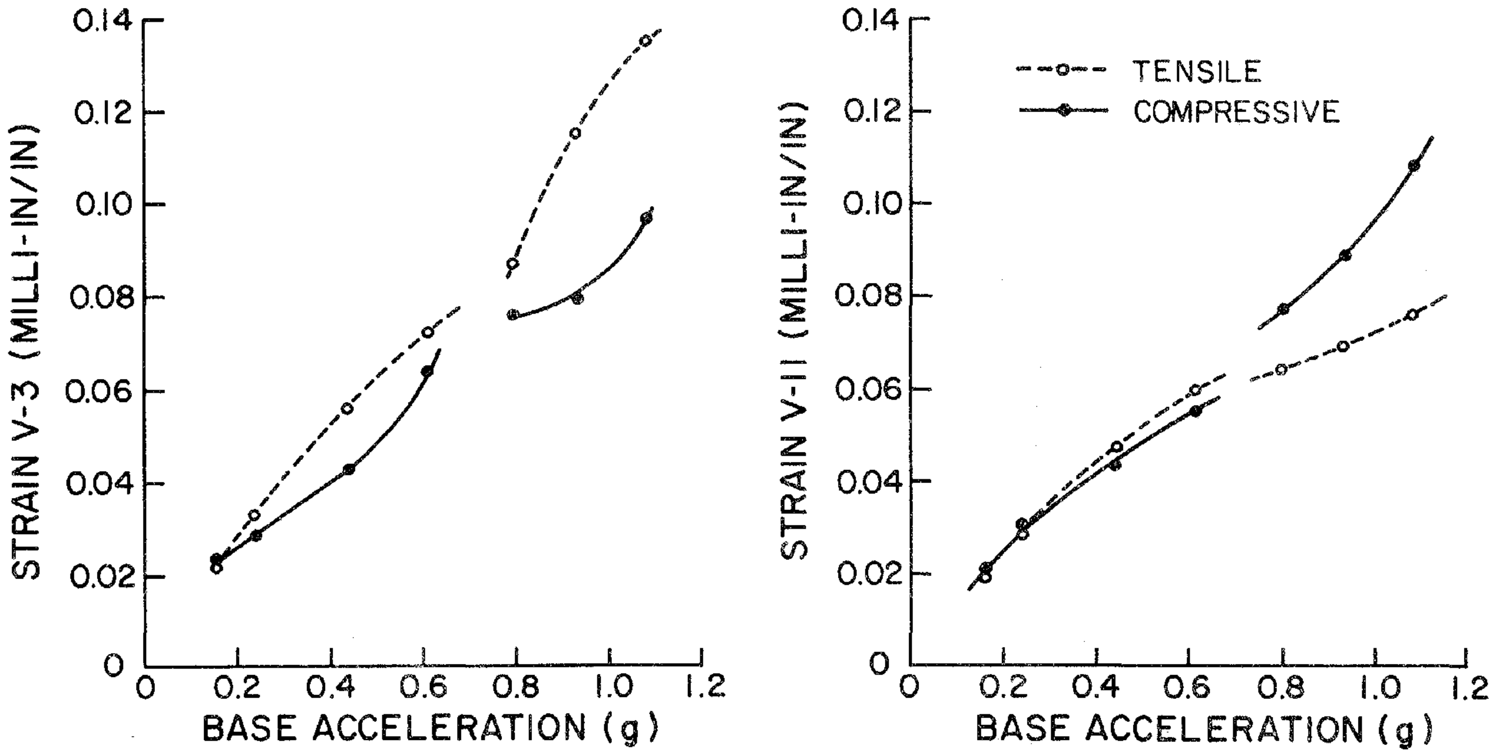

(c) Vertical Strain near Critical Section

(d) Vertical Strain at Base

Fig. 4.15 (Cont.) Influence of Cavitation on Response of Koyna Model

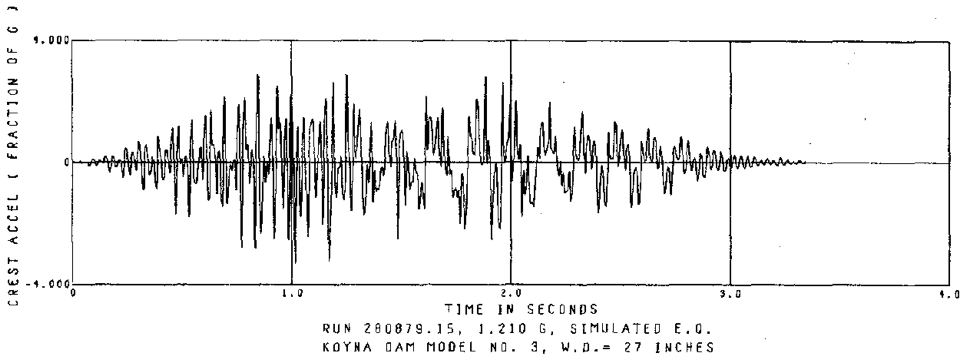

(a) Crest Acceleration

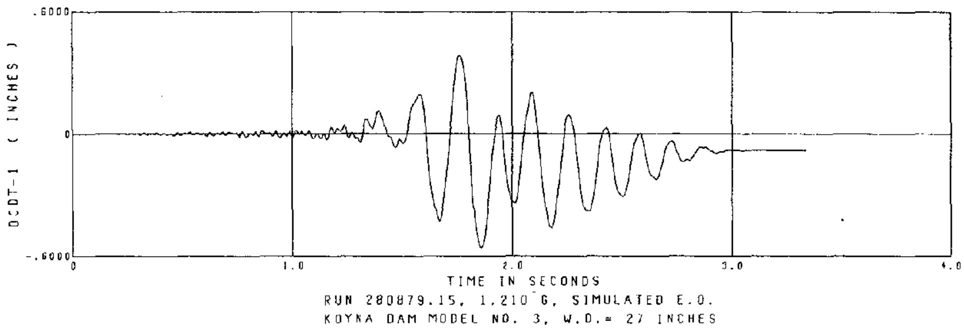

(b) Crest Displacement

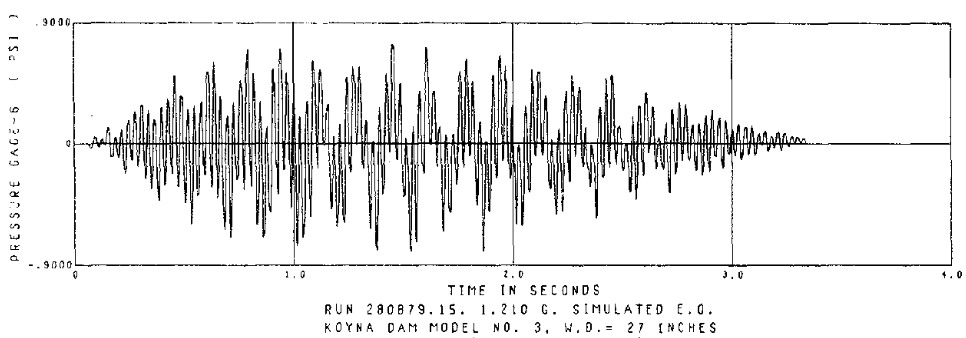

(c) Pressure at Base

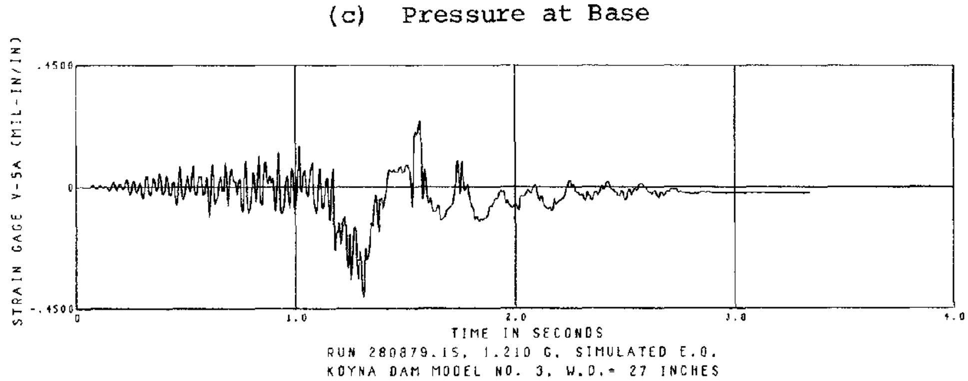

(d) Strain near Critical Section

Fig. 4.16 Cracking Response of Koyna Model

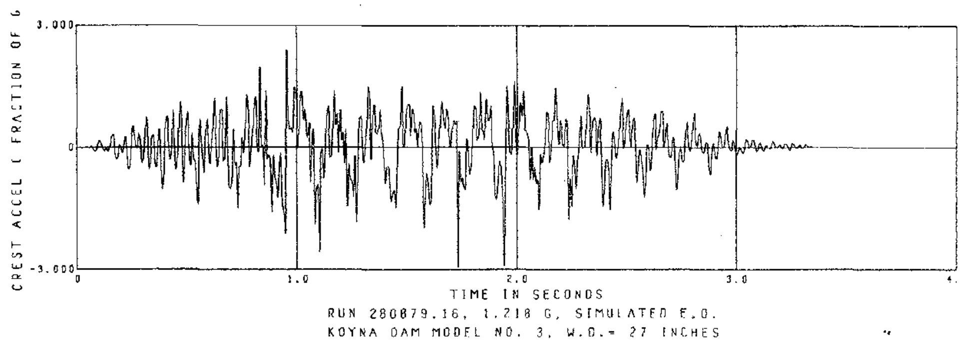

(a) Crest Acceleration

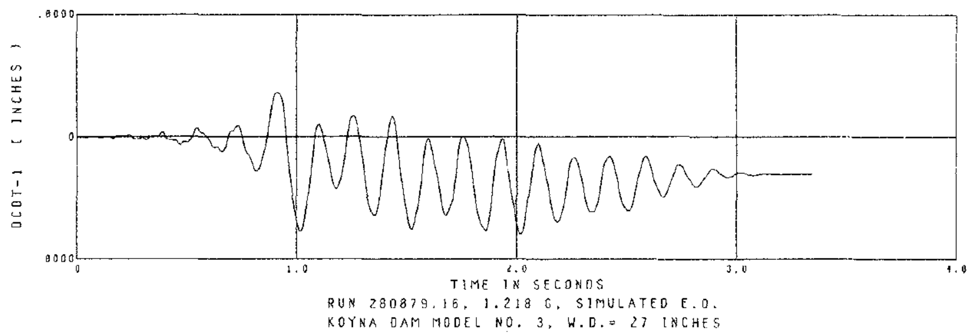

(b) Crest Displacement

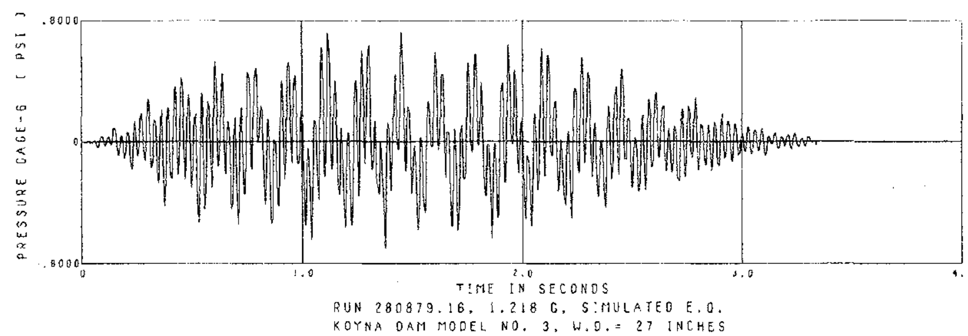

(c) Pressure at Base

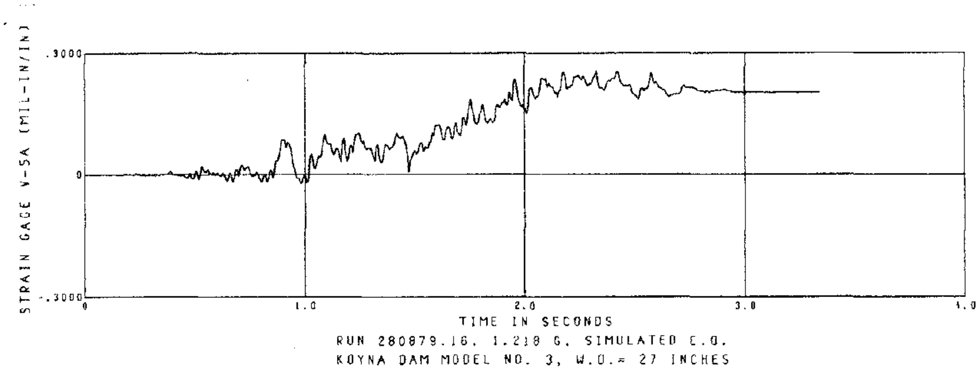

(d) Strain near Critical Section

Fig. 4.17 Post-Cracking Response of Koyna Model

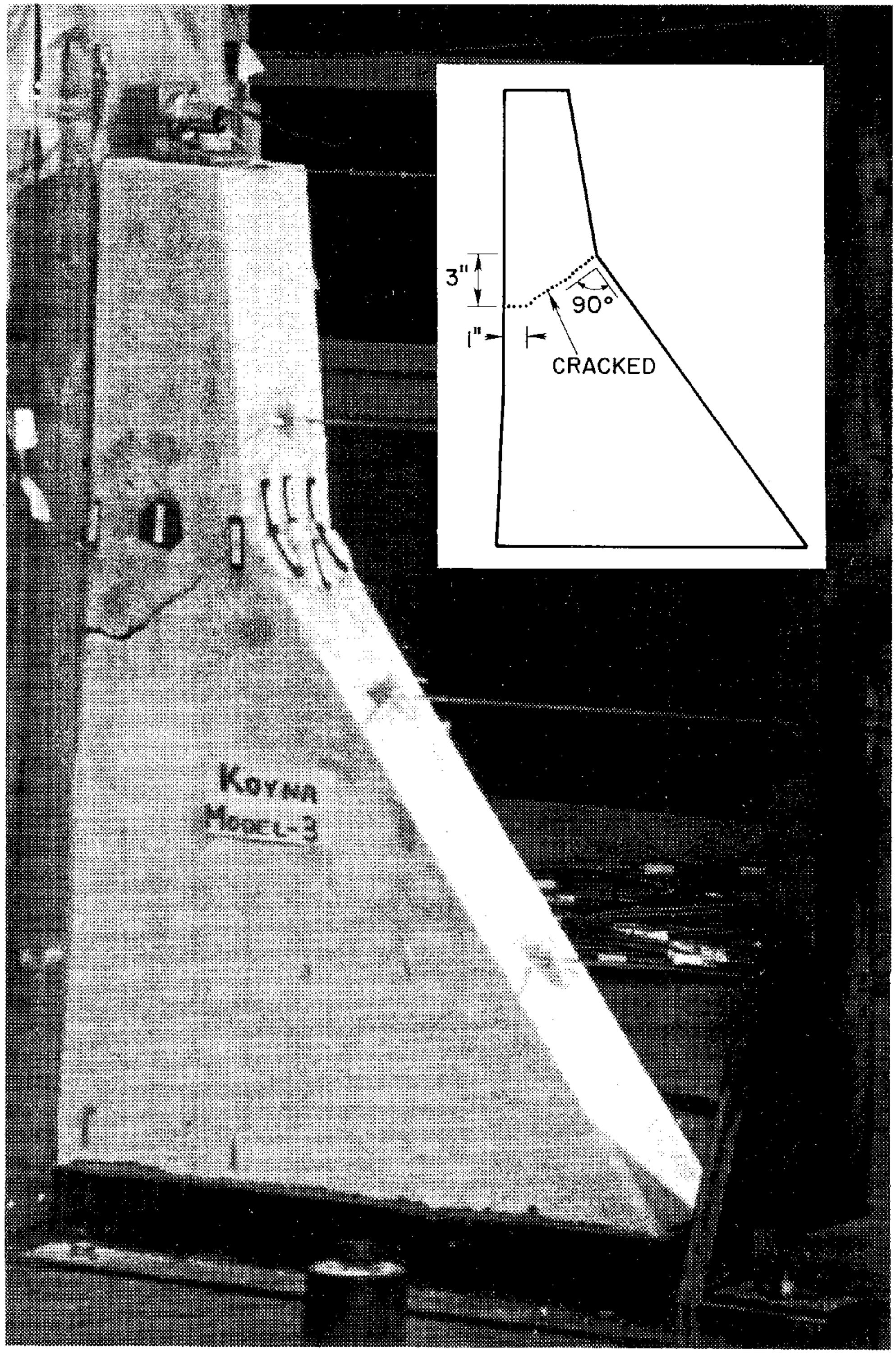

Fig. 4.18 Post-Cracking Response of Koyna Model

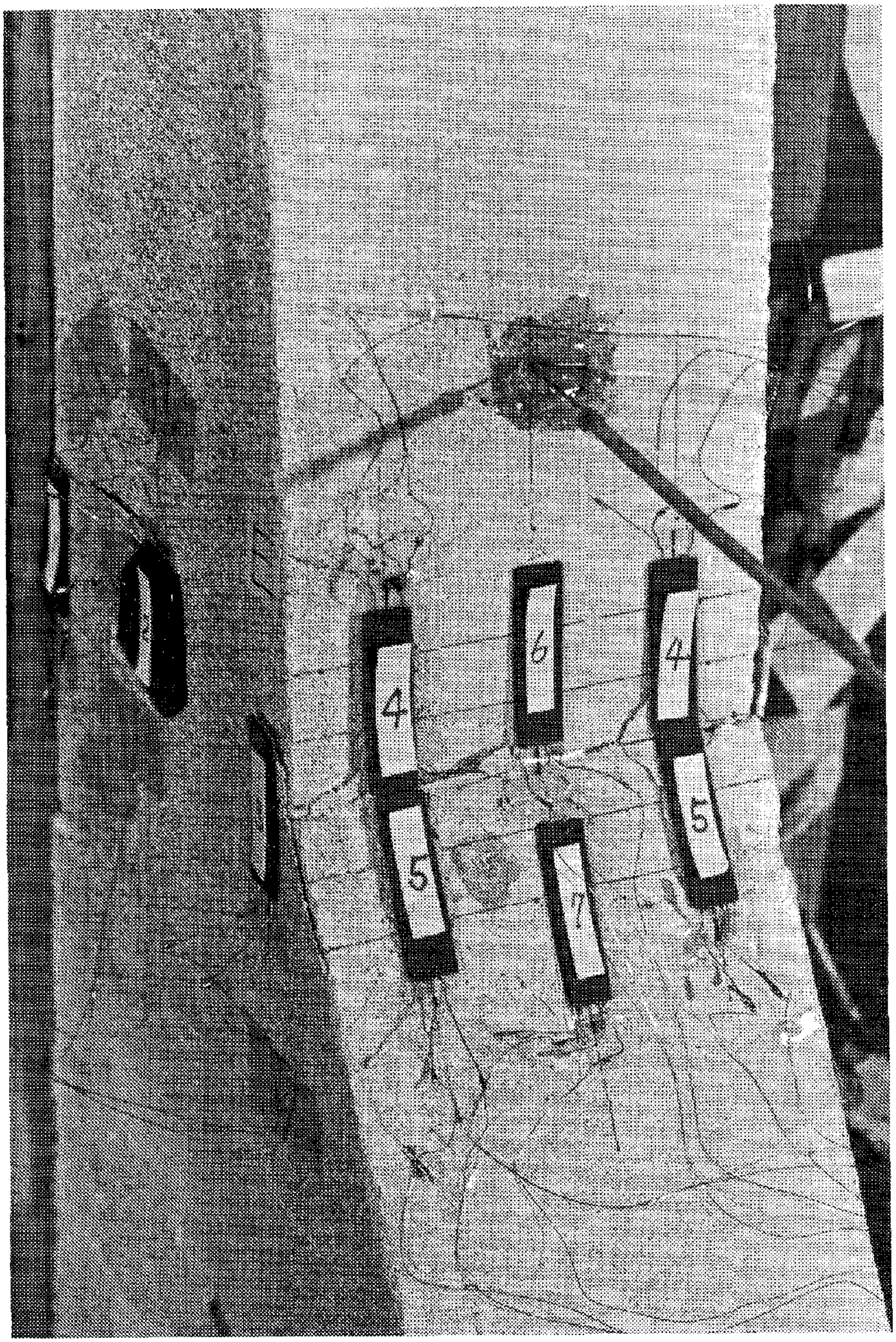

(a) Downstream Face at Critical Section

Fig. 4.19 Cracking Damages in Koyna Model

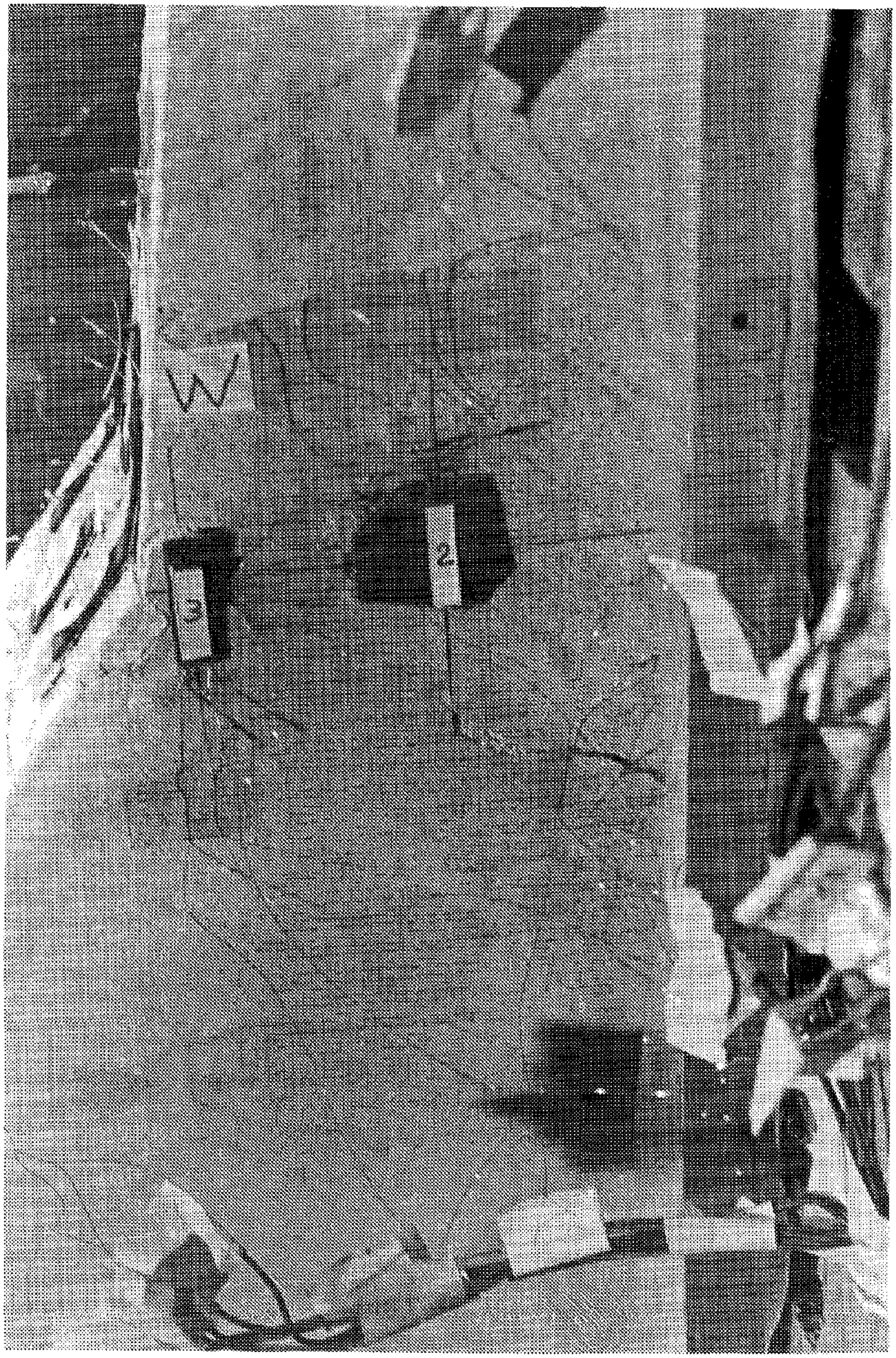

(b) West-Side of Critical Section

Fig. 4.19 (Cont.) Cracking Damages in Koyna Model

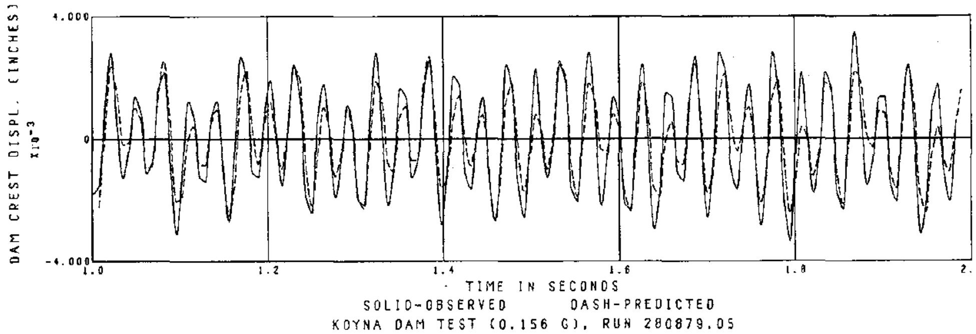

(a) Crest Displacement

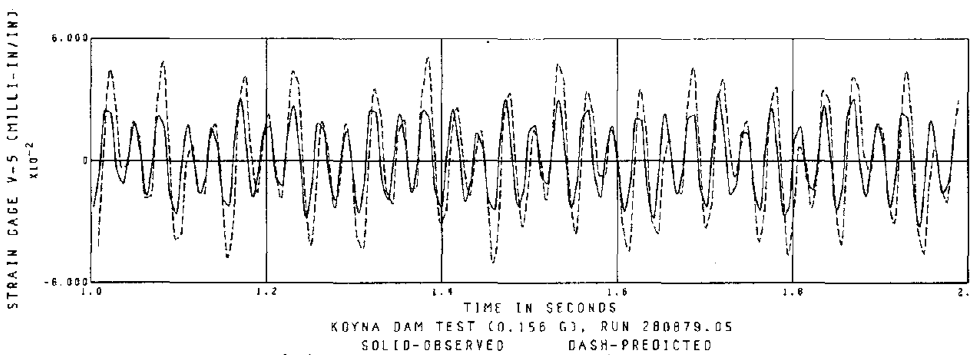

(b) Strain near Critical Section

Fig. 4.20 Correlation for Low Intensity Excitation Test of Koyna Model

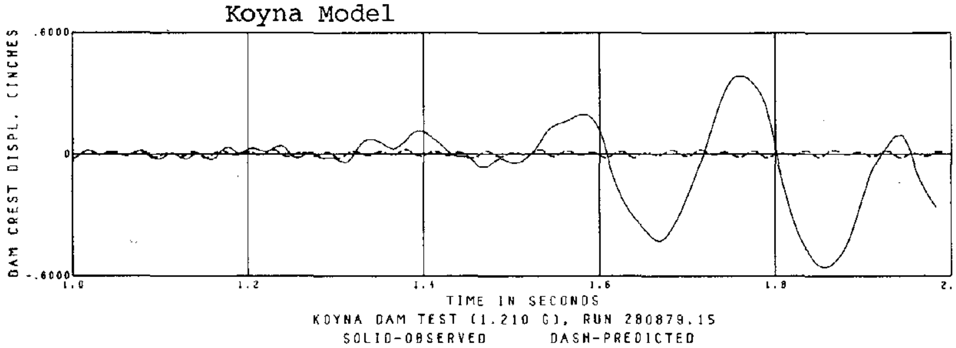

(a) Crest Displacement

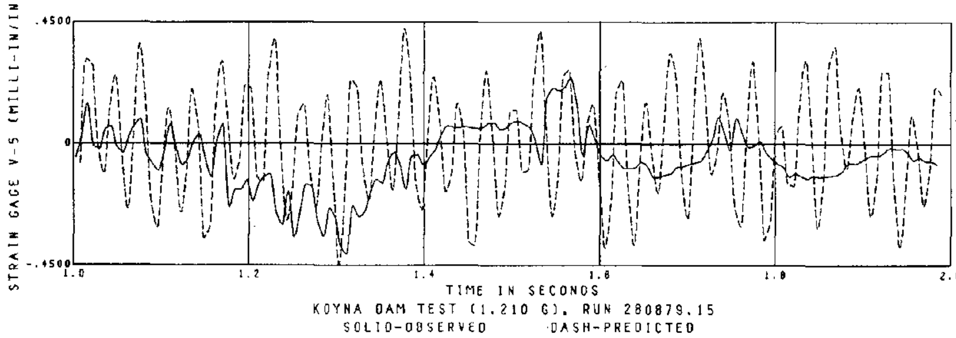

(b) Strain near Critical Section

Fig. 4.21 Correlation for Severe Excitation Test of Koyna Model

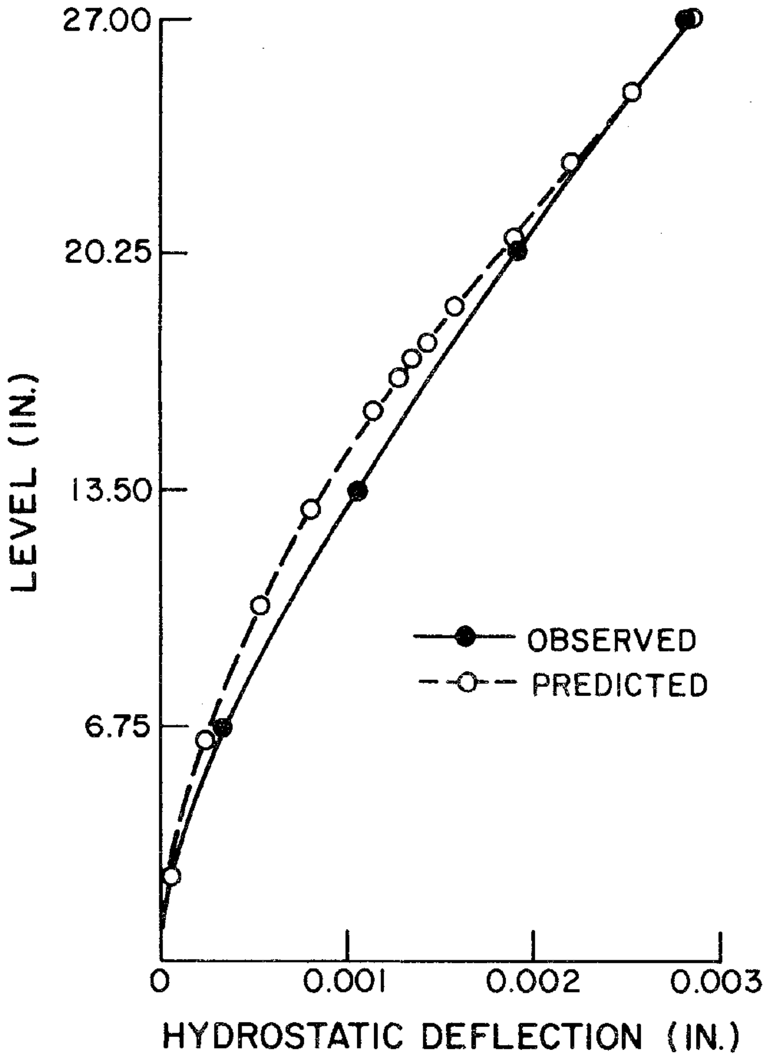

(a) Deflection

Fig. 4.22 Correlation for Hydrostatic Test of Koyna Model

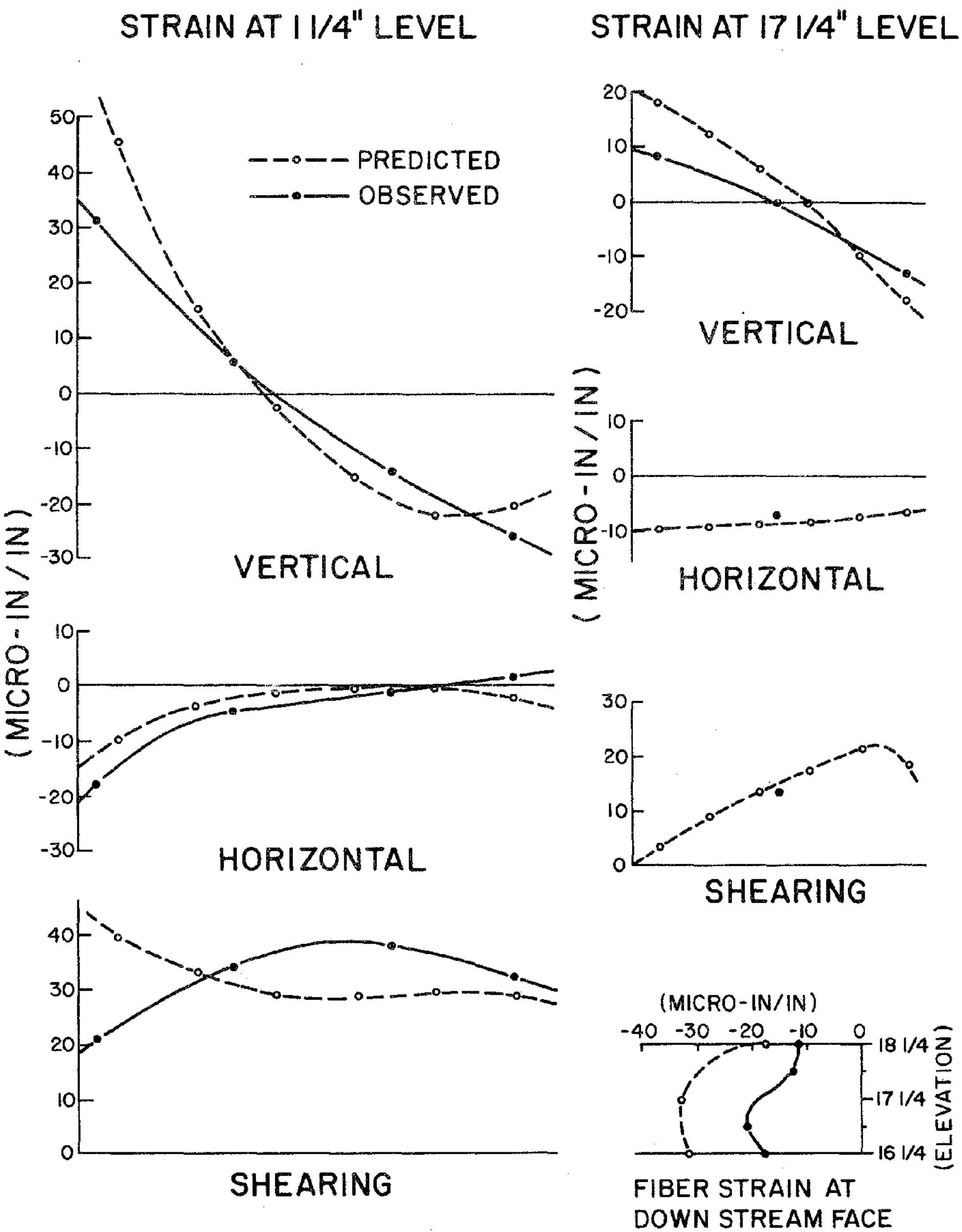

(b) Strain

Fig. 4.22 (Cont.) Correlation for Hydrostatic Test of Koyna Model

5. CONCLUSIONS

The principal conclusions that can be made from this investigation are as follows:

1. Plaster-celite-sand mixtures can be made to simulate all essential mechanical properties of mass concrete, except unit weight, for model length scales as small as 1/150.

2. Addition of lead powder to satisfy the unit weight requirement leads to some distortion with respect to strength and modulus but a fair degree of similitude can be attained for length scales as small as 1/150; better similitude could be achieved for somewhat larger scales.

3. Arch segment models appear to reproduce the joint opening mechanisms that are expected in the earthquake response of arch dams, at least that component of the opening induced by arch flexure. Joint opening effectively suppresses development of actual tensile stress in the arch ring direction, but significantly intensifies compressive stresses at the joint faces due to reduction in joint contact area.

4. The Koyna Dam model tests demonstrated that a cracked gravity dam can still retain the reservoir, and thus that cracking should not be considered to represent failure of such structures. It is believed that arch dams can undergo even more significant cracking without loss of the reservoir; however, model studies of a complete arch dam-reservoir system will be required to demonstrate the post-cracking behavior of such structures.

5. Cavitation mechanisms may have an important influence in the dynamic response of arch dams. Impact action due to cavitating reservoir interaction could significantly amplify the stress response in the upper part of the dam; on the other hand, the reservoir separation could reduce the upstream forces acting on the structure. Thus, further study of this problem is needed.

6. Based on the results of this investigation, it is concluded that shaking table testing of complete arch dam model is feasible, and that results of such a research program would provide invaluable insight into the nonlinear earthquake response and failure mechanisms of thin shell concrete arch dams.

REFERENCES

1. Priscu, R., Popovici, A., and Stere, C., "Consequences of Partially Grouted Joints Upon the Arch Dam Seismic Behavior", Proceedings of Seminar on Construction in Seismic Zones, Bergamo, Italy, May 1978.

2. Pal, N., "Nonlinear Earthquake Response of Concrete Gravity Dams", Report No. EERC-74/14, University of California, Berkeley, December 1974.

3. Clough, R. W., and Chang, C. H., "Cavitation Analysis of Gravity Dam Due to Strong Ground Motion", Earthquake Engineering Research Center, University of California, Berkeley, June 1980.

4. Baba, K., "Model and Full-Scale Concrete Dam Studies in Japan", Proceedings of Research Conference on Earthquake Engineering, Skopje, Yugoslavia, June 1980.

5. Chakrabarti, P., and Chopra, A. K., "A Computer Program for Earthquake Analysis of Gravity Dams Including Hydrodynamic Interaction", Report No. EERC 73-7, University of California, Berkeley, May 1973.

6. Oberti, G., "Construction of Models to the Modern Design and Safety Control of Large Concrete Dams", ISMES Report No. 116, Instito Sperimentale Modelli e Strutture, Bergamo, Italy, March 1979.

7. Raphael, J. M., "Structural Model Investigations for Oroville Dam", Institute of Engineering Research, University of California, Berkeley, February 1960.

8. Saini, S. S. and Krishna, J., "Overturning of Top Profile of Koyna Dam During Severe Ground Motion", International Journal of Earthquake Engineering and Structural Dynamics, Vol. 2, Issue No. 3, 1974.

EARTHQUAKE ENGINEERING RESEARCH CENTER REPORTS

NOTE: Numbers in parenthesis are Accession Numbers assigned by the National Technical Information Service; these are followed by a price code. Copies of the reports may be ordered from the National Technical Information Service, 5285 Port Royal Road, Springfield, Virginia, 22161. Accession Numbers should be quoted on orders for reports (PB --- ---) and remittance must accompany each order. Reports without this information were not available at time of printing. Upon request, EERC will mail inquirers this information when it becomes available.

EERC 67-1 "Feasibility Study Large-Scale Earthquake Simulator Facility," by J. Penzien, J.G. Bouwkamp, R.W. Clough and D. Rea - 1967 (PB 187 905)A07

EERC 68-1 Unassigned

EERC 68-2 "Inelastic Behavior of Beam-to-Column Subassemblages Under Repeated Loading," by V.V. Bertero - 1968 (PB 184 888)A05

EERC 68-3 "A Graphical Method for Solving the Wave Reflection-Refraction Problem," by H.D. McNiven and Y. Mengi - 1968 (PB 187 943)A03

EERC 68-4 "Dynamic Properties of McKinley School Buildings," by D. Rea, J.G. Bouwkamp and R.W. Clough - 1968 (PB 187 902)A07

EERC 68-5 "Characteristics of Rock Motions During Earthquakes," by H.B. Seed, I.M. Idriss and F.W. Kiefer - 1968 (PB 188 338)A03

EERC 69-1 "Earthquake Engineering Research at Berkeley," - 1969 (PB 187 906)A11

EERC 69-2 "Nonlinear Seismic Response of Earth Structures," by M. Dibaj and J. Penzien - 1969 (PB 187 904)A08

EERC 69-3 "Probabilistic Study of the Behavior of Structures During Earthquakes," by R. Ruiz and J. Penzien - 1969 (PB 187 886)A06

EERC 69-4 "Numerical Solution of Boundary Value Problems in Structural Mechanics by Reduction to an Initial Value Formulation," by N. Distefano and J. Schujman - 1969 (PB 187 942)A02

EERC 69-5 "Dynamic Programming and the Solution of the Biharmonic Equation," by N. Distefano - 1969 (PB 187 941)A03

EERC 69-6 "Stochastic Analysis of Offshore Tower Structures," by A.K. Malhotra and J. Penzien - 1969 (PB 187 903)A09

EERC 69-7 "Rock Motion Accelerograms for High Magnitude Earthquakes," by H.B. Seed and I.M. Idriss - 1969 (PB 187 940)A02

EERC 69-8 "Structural Dynamics Testing Facilities at the University of California, Berkeley," by R.M. Stephen, J.G. Bouwkamp, R.W. Clough and J. Penzien - 1969 (PB 189 111)A04

EERC 69-9 "Seismic Response of Soil Deposits Underlain by Sloping Rock Boundaries," by H. Dezfulian and H.B. Seed 1969 (PB 189 114)A03

EERC 69-10 "Dynamic Stress Analysis of Axisymmetric Structures Under Arbitrary Loading," by S. Ghosh and E.L. Wilson 1969 (PB 189 026)A10

EERC 69-11 "Seismic Behavior of Multistory Frames Designed by Different Philosophies," by J.C. Anderson and V. V. Bertero - 1969 (PB 190 662)A10

EERC 69-12 "Stiffness Degradation of Reinforcing Concrete Members Subjected to Cyclic Flexural Moments," by V.V. Bertero, B. Bresler and H. Ming Liao - 1969 (PB 202 942)A07

EERC 69-13 "Response of Non-Uniform Soil Deposits to Travelling Seismic Waves," by H. Dezfulian and H.B. Seed - 1969 (PB 191 023)A03

EERC 69-14 "Damping Capacity of a Model Steel Structure," by D. Rea, R.W. Clough and J.G. Bouwkamp - 1969 (PB 190 663)A06

EERC 69-15 "Influence of Local Soil Conditions on Building Damage Potential during Earthquakes," by H.B. Seed and I.M. Idriss - 1969 (PB 191 036)A03

EERC 69-16 "The Behavior of Sands Under Seismic Loading Conditions," by M.L. Silver and H.B. Seed - 1969 (AD 714 982)A07

EERC 70-1 "Earthquake Response of Gravity Dams," by A.K. Chopra - 1970 (AD 709 640)A03

EERC 70-2 "Relationships between Soil Conditions and Building Damage in the Caracas Earthquake of July 29, 1967," by H.B. Seed, I.M. Idriss and H. Dezfulian - 1970 (PB 195 762)A05

EERC 70-3 "Cyclic Loading of Full Size Steel Connections," by E.P. Popov and R.M. Stephen - 1970 (PB 213 545)A04

EERC 70-4 "Seismic Analysis of the Charaima Building, Caraballeda, Venezuela," by Subcommittee of the SEAONC Research Committee: V.V. Bertero, P.F. Fratessa, S.A. Mahin, J.H. Sexton, A.C. Scordelis, E.L. Wilson, L.A. Wyllie, H.B. Seed and J. Penzien, Chairman - 1970 (PB 201 455)A06

EERC 70-5 "A Computer Program for Earthquake Analysis of Dams," by A.K. Chopra and P. Chakrabarti - 1970 (AD 723 994)A05

EERC 70-6 "The Propagation of Love Waves Across Non-Horizontally Layered Structures," by J. Lysmer and L.A. Drake 1970 (PB 197 896)A03

EERC 70-7 "Influence of Base Rock Characteristics on Ground Response," by J. Lysmer, H.B. Seed and P.B. Schnabel 1970 (PB 197 897)A03

EERC 70-8 "Applicability of Laboratory Test Procedures for Measuring Soil Liquefaction Characteristics under Cyclic Loading," by H.B. Seed and W.H. Peacock - 1970 (PB 198 016)A03

EERC 70-9 "A Simplified Procedure for Evaluating Soil Liquefaction Potential," by H.B. Seed and I.M. Idriss - 1970 (PB 198 009)A03

EERC 70-10 "Soil Moduli and Damping Factors for Dynamic Response Analysis," by H.B. Seed and I.M. Idriss - 1970 (PB 197 869)A03

EERC 71-1 "Koyna Earthquake of December 11, 1967 and the Performance of Koyna Dam," by A.K. Chopra and P. Chakrabarti 1971 (AD 731 496)A06

EERC 71-2 "Preliminary In-Situ Measurements of Anelastic Absorption in Soils Using a Prototype Earthquake Simulator," by R.D. Borcherdt and P.W. Rodgers - 1971 (PB 201 454)A03

EERC 71-3 "Static and Dynamic Analysis of Inelastic Frame Structures," by F.L. Porter and G.H. Powell - 1971 (PB 210 135)A06

EERC 71-4 "Research Needs in Limit Design of Reinforced Concrete Structures," by V.V. Bertero - 1971 (PB 202 943)A04

EERC 71-5 "Dynamic Behavior of a High-Rise Diagonally Braced Steel Building," by D. Rea, A.A. Shah and J.G. Bouwkamp 1971 (PB 203 584)A06

EERC 71-6 "Dynamic Stress Analysis of Porous Elastic Solids Saturated with Compressible Fluids," by J. Ghaboussi and E. L. Wilson - 1971 (PB 211 396)A06

EERC 71-7 "Inelastic Behavior of Steel Beam-to-Column Subassemblages," by H. Krawinkler, V.V. Bertero and E.P. Popov 1971 (PB 211 335)A14

EERC 71-8 "Modification of Seismograph Records for Effects of Local Soil Conditions," by P. Schnabel, H.B. Seed and J. Lysmer - 1971 (PB 214 450)A03

EERC 72-1 "Static and Earthquake Analysis of Three Dimensional Frame and Shear Wall Buildings," by E.L. Wilson and H.H. Dovey - 1972 (PB 212 904)A05

EERC 72-2 "Accelerations in Rock for Earthquakes in the Western United States," by P.B. Schnabel and H.B. Seed - 1972 (PB 213 100)A03

EERC 72-3 "Elastic-Plastic Earthquake Response of Soil-Building Systems," by T. Minami - 1972 (PB 214 868)A08

EERC 72-4 "Stochastic Inelastic Response of Offshore Towers to Strong Motion Earthquakes," by M.K. Kaul - 1972 (PB 215 713)A05

EERC 72-5 "Cyclic Behavior of Three Reinforced Concrete Flexural Members with High Shear," by E.P. Popov, V.V. Bertero and H. Krawinkler - 1972 (PB 214 555)A05

EERC 72-6 "Earthquake Response of Gravity Dams Including Reservoir Interaction Effects," by P. Chakrabarti and A.K. Chopra - 1972 (AD 762 330)A08

EERC 72-7 "Dynamic Properties of Pine Flat Dam," by D. Rea, C.Y. Liaw and A.K. Chopra - 1972 (AD 763 928)A05

EERC 72-8 "Three Dimensional Analysis of Building Systems," by E.L. Wilson and H.H. Dovey - 1972 (PB 222 438)A06

EERC 72-9 "Rate of Loading Effects on Uncracked and Repaired Reinforced Concrete Members," by S. Mahin, V.V. Bertero, D. Rea and M. Atalay - 1972 (PB 224 520)A08

EERC 72-10 "Computer Program for Static and Dynamic Analysis of Linear Structural Systems," by E.L. Wilson, K.-J. Bathe, J.E. Peterson and H.H.Dovey - 1972 (PB 220 437)A04

EERC 72-11 "Literature Survey - Seismic Effects on Highway Bridges," by T. Iwasaki, J. Penzien and R.W. Clough - 1972 (PB 215 613)A19

EERC 72-12 "SHAKE-A Computer Program for Earthquake Response Analysis of Horizontally Layered Sites," by P.B. Schnabel and J. Lysmer - 1972 (PB 220 207)A06

EERC 73-1 "Optimal Seismic Design of Multistory Frames," by V.V. Bertero and H. Kamil - 1973

EERC 73-2 "Analysis of the Slides in the San Fernando Dams During the Earthquake of February 9, 1971," by H.B. Seed, K.L. Lee, I.M. Idriss and F. Makdisi - 1973 (PB 223 402)A14

EERC 73-3 "Computer Aided Ultimate Load Design of Unbraced Multistory Steel Frames," by M.B. El-Hafez and G.H. Powell 1973 (PB 248 315)A09

EERC 73-4 "Experimental Investigation into the Seismic Behavior of Critical Regions of Reinforced Concrete Components as Influenced by Moment and Shear," by M. Celebi and J. Penzien - 1973 (PB 215 884)A09

EERC 73-5 "Hysteretic Behavior of Epoxy-Repaired Reinforced Concrete Beams," by M. Celebi and J. Penzien - 1973 (PB 239 568)A03

EERC 73-6 "General Purpose Computer Program for Inelastic Dynamic Response of Plane Structures," by A. Kanaan and G.H. Powell - 1973 (PB 221 260)A08

EERC 73-7 "A Computer Program for Earthquake Analysis of Gravity Dams Including Reservoir Interaction," by P. Chakrabarti and A.K. Chopra - 1973 (AD 766 271)A04

EERC 73-8 "Behavior of Reinforced Concrete Deep Beam-Column Subassemblages Under Cyclic Loads," by O. Küstü and J.G. Bouwkamp - 1973 (PB 246 117)A12

EERC 73-9 "Earthquake Analysis of Structure-Foundation Systems," by A.K. Vaish and A.K. Chopra - 1973 (AD 766 272)A07

EERC 73-10 "Deconvolution of Seismic Response for Linear Systems," by R.B. Reimer - 1973 (PB 227 179)A08

EERC 73-11 "SAP IV: A Structural Analysis Program for Static and Dynamic Response of Linear Systems," by K.-J. Bathe, E.L. Wilson and F.E. Peterson - 1973 (PB 221 967)A09

EERC 73-12 "Analytical Investigations of the Seismic Response of Long, Multiple Span Highway Bridges," by W.S. Tseng and J. Penzien - 1973 (PB 227 816)A10

EERC 73-13 "Earthquake Analysis of Multi-Story Buildings Including Foundation Interaction," by A.K. Chopra and J.A. Gutierrez - 1973 (PB 222 970)A03

EERC 73-14 "ADAP: A Computer Program for Static and Dynamic Analysis of Arch Dams," by R.W. Clough, J.M. Raphael and S. Mojtahedi - 1973 (PB 223 763)A09

EERC 73-15 "Cyclic Plastic Analysis of Structural Steel Joints," by R.B. Pinkney and R.W. Clough - 1973 (PB 226 843)A08

EERC 73-16 "QUAD-4: A Computer Program for Evaluating the Seismic Response of Soil Structures by Variable Damping Finite Element Procedures," by I.M. Idriss, J. Lysmer, R. Hwang and H.B. Seed - 1973 (PB 229 424)A05

EERC 73-17 "Dynamic Behavior of a Multi-Story Pyramid Shaped Building," by R.M. Stephen, J.P. Hollings and J.G. Bouwkamp - 1973 (PB 240 718)A06

EERC 73-18 "Effect of Different Types of Reinforcing on Seismic Behavior of Short Concrete Columns," by V.V. Bertero, J. Hollings, O. Küstü, R.M. Stephen and J.G. Bouwkamp - 1973

EERC 73-19 "Olive View Medical Center Materials Studies, Phase I," by B. Bresler and V.V. Bertero - 1973 (PB 235 986)A06

EERC 73-20 "Linear and Nonlinear Seismic Analysis Computer Programs for Long Multiple-Span Highway Bridges," by W.S. Tseng and J. Penzien - 1973

EERC 73-21 "Constitutive Models for Cyclic Plastic Deformation of Engineering Materials," by J.M. Kelly and P.P. Gillis 1973 (PB 226 024)A03

EERC 73-22 "DRAIN - 2D User's Guide," by G.H. Powell - 1973 (PB 227 016)A05

EERC 73-23 "Earthquake Engineering at Berkeley - 1973," (PB 226 033)A11

EERC 73-24 Unassigned

EERC 73-25 "Earthquake Response of Axisymmetric Tower Structures Surrounded by Water," by C.Y. Liaw and A.K. Chopra 1973 (AD 773 052)A09

EERC 73-26 "Investigation of the Failures of the Olive View Stairtowers During the San Fernando Earthquake and Their Implications on Seismic Design," by V.V. Bertero and R.G. Collins - 1973 (PB 235 106)A13

EERC 73-27 "Further Studies on Seismic Behavior of Steel Beam-Column Subassemblages," by V.V. Bertero, H. Krawinkler and E.P. Popov - 1973 (PB 234 172)A06

EERC 74-1 "Seismic Risk Analysis," by C.S. Oliveira - 1974 (PB 235 920)A06

EERC 74-2 "Settlement and Liquefaction of Sands Under Multi-Directional Shaking," by R. Pyke, C.K. Chan and H.B. Seed 1974

EERC 74-3 "Optimum Design of Earthquake Resistant Shear Buildings," by D. Ray, K.S. Pister and A.K. Chopra - 1974 (PB 231 172)A06

EERC 74-4 "LUSH - A Computer Program for Complex Response Analysis of Soil-Structure Systems," by J. Lysmer, T. Udaka, H.B. Seed and R. Hwang - 1974 (PB 236 796)A05

EERC 74-5 "Sensitivity Analysis for Hysteretic Dynamic Systems: Applications to Earthquake Engineering," by D. Ray 1974 (PB 233 213)A06

EERC 74-6 "Soil Structure Interaction Analyses for Evaluating Seismic Response," by H.B. Seed, J. Lysmer and R. Hwang 1974 (PB 236 519)A04

EERC 74-7 Unassigned

EERC 74-8 "Shaking Table Tests of a Steel Frame - A Progress Report," by R.W. Clough and D. Tang - 1974 (PB 240 869)A03

EERC 74-9 "Hysteretic Behavior of Reinforced Concrete Flexural Members with Special Web Reinforcement," by V.V. Bertero, E.P. Popov and T.Y. Wang - 1974 (PB 236 797)A07

EERC 74-10 "Applications of Reliability-Based, Global Cost Optimization to Design of Earthquake Resistant Structures," by E. Vitiello and K.S. Pister - 1974 (PB 237 231)A06

EERC 74-11 "Liquefaction of Gravelly Soils Under Cyclic Loading Conditions," by R.T. Wong, H.B. Seed and C.K. Chan 1974 (PB 242 042)A03

EERC 74-12 "Site-Dependent Spectra for Earthquake-Resistant Design," by H.B. Seed, C. Ugas and J. Lysmer - 1974 (PB 240 953)A03

EERC 74-13 "Earthquake Simulator Study of a Reinforced Concrete Frame," by P. Hidalgo and R.W. Clough - 1974 (PB 241 944)A13

EERC 74-14 "Nonlinear Earthquake Response of Concrete Gravity Dams," by N. Pal - 1974 (AD/A 006 583)A06

EERC 74-15 "Modeling and Identification in Nonlinear Structural Dynamics - I. One Degree of Freedom Models," by N. Distefano and A. Rath - 1974 (PB 241 548)A06

EERC 75-1 "Determination of Seismic Design Criteria for the Dumbarton Bridge Replacement Structure, Vol. I: Description, Theory and Analytical Modeling of Bridge and Parameters," by F. Baron and S.-H. Pang - 1975 (PB 259 407)A15

EERC 75-2 "Determination of Seismic Design Criteria for the Dumbarton Bridge Replacement Structure, Vol. II: Numerical Studies and Establishment of Seismic Design Criteria," by F. Baron and S.-H. Pang - 1975 (PB 259 408)A11 (For set of EERC 75-1 and 75-2 (PB 259 406))

EERC 75-3 "Seismic Risk Analysis for a Site and a Metropolitan Area," by C.S. Oliveira - 1975 (PB 248 134)A09

EERC 75-4 "Analytical Investigations of Seismic Response of Short, Single or Multiple-Span Highway Bridges," by M.-C. Chen and J. Penzien - 1975 (PB 241 454)A09

EERC 75-5 "An Evaluation of Some Methods for Predicting Seismic Behavior of Reinforced Concrete Buildings," by S.A. Mahin and V.V. Bertero - 1975 (PB 246 306)A16

EERC 75-6 "Earthquake Simulator Study of a Steel Frame Structure, Vol. I: Experimental Results," by R.W. Clough and D.T. Tang - 1975 (PB 243 981)A13

EERC 75-7 "Dynamic Properties of San Bernardino Intake Tower," by D. Rea, C.-Y. Liaw and A.K. Chopra - 1975 (AD/A008 406) A05

EERC 75-8 "Seismic Studies of the Articulation for the Dumbarton Bridge Replacement Structure, Vol. I: Description, Theory and Analytical Modeling of Bridge Components," by F. Baron and R.E. Hamati - 1975 (PB 251 539)A07

EERC 75-9 "Seismic Studies of the Articulation for the Dumbarton Bridge Replacement Structure, Vol. 2: Numerical Studies of Steel and Concrete Girder Alternates," by F. Baron and R.E. Hamati - 1975 (PB 251 540)A10

EERC 75-10 "Static and Dynamic Analysis of Nonlinear Structures," by D.P. Mondkar and G.H. Powell - 1975 (PB 242 434)A08

EERC 75-11 "Hysteretic Behavior of Steel Columns," by E.P. Popov, V.V. Bertero and S. Chandramouli - 1975 (PB 252 365)A11

EERC 75-12 "Earthquake Engineering Research Center Library Printed Catalog," - 1975 (PB 243 711)A26

EERC 75-13 "Three Dimensional Analysis of Building Systems (Extended Version)," by E.L. Wilson, J.P. Hollings and H.H. Dovey - 1975 (PB 243 989)A07

EERC 75-14 "Determination of Soil Liquefaction Characteristics by Large-Scale Laboratory Tests," by P. De Alba, C.K. Chan and H.B. Seed - 1975 (NUREG 0027)A08

EERC 75-15 "A Literature Survey - Compressive, Tensile, Bond and Shear Strength of Masonry," by R.L. Mayes and R.W. Clough - 1975 (PB 246 292)A10

EERC 75-16 "Hysteretic Behavior of Ductile Moment Resisting Reinforced Concrete Frame Components," by V.V. Bertero and E.P. Popov - 1975 (PB 246 388)A05

EERC 75-17 "Relationships Between Maximum Acceleration, Maximum Velocity, Distance from Source, Local Site Conditions for Moderately Strong Earthquakes," by H.B. Seed, R. Murarka, J. Lysmer and I.M. Idriss - 1975 (PB 248 172)A03

EERC 75-18 "The Effects of Method of Sample Preparation on the Cyclic Stress-Strain Behavior of Sands," by J. Mulilis, C.K. Chan and H.B. Seed - 1975 (Summarized in EERC 75-28)

EERC 75-19 "The Seismic Behavior of Critical Regions of Reinforced Concrete Components as Influenced by Moment, Shear and Axial Force," by M.B. Atalay and J. Penzien - 1975 (PB 258 842)A11

EERC 75-20 "Dynamic Properties of an Eleven Story Masonry Building," by R.M. Stephen, J.P. Hollings, J.G. Bouwkamp and D. Jurukovski - 1975 (PB 246 945)A04

EERC 75-21 "State-of-the-Art in Seismic Strength of Masonry - An Evaluation and Review," by R.L. Mayes and R.W. Clough 1975 (PB 249 040)A07

EERC 75-22 "Frequency Dependent Stiffness Matrices for Viscoelastic Half-Plane Foundations," by A.K. Chopra, P. Chakrabarti and G. Dasgupta - 1975 (PB 248 121)A07

EERC 75-23 "Hysteretic Behavior of Reinforced Concrete Framed Walls," by T.Y. Wong, V.V. Bertero and E.P. Popov - 1975

EERC 75-24 "Testing Facility for Subassemblages of Frame-Wall Structural Systems," by V.V. Bertero, E.P. Pöpov and T. Endo - 1975

EERC 75-25 "Influence of Seismic History on the Liquefaction Characteristics of Sands," by H.B. Seed, K. Mori and C.K. Chan - 1975 (Summarized in EERC 75-28)

EERC 75-26 "The Generation and Dissipation of Pore Water Pressures during Soil Liquefaction," by H.B. Seed, P.P. Martin and J. Lysmer - 1975 (PB 252 648)A03

EERC 75-27 "Identification of Research Needs for Improving Aseismic Design of Building Structures," by V.V. Bertero 1975 (PB 248 136)A05

EERC 75-28 "Evaluation of Soil Liquefaction Potential during Earthquakes," by H.B. Seed, I. Arango and C.K. Chan - 1975 (NUREG 0026)A13

EERC 75-29 "Representation of Irregular Stress Time Histories by Equivalent Uniform Stress Series in Liquefaction Analyses," by H.B. Seed, I.M. Idriss, F. Makdisi and N. Banerjee - 1975 (PB 252 635)A03

EERC 75-30 "FLUSH - A Computer Program for Approximate 3-D Analysis of Soil-Structure Interaction Problems," by J. Lysmer, T. Udaka, C.-F. Tsai and H.B. Seed - 1975 (PB 259 332)A07

EERC 75-31 "ALUSH - A Computer Program for Seismic Response Analysis of Axisymmetric Soil-Structure Systems," by E. Berger, J. Lysmer and H.B. Seed - 1975

EERC 75-32 "TRIP and TRAVEL - Computer Programs for Soil-Structure Interaction Analysis with Horizontally Travelling Waves," by T. Udaka, J. Lysmer and H.B. Seed - 1975

EERC 75-33 "Predicting the Performance of Structures in Regions of High Seismicity," by J. Penzien - 1975 (PB 248 130)A03

EERC 75-34 "Efficient Finite Element Analysis of Seismic Structure - Soil - Direction," by J. Lysmer, H.B. Seed, T. Udaka, R.N. Hwang and C.-F. Tsai - 1975 (PB 253 570)A03

EERC 75-35 "The Dynamic Behavior of a First Story Girder of a Three-Story Steel Frame Subjected to Earthquake Loading," by R.W. Clough and L.-Y. Li - 1975 (PB 248 841)A05

EERC 75-36 "Earthquake Simulator Study of a Steel Frame Structure, Volume II - Analytical Results," by D.T. Tang - 1975 (PB 252 926)A10

EERC 75-37 "ANSR-I General Purpose Computer Program for Analysis of Non-Linear Structural Response," by D.P. Mondkar and G.H. Powell - 1975 (PB 252 386)A08

EERC 75-38 "Nonlinear Response Spectra for Probabilistic Seismic Design and Damage Assessment of Reinforced Concrete Structures," by M. Murakami and J. Penzien - 1975 (PB 259 530)A05

EERC 75-39 "Study of a Method of Feasible Directions for Optimal Elastic Design of Frame Structures Subjected to Earthquake Loading," by N.D. Walker and K.S. Pister - 1975 (PB 257 781)A06

EERC 75-40 "An Alternative Representation of the Elastic-Viscoelastic Analogy," by G. Dasgupta and J.L. Sackman - 1975 (PB 252 173)A03

EERC 75-41 "Effect of Multi-Directional Shaking on Liquefaction of Sands," by H.B. Seed, R. Pyke and G.R. Martin - 1975 (PB 258 781)A03

EERC 76-1 "Strength and Ductility Evaluation of Existing Low-Rise Reinforced Concrete Buildings - Screening Method," by T. Okada and B. Bresler - 1976 (PB 257 906)A11

EERC 76-2 "Experimental and Analytical Studies on the Hysteretic Behavior of Reinforced Concrete Rectangular and T-Beams," by S.-Y.M. Ma, E.P. Popov and V.V. Bertero - 1976 (PB 260 843)A12

EERC 76-3 "Dynamic Behavior of a Multistory Triangular-Shaped Building," by J. Petrovski, R.M. Stephen, E. Gartenbaum and J.G. Bouwkamp - 1976 (PB 273 279)A07

EERC 76-4 "Earthquake Induced Deformations of Earth Dams," by N. Serff, H.B. Seed, F.I. Makdisi & C.-Y. Chang - 1976 (PB 292 065)A08

EERC 76-5 "Analysis and Design of Tube-Type Tall Building Structures," by H. de Clercq and G.H. Powell - 1976 (PB 252 220) A10

EERC 76-6 "Time and Frequency Domain Analysis of Three-Dimensional Ground Motions, San Fernando Earthquake," by T. Kubo and J. Penzien (PB 260 556)A11

EERC 76-7 "Expected Performance of Uniform Building Code Design Masonry Structures," by R.L. Mayes, Y. Omote, S.W. Chen and R.W. Clough - 1976 (PB 270 098)A05

EERC 76-8 "Cyclic Shear Tests of Masonry Piers, Volume 1 - Test Results," by R.L. Mayes, Y. Omote, R.W. Clough - 1976 (PB 264 424)A06

EERC 76-9 "A Substructure Method for Earthquake Analysis of Structure - Soil Interaction," by J.A. Gutierrez and A.K. Chopra - 1976 (PB 257 783)A08

EERC 76-10 "Stabilization of Potentially Liquefiable Sand Deposits using Gravel Drain Systems," by H.B. Seed and J.R. Booker - 1976 (PB 258 820)A04

EERC 76-11 "Influence of Design and Analysis Assumptions on Computed Inelastic Response of Moderately Tall Frames," by G.H. Powell and D.G. Row - 1976 (PB 271 409)A06

EERC 76-12 "Sensitivity Analysis for Hysteretic Dynamic Systems: Theory and Applications," by D. Ray, K.S. Pister and E. Polak - 1976 (PB 262 859)A04

EERC 76-13 "Coupled Lateral Torsional Response of Buildings to Ground Shaking," by C.L. Kan and A.K. Chopra - 1976 (PB 257 907)A09

EERC 76-14 "Seismic Analyses of the Banco de America," by V.V. Bertero, S.A. Mahin and J.A. Hollings - 1976

EERC 76-15 "Reinforced Concrete Frame 2: Seismic Testing and Analytical Correlation," by R.W. Clough and J. Gidwani - 1976 (PB 261 323)A08

EERC 76-16 "Cyclic Shear Tests of Masonry Piers, Volume 2 - Analysis of Test Results," by R.L. Mayes, Y. Omote and R.W. Clough - 1976

EERC 76-17 "Structural Steel Bracing Systems: Behavior Under Cyclic Loading," by E.P. Popov, K. Takanashi and C.W. Roeder - 1976 (PB 260 715)A05

EERC 76-18 "Experimental Model Studies on Seismic Response of High Curved Overcrossings," by D. Williams and W.G. Godden - 1976 (PB 269 548)A08

EERC 76-19 "Effects of Non-Uniform Seismic Disturbances on the Dumbarton Bridge Replacement Structure," by F. Baron and R.E. Hamati - 1976 (PB 282 981)A16

EERC 76-20 "Investigation of the Inelastic Characteristics of a Single Story Steel Structure Using System Identification and Shaking Table Experiments," by V.C. Matzen and H.D. McNiven - 1976 (PB 258 453)A07

EERC 76-21 "Capacity of Columns with Splice Imperfections," by E.P. Popov, R.M. Stephen and R. Philbrick - 1976 (PB 260 378)A04

EERC 76-22 "Response of the Olive View Hospital Main Building during the San Fernando Earthquake," by S. A. Mahin, V.V. Bertero, A.K. Chopra and R. Collins - 1976 (PB 271 425)A14

EERC 76-23 "A Study on the Major Factors Influencing the Strength of Masonry Prisms," by N.M. Mostaghel, R.L. Mayes, R. W. Clough and S.W. Chen - 1976 (Not published)

EERC 76-24 "GADFLEA - A Computer Program for the Analysis of Pore Pressure Generation and Dissipation during Cyclic or Earthquake Loading," by J.R. Booker, M.S. Rahman and H.B. Seed - 1976 (PB 263 947)A04

EERC 76-25 "Seismic Safety Evaluation of a R/C School Building," by B. Bresler and J. Axley - 1976

EERC 76-26 "Correlative Investigations on Theoretical and Experimental Dynamic Behavior of a Model Bridge Structure," by K. Kawashima and J. Penzien - 1976 (PB 263 388)A11

EERC 76-27 "Earthquake Response of Coupled Shear Wall Buildings," by T. Srichatrapimuk - 1976 (PB 265 157)A07

EERC 76-28 "Tensile Capacity of Partial Penetration Welds," by E.P. Popov and R.M. Stephen - 1976 (PB 262 899)A03

EERC 76-29 "Analysis and Design of Numerical Integration Methods in Structural Dynamics," by H.M. Hilber - 1976 (PB 264 410)A06

EERC 76-30 "Contribution of a Floor System to the Dynamic Characteristics of Reinforced Concrete Buildings," by L.E. Malik and V.V. Bertero - 1976 (PB 272 247)A13

EERC 76-31 "The Effects of Seismic Disturbances on the Golden Gate Bridge," by F. Baron, M. Arikan and R.E. Hamati - 1976 (PB 272 279)A09

EERC 76-32 "Infilled Frames in Earthquake Resistant Construction," by R.E. Klingner and V.V. Bertero - 1976 (PB 265 892)A13

UCB/EERC-77/01 "PLUSH - A Computer Program for Probabilistic Finite Element Analysis of Seismic Soil-Structure Interaction," by M.P. Romo Organista, J. Lysmer and H.B. Seed - 1977

UCB/EERC-77/02 "Soil-Structure Interaction Effects at the Humboldt Bay Power Plant in the Ferndale Earthquake of June 7, 1975," by J.E. Valera, H.B. Seed, C.F. Tsai and J. Lysmer - 1977 (PB 265 795)A04

UCB/EERC-77/03 "Influence of Sample Disturbance on Sand Response to Cyclic Loading," by K. Mori, H.B. Seed and C.K. Chan - 1977 (PB 267 352)A04

UCB/EERC-77/04 "Seismological Studies of Strong Motion Records," by J. Shoja-Taheri - 1977 (PB 269 655)A10

UCB/EERC-77/05 "Testing Facility for Coupled-Shear Walls," by L. Li-Hyung, V.V. Bertero and E.P. Popov - 1977

UCB/EERC-77/06 "Developing Methodologies for Evaluating the Earthquake Safety of Existing Buildings," by No. 1 - B. Bresler; No. 2 - B. Bresler, T. Okada and D. Zisling; No. 3 - T. Okada and B. Bresler; No. 4 - V.V. Bertero and B. Bresler - 1977 (PB 267 354)A08

UCB/EERC-77/07 "A Literature Survey - Transverse Strength of Masonry Walls," by Y. Omote, R.L. Mayes, S.W. Chen and R.W. Clough - 1977 (PB 277 933)A07

UCB/EERC-77/08 "DRAIN-TABS: A Computer Program for Inelastic Earthquake Response of Three Dimensional Buildings," by R. Guendelman-Israel and G.H. Powell - 1977 (PB 270 693)A07

UCB/EERC-77/09 "SUBWALL: A Special Purpose Finite Element Computer Program for Practical Elastic Analysis and Design of Structural Walls with Substructure Option," by D.Q. Le, H. Peterson and E.P. Popov - 1977 (PB 270 567)A05

UCB/EERC-77/10 "Experimental Evaluation of Seismic Design Methods for Broad Cylindrical Tanks," by D.P. Clough (PB 272 280)A13

UCB/EERC-77/11 "Earthquake Engineering Research at Berkeley - 1976," - 1977 (PB 273 507)A09

UCB/EERC-77/12 "Automated Design of Earthquake Resistant Multistory Steel Building Frames," by N.D. Walker, Jr. - 1977 (PB 276 526)A09

UCB/EERC-77/13 "Concrete Confined by Rectangular Hoops Subjected to Axial Loads," by J. Vallenas, V.V. Bertero and E.P. Popov - 1977 (PB 275 165)A06

UCB/EERC-77/14 "Seismic Strain Induced in the Ground During Earthquakes," by Y. Sugimura - 1977 (PB 284 201)A04

UCB/EERC-77/15 "Bond Deterioration under Generalized Loading," by V.V. Bertero, E.P. Popov and S. Viwathanatepa - 1977

UCB/EERC-77/16 "Computer Aided Optimum Design of Ductile Reinforced Concrete Moment Resisting Frames," by S.W. Zagajeski and V.V. Bertero - 1977 (PB 280 137)A07

UCB/EERC-77/17 "Earthquake Simulation Testing of a Stepping Frame with Energy-Absorbing Devices," by J.M. Kelly and D.F. Tsztoo - 1977 (PB 273 506)A04

UCB/EERC-77/18 "Inelastic Behavior of Eccentrically Braced Steel Frames under Cyclic Loadings," by C.W. Roeder and E.P. Popov - 1977 (PB 275 526)A15

UCB/EERC-77/19 "A Simplified Procedure for Estimating Earthquake-Induced Deformations in Dams and Embankments," by F.I. Makdisi and H.B. Seed - 1977 (PB 276 820)A04

UCB/EERC-77/20 "The Performance of Earth Dams during Earthquakes," by H.B. Seed, F.I. Makdisi and P. de Alba - 1977 (PB 276 821)A04

UCB/EERC-77/21 "Dynamic Plastic Analysis Using Stress Resultant Finite Element Formulation," by P. Lukkunapvasit and J.M. Kelly - 1977 (PB 275 453)A04

UCB/EERC-77/22 "Preliminary Experimental Study of Seismic Uplift of a Steel Frame," by R.W. Clough and A.A. Huckelbridge 1977 (PB 278 769)A08

UCB/EERC-77/23 "Earthquake Simulator Tests of a Nine-Story Steel Frame with Columns Allowed to Uplift," by A.A. Huckelbridge - 1977 (PB 277 944)A09

UCB/EERC-77/24 "Nonlinear Soil-Structure Interaction of Skew Highway Bridges," by M.-C. Chen and J. Penzien - 1977 (PB 276 176)A07

UCB/EERC-77/25 "Seismic Analysis of an Offshore Structure Supported on Pile Foundations," by D.D.-N. Liou and J. Penzien 1977 (PB 283 180)A06

UCB/EERC-77/26 "Dynamic Stiffness Matrices for Homogeneous Viscoelastic Half-Planes," by G. Dasgupta and A.K. Chopra - 1977 (PB 279 654)A06

UCB/EERC-77/27 "A Practical Soft Story Earthquake Isolation System," by J.M. Kelly, J.M. Eidinger and C.J. Derham - 1977 (PB 276 814)A07

UCB/EERC-77/28 "Seismic Safety of Existing Buildings and Incentives for Hazard Mitigation in San Francisco: An Exploratory Study," by A.J. Meltsner - 1977 (PB 281 970)A05

UCB/EERC-77/29 "Dynamic Analysis of Electrohydraulic Shaking Tables," by D. Rea, S. Abedi-Hayati and Y. Takahashi 1977 (PB 282 569)A04

UCB/EERC-77/30 "An Approach for Improving Seismic - Resistant Behavior of Reinforced Concrete Interior Joints," by B. Galunic, V.V. Bertero and E.P. Popov - 1977 (PB 290 870)A06

UCB/EERC-78/01 "The Development of Energy-Absorbing Devices for Aseismic Base Isolation Systems," by J.M. Kelly and D.F. Tsztoo - 1978 (PB 284 978)A04

UCB/EERC-78/02 "Effect of Tensile Prestrain on the Cyclic Response of Structural Steel Connections, by J.G. Bouwkamp and A. Mukhopadhyay - 1978

UCB/EERC-78/03 "Experimental Results of an Earthquake Isolation System using Natural Rubber Bearings," by J.M. Eidinger and J.M. Kelly - 1978 (PB 281 686)A04

UCB/EERC-78/04 "Seismic Behavior of Tall Liquid Storage Tanks," by A. Niwa - 1978 (PB 284 017)A14

UCB/EERC-78/05 "Hysteretic Behavior of Reinforced Concrete Columns Subjected to High Axial and Cyclic Shear Forces," by S.W. Zagajeski, V.V. Bertero and J.G. Bouwkamp - 1978 (PB 283 858)A13

UCB/EERC-78/06 "Inelastic Beam-Column Elements for the ANSR-I Program," by A. Riahi, D.G. Row and G.H. Powell - 1978

UCB/EERC-78/07 "Studies of Structural Response to Earthquake Ground Motion," by O.A. Lopez and A.K. Chopra - 1978 (PB 282 790)A05

UCB/EERC-78/08 "A Laboratory Study of the Fluid-Structure Interaction of Submerged Tanks and Caissons in Earthquakes," by R.C. Byrd - 1978 (PB 284 957)A08

UCB/EERC-78/09 "Model for Evaluating Damageability of Structures," by I. Sakamoto and B. Bresler - 1978

UCB/EERC-78/10 "Seismic Performance of Nonstructural and Secondary Structural Elements," by I. Sakamoto - 1978

UCB/EERC-78/11 "Mathematical Modelling of Hysteresis Loops for Reinforced Concrete Columns," by S. Nakata, T. Sproul and J. Penzien - 1978

UCB/EERC-78/12 "Damageability in Existing Buildings," by T. Blejwas and B. Bresler - 1978

UCB/EERC-78/13 "Dynamic Behavior of a Pedestal Base Multistory Building," by R.M. Stephen, E.L. Wilson, J.G. Bouwkamp and M. Button - 1978 (PB 286 650)A08

UCB/EERC-78/14 "Seismic Response of Bridges - Case Studies," by R.A. Imbsen, V. Nutt and J. Penzien - 1978 (PB 286 503)A10

UCB/EERC-78/15 "A Substructure Technique for Nonlinear Static and Dynamic Analysis," by D.G. Row and G.H. Powell - 1978 (PB 288 077)A10

UCB/EERC-78/16 "Seismic Risk Studies for San Francisco and for the Greater San Francisco Bay Area," by C.S. Oliveira - 1978

UCB/EERC-78/17 "Strength of Timber Roof Connections Subjected to Cyclic Loads," by P. Gülkan, R.L. Mayes and R.W. Clough - 1978

UCB/EERC-78/18 "Response of K-Braced Steel Frame Models to Lateral Loads," by J.G. Bouwkamp, R.M. Stephen and E.P. Popov - 1978

UCB/EERC-78/19 "Rational Design Methods for Light Equipment in Structures Subjected to Ground Motion," by J.L. Sackman and J.M. Kelly - 1978 (PB 292 357)A04

UCB/EERC-78/20 "Testing of a Wind Restraint for Aseismic Base Isolation," by J.M. Kelly and D.E. Chitty - 1978 (PB 292 833)A03

UCB/EERC-78/21 "APOLLO - A Computer Program for the Analysis of Pore Pressure Generation and Dissipation in Horizontal Sand Layers During Cyclic or Earthquake Loading," by P.P. Martin and H.B. Seed - 1978 (PB 292 835)A04

UCB/EERC-78/22 "Optimal Design of an Earthquake Isolation System," by M.A. Bhatti, K.S. Pister and E. Polak - 1978 (PB 294 735)A06

UCB/EERC-78/23 "MASH - A Computer Program for the Non-Linear Analysis of Vertically Propagating Shear Waves in Horizontally Layered Deposits," by P.P. Martin and H.B. Seed - 1978 (PB 293 101)A05

UCB/EERC-78/24 "Investigation of the Elastic Characteristics of a Three Story Steel Frame Using System Identification," by I. Kaya and H.D. McNiven - 1978

UCB/EERC-78/25 "Investigation of the Nonlinear Characteristics of a Three-Story Steel Frame Using System Identification," by I. Kaya and H.D. McNiven - 1978

UCB/EERC-78/26 "Studies of Strong Ground Motion in Taiwan," by Y.M. Hsiung, B.A. Bolt and J. Penzien - 1978

UCB/EERC-78/27 "Cyclic Loading Tests of Masonry Single Piers: Volume 1 - Height to Width Ratio of 2," by P.A. Hidalgo, R.L. Mayes, H.D. McNiven and R.W. Clough - 1978

UCB/EERC-78/28 "Cyclic Loading Tests of Masonry Single Piers: Volume 2 - Height to Width Ratio of 1," by S.-W.J. Chen, P.A. Hidalgo, R.L. Mayes, R.W. Clough and H.D. McNiven - 1978

UCB/EERC-78/29 "Analytical Procedures in Soil Dynamics," by J. Lysmer - 1978

UCB/EERC-79/01 "Hysteretic Behavior of Lightweight Reinforced Concrete Beam-Column Subassemblages," by B. Forzani, E.P. Popov, and V.V. Bertero - 1979

UCB/EERC-79/02 "The Development of a Mathematical Model to Predict the Flexural Response of Reinforced Concrete Beams to Cyclic Loads, Using System Identification," by J.F. Stanton and H.D. McNiven - 1979

UCB/EERC-79/03 "Linear and Nonlinear Earthquake Response of Simple Torsionally Coupled Systems," by C.L. Kan and A.K. Chopra - 1979

UCB/EERC-79/04 "A Mathematical Model of Masonry for Predicting Its Linear Seismic Response Characteristics," by Y. Mengi and H.D. McNiven - 1979

UCB/EERC-79/05 "Mechanical Behavior of Lightweight Concrete Confined by Different Types of Lateral Reinforcement," by M.A. Manrique, V.V. Bertero and E.P. Popov - 1979

UCB/EERC-79/06 "Static Tilt Tests of a Tall Cylindrical Liquid Storage Tank," by R.W. Clough and A. Niwa - 1979

UCB/EERC-79/07 "The Design of Steel Energy Absorbing Restrainers and Their Incorporation Into Nuclear Power Plants for Enhanced Safety: Volume 1 - Summary Report," by P.N. Spencer, V.F. Zackay, and E.R. Parker - 1979

UCB/EERC-79/08 "The Design of Steel Energy Absorbing Restrainers and Their Incorporation Into Nuclear Power Plants for Enhanced Safety: Volume 2 - The Development of Analyses for Reactor System Piping," "Simple Systems" by M.C. Lee, J. Penzien, A.K. Chopra, and K. Suzuki "Complex Systems" by G.H. Powell, E.L. Wilson, R.W. Clough and D.G. Row - 1979

UCB/EERC-79/09 "The Design of Steel Energy Absorbing Restrainers and Their Incorporation Into Nuclear Power Plants for Enhanced Safety: Volume 3 - Evaluation of Commerical Steels," by W.S. Owen, R.M.N. Pelloux, R.O. Ritchie, M. Faral, T. Ohhashi, J. Toplosky, S.J. Hartman, V.F. Zackay, and E.R. Parker - 1979

UCB/EERC-79/10 "The Design of Steel Energy Absorbing Restrainers and Their Incorporation Into Nuclear Power Plants for Enhanced Safety: Volume 4 - A Review of Energy-Absorbing Devices," by J.M. Kelly and M.S. Skinner - 1979

UCB/EERC-79/11 "Conservatism In Summation Rules for Closely Spaced Modes," by J.M. Kelly and J.L. Sackman - 1979

UCB/EERC-79/12 "Cyclic Loading Tests of Masonry Single Piers Volume 3 - Height to Width Ratio of 0.5," by P.A. Hidalgo, R.L. Mayes, H.D. McNiven and R.W. Clough - 1979

UCB/EERC-79/13 "Cyclic Behavior of Dense Coarse-Grained Materials in Relation to the Seismic Stability of Dams," by N.G. Banerjee, H.B. Seed and C.K. Chan - 1979

UCB/EERC-79/14 "Seismic Behavior of Reinforced Concrete Interior Beam-Column Subassemblages," by S. Viwathanatepa, E.P. Popov and V.V. Bertero - 1979

UCB/EERC-79/15 "Optimal Design of Localized Nonlinear Systems with Dual Performance Criteria Under Earthquake Excitations," by M.A. Bhatti - 1979

UCB/EERC-79/16 "OPTDYN - A General Purpose Optimization Program for Problems with or without Dynamic Constraints," by M.A. Bhatti, E. Polak and K.S. Pister - 1979

UCB/EERC-79/17 "ANSR-II, Analysis of Nonlinear Structural Response, Users Manual," by D.P. Mondkar and G.H. Powell - 1979

UCB/EERC-79/18 "Soil Structure Interaction in Different Seismic Environments," A. Gomez-Masso, J. Lysmer, J.-C. Chen and H.B. Seed - 1979

UCB/EERC-79/19 "ARMA Models for Earthquake Ground Motions," by M.K. Chang, J.W. Kwiatkowski, R.F. Nau, R.M. Oliver and K.S. Pister - 1979

UCB/EERC-79/20 "Hysteretic Behavior of Reinforced Concrete Structural Walls," by J.M. Vallenas, V.V. Bertero and E.P. Popov - 1979

UCB/EERC-79/21 "Studies on High-Frequency Vibrations of Buildings I: The Column Effects," by J. Lubliner - 1979

UCB/EERC-79/22 "Effects of Generalized Loadings on Bond Reinforcing Bars Embedded in Confined Concrete Blocks," by S. Viwathanatepa, E.P. Popov and V.V. Bertero - 1979

UCB/EERC-79/23 "Shaking Table Study of Single-Story Masonry Houses, Volume 1: Test Structures 1 and 2," by P. Gülkan, R.L. Mayes and R.W. Clough - 1979

UCB/EERC-79/24 "Shaking Table Study of Single-Story Masonry Houses, Volume 2: Test Structures 3 and 4," by P. Gülkan, R.L. Mayes and R.W. Clough - 1979

UCB/EERC-79/25 "Shaking Table Study of Single-Story Masonry Houses, Volume 3: Summary, Conclusions and Recommendations," by R.W. Clough, R.L. Mayes and P. Gülkan - 1979

UCB/EERC-79/26 "Recommendations for a U.S.-Japan Cooperative Research Program Utilizing Large-Scale Testing Facilities," by U.S.-Japan Planning Group - 1979

UCB/EERC-79/27 "Earthquake-Induced Liquefaction Near Lake Amatitlan, Guatemala," by H.B. Seed, I. Arango, C.K. Chan, A. Gomez-Masso and R. Grant de Ascoli - 1979

UCB/EERC-79/28 "Infill Panels: Their Influence on Seismic Response of Buildings," by J.W. Axley and V.V. Bertero - 1979

UCB/EERC-79/29 "3D Truss Bar Element (Type 1) for the ANSR-II Program," by D.P. Mondkar and G.H. Powell - 1979

UCB/EERC-79/30 "2D Beam-Column Element (Type 5 - Parallel Element Theory) for the ANSR-II Program," by D.G. Row, G.H. Powell and D.P. Mondkar

UCB/EERC-79/31 "3D Beam-Column Element (Type 2 - Parallel Element Theory) for the ANSR-II Program," by A. Riahi, G.H. Powell and D.P. Mondkar - 1979

UCB/EERC-79/32 "On Response of Structures to Stationary Excitation," by A. Der Kiureghian - 1979

UCB/EERC-79/33 "Undisturbed Sampling and Cyclic Load Testing of Sands," by S. Singh, H.B. Seed and C.K. Chan - 1979

UCB/EERC-79/34 "Interaction Effects of Simultaneous Torsional and Compressional Cyclic Loading of Sand," by P.M. Griffin and W.N. Houston - 1979

UCB/EERC-80/01 "Earthquake Response of Concrete Gravity Dams Including Hydrodynamic and Foundation Interaction Effects," by A.K. Chopra, P. Chakrabarti and S. Gupta - 1980

UCB/EERC-80/02 "Rocking Response of Rigid Blocks to Earthquakes," by C.S. Yim, A.K. Chopra and J. Penzien - 1980

UCB/EERC-80/03 "Optimum Inelastic Design of Seismic-Resistant Reinforced Concrete Frame Structures," by S.W. Zagajeski and V.V. Bertero - 1980

UCB/EERC-80/04 "Effects of Amount and Arrangement of Wall-Panel Reinforcement on Hysteretic Behavior of Reinforced Concrete Walls," by R. Iliya and V.V. Bertero - 1980

UCB/EERC-80/05 "Shaking Table Research on Concrete Dam Models," by A. Niwa and R.W. Clough - 1980